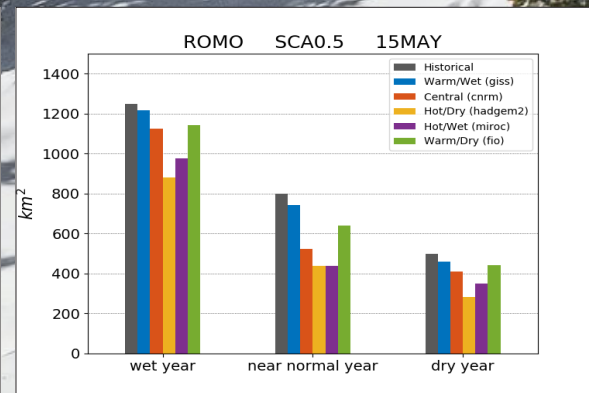
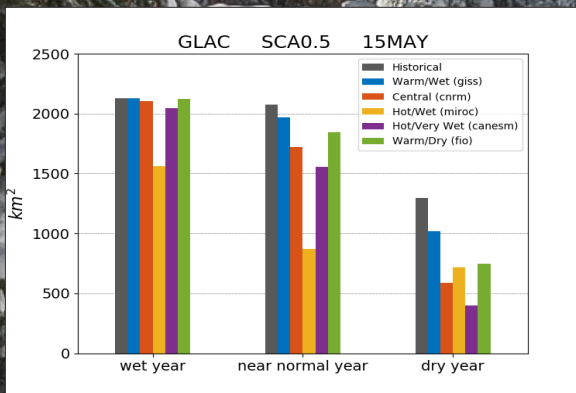


Future Snow Persistence in Rocky Mountain and Glacier National Parks

An analysis to inform the USFWS Wolverine Species Status Assessment



A Report to the U.S. Fish and Wildlife Service Region 6
September 7, 2017



Acknowledgements: The authors acknowledge funding from USFWS Region 6 and the NOAA Physical Sciences Laboratory (PSL). This project built on ongoing work at the NOAA/PSL and the University of Colorado on snow hydrology. and wish to acknowledge CU Support Scientist Leanne Lestak for her work in preparation of DEM, soils, and other input files for DHSVM. We are grateful for the feedback from the many USFWS Region 6 biologists and managers who provided feedback, and in particular to Kevin Swensen. We thank Kevin McKelvey, Jeff Copeland, and Jeremy Littell for their willingness to discuss their earlier projects with us and share their data. We thank Barbara DeLuisi, PSL, for the report cover design. We also acknowledge the World Climate Research Programme's Working Group on Coupled Modelling, and the modeling groups that supplied data to IPCC/CMIP5.

Data: Snow projection data is available here: ftp://ftp2.psl.noaa.gov/Projects/FAIR_paper_data/20200914_01/

Cover Images: Glacier National Park by Andrew Gloor at Unsplash.com; Wolverine by William F. Wood at Wikimedia Commons (CC BY-SA 4.0); Graphs - see figures 5-12 and 5-19 in this report.

Suggested citation: Ray, Andrea J., Barsugli, Joseph J. Jr., Livneh, Ben, Dewes, Candida F., Rangwala, Imtiaz, Heldmyer, Aaron, Stewart, Jenna. 2017. Future snow persistence in Rocky Mountain and Glacier National Parks: An analysis to inform the USFWS Wolverine Species Status Assessment. NOAA Report to the U.S. Fish and Wildlife Service. 101pp. Available at: <https://psl.noaa.gov/assessments/pdf/noaa-future-snow-persistence-report-2017.pdf>

A peer-reviewed article based on this work is in press (as of Sept 2020) in an American Geophysical Union journal, Barsugli, Joseph J. Jr., Ray, Andrea J. Livneh, Ben, Dewes, Candida F., Rangwala, Imtiaz, Heldmyer, Aaron, Guinotte, John, and Torbit, Stephen. (2020). Projections of mountain snowpack loss for wolverine denning elevations in the Rocky Mountains, *Earth's Future*, in press (Sept 2020).

Future snow persistence in Rocky Mountain and
Glacier National Parks:
An analysis to inform the USFWS Wolverine
Species Status Assessment

A Report to the U.S. Fish and Wildlife Service Region 6

7 September 2017

Andrea J. Ray¹, Joseph J. Barsugli², Ben Livneh³, Candida F. Dewes², Imtiaz Rangwala²,
Aaron Heldmyer³, Jenna Stewart³

¹NOAA Physical Sciences Laboratory

²CU/Cooperative Institute for Research in Environmental Sciences (CIRES)

³CU Civil, Environmental & Architectural Engineering

All Boulder, CO

Corresponding Author:

Andrea J. Ray, Ph.D.

303-497-6434

andrea.ray@noaa.gov

This page intentionally left blank.

Executive Summary

Overview: This study is a fine-scale assessment of snow extent and depth for two areas within and surrounding Glacier and Rocky Mountain National Parks. The analysis was done for both the recent past, using MODIS satellite-based remote sensing, and in historic simulations and projections of future snowpack using a high-resolution hydrologic model. The fine scale hydrologic modeling allows for the consideration of snow processes such as dependence on terrain slope and aspect that are important to understanding high elevation snow persistence in a changing climate and were not considered in previous work.

Methods: The report intentionally builds on previous work by McKelvey et al. (2011) extending that work by providing a higher resolution spatial scale analysis for two case study areas, and a broader range of future scenarios. Two areas were studied: a high latitude area near tree line within Glacier National Park, where tree line occurs at ~1800-2100 m (Figure 2-1) that is currently occupied by wolverines; and a lower latitude area within Rocky Mountain National Park, where tree line occurs at higher elevation (~ 3500 m) (ROMO, Figure 2-2). These sites were chosen to bracket the range of latitude and elevation wolverines currently occupy in the contiguous U.S. A detailed comparison of their methodologies and ours is provided in Table 2-1, and a discussion of results in Section 6. Note however that the primary difference between McKelvey et al. (2011) and this study is in the choice of study areas – west-wide vs. much smaller selected areas near treeline, which has implications for the biological hypotheses that may be addressed. Their work focused on May 1st snow depth as a proxy for May 15th snow disappearance, while we focus directly on May 15th snow disappearance. We also analyze our model results for the presence or absence of deeper snow (nominally greater than or equal to 0.5 meters depth) on April 15th and May 1st.¹

The project uses methods from the peer-reviewed, published literature to:

- Explicitly model the effects of slope and aspect, using fine-scale spatial models to analyze topographic effects on snow
- Better represent the range of plausible future changes (climate scenarios)
- Analyze year-to-year variability during the main study period (2000-2013, the years for which both MODIS satellite and hydrologic modeling were available) including wet and dry extremes within that period. We selected representative wet, dry, and near normal years from the main study period for detailed analysis and assessed how these would change under different future climate scenarios. For the two areas, these are:
 - Representative years for GLAC: 2011 (wet), 2005 (dry), 2009 (near normal).
 - Representative years for ROMO: 2011 (wet), 2002 (dry), 2007 (near normal).
- Assessing change in snow persistence by elevation, with emphasis on elevations used by wolverines for denning in GLAC, 1500m -2250.² Linear regression of den site elevations

¹ The study originally focused on May 15th to compare to the McKelvey, et al (2011) study, and June 1st to bracket the snowmelt season. However, as the study progressed, biologists became more interested in April snowcovered area.

² Actual locations of specific dens are confidential and are not provided in this report. The full range in GLAC is ~1500m - ~2250. All but three of 14 documented dens in GLAC are between

and latitude in the contiguous U.S. indicated den sites in the ROMO study area would be located in an elevation range of 2700-3600 m, but documented den sites do not exist in ROMO (Guinotte, personal communication). In contrast to McKelvey's study, which included , the modeling for our study areas are near tree line and above (~1000m – 3166 m in GLAC, and ~2500 m – 4253 m in ROMO).

MODIS Observed Historic Snowpack Variability Analysis: Satellite-based MODIS snowcover data was used to assess the historical variability of snowcover in the study areas and as a basis for the spatial evaluation of the hydrologic model simulations. The historical observed snowcover was analyzed for its dependence on terrain elevation and aspect (compass direction that the slope faces).

- In GLAC, snowcovered area varies considerably by year, including wet years such as 2011 with very persistent snow, years with strong melt in early May, such as 2012, or in late May (2009, 2001), and dry years (2004, 2005; Section 4.3).
- Even in dry years, NE-facing slopes in GLAC tend to hold more snow and melt later in the season. There is > 80% snowcover above ~2000 m elevation on May 1 during dry years, and > 95% snowcover above ~1200 m during wet years (Figure 4-6).
- In ROMO, snowcovered area also varies considerably by year (Section 4-4).
- Northwest-facing slopes in ROMO tend to hold more snow even during dry years. In very dry years, snowcover peaks at intermediate elevations, suggesting that the high-altitude snowpack may be particularly vulnerable in this region under warm/dry conditions (Figure 4-13).

Future Snowpack Projections (Section 5): The Distributed Hydrology Soil Vegetation model (DHSVM) was run in historical simulations of the period 1998-2013. The model was validated against SNOTEL in-situ snow observations and MODIS snowcover. The model was then run for five scenarios of the future which represent a nominal 2055 climate. Scenarios were selected from CMIP5 global climate model (GCM) projections, and were chosen to span a large fraction of the range of the CMIP5 ensemble projections in each study area in terms of precipitation and temperature changes. Representative Wet, Near Normal, and Dry years were analyzed for the historical simulations and how each of these years plays out under these five future scenarios. The number of years (out of 16) with snow above 0.5m depth was also analyzed as was the change in snowcovered area (SCA) with depth greater than 0.5m. The average change in SCA and snow water equivalent (SWE) was analyzed as a function of elevation, and for GLAC was overlaid with the elevations of wolverine den sites.

Data is available at: ftp://ftp2.psl.noaa.gov/Projects/FAIR_paper_data/20200914_01/

While SCA changes provide an overall metrics for the study areas, the interpretation of these reported changes should be done with care. The area-wide SCA results include snowcover changes in both forested and above-treeline terrain, which may have different implications for

1800 and 2000m (Fig. 5-22, 23); two are above 2000m and one is below ~1500m. Our analysis highlights this 1800-2000m band, although results are reported below and above that band.

wolverine biology. Acknowledging this limitation, SWE raster data was provided to the FWS for further analysis.

For the study area in Glacier National Park (GLAC):

- Projections for April 15th, May 1st, and May 15th snowcovered area and area with snow depth greater than 0.5 meters show declines on average in all scenarios, except for small increases in the Warm/Wet scenario and for almost all years (Section 5-11).
- For April 15th for the study area as a whole (Figure 2-1), there is a decline of 3-23 percent in snowcovered area with light snowcover (depth \geq 5 mm), and a 7-44% percent decline in area with significant snow (depth $>$ 0.5 m) for the five scenarios considered, compared to the 2000-2013 historic average. For May 15th, the area with light snowcover declines 10-36 percent, and the area with significant snowcover declines 13-50 percent (Tables 5-4, 5-5)
- On April 15th, the Warm/Wet scenario shows the least change in average SCA (2121 sq-km) compared to the historic snowcover (2609 sq-km, 7% decline) for significant (\geq 0.5 meter) snowcover. The largest decrease is the Hot/Wet scenario (1520 sq-km) with 44% decrease. Under the Hot/Wet scenario, the April 15th significant snowpack has been diminished below the level of the historic May 15th snowpack – a month shift (Fig. 5-14).
- All projections show declines in the number of years with significant snow. In each study domain, the areas with frequent availability (at least 14 out of 16 years) of significant snow (\geq 0.5 m) become concentrated in smaller high elevation areas, as seen in the maps in Figs. 5-13, 5-14 (GLAC), and 5-20, 5-21 (ROMO). In contrast, lower elevation areas had the largest changes, or decreases in the number of years with significant snowcover.
- Most of the known den sites are located between 1800 and 2000m in GLAC. Below that elevation band large snow losses are predicted (40-70% decreases for two of the scenarios, 16-20% for the other three), above that elevation band there is little change in SCA for four of the five scenarios (2-8%) except in maximum warming scenario (-40%, Figure 5-22). In that 1800-2000m band, the snowpack change is sensitive to elevation and to the particular future climate scenario.
- This phenomenon of elevation-dependent snowpack change in the Western US is well supported in the literature. (Section 5-13)
- For representative wet years, the higher elevations of our study areas experience only 2-7% loss of snowpack under the scenarios with “least” change and the “central” change (Figure 5-8, 5-12), although for the dry years, losses range 18-57% (Table 5-5).
- Modest declines in SWE may occur without affecting the area with significant snow depth. On May 1st, for areas at 1800m and above in GLAC, losses of ~10-30% SWE (Figure 5-23) result in losses of only ~10% snowcover. The implication is that the wet, cold climate of the GLAC study area could act as a “buffer” to change in the area of 0.5 m deep snow on May 1st, at least at the elevations above 1800m.

For the study area in and around Rocky Mountain National Park (ROMO):

- Projections of May 15th Snowcovered Area in ROMO declines on average in all scenarios, except for small increases in the Warm/Wet scenario, and for almost all years (Section 5-12).
- For April 15th for the study area as a whole (Figure 2-2), there is decline of 3-18% in area with light snowcover (depth \geq 5 mm), and a change of -1 - +16 in area with significant

snowcover (depth > 0.5 m) for the five scenarios considered, compared to the 2000-2013 historic average. For May 15th, the area with light snowcover declines 8-35 %, and the area with significant snowcover declines 6-38 percent (Tables 5-6, 5-7).

- Snowcovered Area in ROMO (≥ 0.5 m threshold on May 15) generally declines in wet years, shows a slight increase in (1-5%) in some years for the Warm/Wet scenarios with increased precipitation.
- One scenario with increased precipitation (Warm/Wet, giss) shows increases in April 15th SCA (Table 5-7). There are also slight increases in SWE for two scenarios at elevations at and above 3400m (Figure 5-25), but decreases in SWE for all scenarios below 3400m.
- Although no dens have been documented in ROMO, the elevation band for denning, modeled by regression analysis, is estimated to be 2700-3600m (Guinotte, personal communication). On May 1st, modest declines in SWE of ~15% and less for areas at 3400m and above result in losses of < result in losses of only ~10% snowcover (Figure 5-24, 25). The implication is that the wet, cold climate of the higher parts of the ROMO study area could also act as a “buffer” to change in the area of 0.5 m deep snow on May 1st. Below that band losses in SWE of $\geq 35\%$ result in higher losses in SCA (20-65%), except in the scenario with least change (Warm/Wet, giss model). As in the denning band in GLAC, in that 2700-3600m band, the snowpack change is sensitive to elevation and to the particular future climate scenario.
- The phenomenon of elevation-dependent snowpack change in the Western US is well supported in the literature. Studies have found little historical change in snowpack in the Western United States above approximately 2500m elevation despite observed warming trends. Other literature on this topic is discussed in Section 5.13.
- ROMO exhibited more uncertainty in projections than GLAC, because compared to GLAC, the GCM climate projections for ROMO are more uncertain, i.e. have a larger spread, as to whether precipitation will increase or decrease (Figure 5-7).
 - For April 15th –May 15th, and for wet years, at the high elevations of the ROMO study area as whole, there is only modest loss of snowcover (<13%) under most scenarios of change (Table 5-7, see 2011 representative wet year). However even in wet years, the area of significant snowpack can decline by up to 26% for the Hot/Dry climate change scenario on May 15th (Table 5-7).

Elevation dependence of change (Section 5.13): **In general, and supported by the literature (see section 5.13), the snowpack at the higher elevations of both areas is more responsive to precipitation change, while at lower elevations it is more responsive to temperature change.** For GLAC, most of the observed and inferred den sites are located within the zone where temperature dominates the future effects of change, and therefore at elevations where the changes in snowpack are highly dependent on the climate scenario and also on elevation. For the elevation of den sites in GLAC (>1800m) loss of SCA on May 1st spans the range of 5-40% loss, with a 70% decreases for the Hot/Wet (mirco GCM) scenario (Fig 5-22). Above 2200m the losses are <5% for all but the Hot/Wet scenario. For ROMO, the range is at 3200 m elevation, the middle of the inferred range for wolverine there. However, at 3600m the loss of SCA in all scenarios is < 5% (Figure 5-24).

Comparison with McKelvey’s results (Section 6): There are challenges in making a direct comparison between the studies due to differences in the goals and spatial scale. McKelvey

investigated persistence of even a light snowcover to May 15th as a correlate of wolverine habitat, as noted in Aubry et al (2008). This study focuses on high-elevation terrain and on the persistence of deeper snowpack.

However, the following comparisons are valid:

- McKelvey reported a 33% decline in snow cover for western North America for the 2030-2059 period in their ensemble mean climate change scenario ("ensemble2040s"), and a 63% decline for the 2070-2099 period ("ensemble2080s"). The closest comparison with this study is to look at May 15th "light snow cover" (≥ 5 mm SWE) for the Central scenario, compared to the Ensemble 2040s results. The Central scenario is not an ensemble mean, but similar to an ensemble mean, was chosen to represent the central tendency of GCM projections in the period 2041-2070. For this scenario, we find losses in ≥ 5 mm SWE of 24% in GLAC and 18% in ROMO (Tables 5-4 and 5-6). Because our modeling used smaller, higher elevation areas focused on denning, we would not expect our results to replicate the snow loss reported in McKelvey. We show smaller losses a decade further in the future. A similar discrepancy holds if one compares only to the Montana and Colorado statewide snow loss reported in McKelvey. Comparable scenarios for the 2080's were beyond the scope of this project.
- Examining the data from McKelvey's study in detail reveals that snowcover persists in the GLAC and ROMO study areas, even for the hotter of the two scenarios of change in their study ("miroc 2080's"). The greatest loss of May 15th snowcover in McKelvey occurs at elevations lower than ~250m below treeline that were deliberately not included in the GLAC or ROMO study areas. (Figure 5-26).
- McKelvey focused exclusively on the persistence of even light snowcover on May 15th. Because of the increased resolution of our study we are able to consider whether any pockets of snow with depth greater than 0.5 meters will persist in these areas. Results vary according to scenario, but generally show declines of 13-50% in SCA in GLAC and 6-38% in ROMO for May 15th by the 2050s. We made projections for April 15th (which McKelvey did not), which shows declines of in SCA of 7-44% in GLAC and changes of -16 - +1% in ROMO for April 1st by the 2050s.
- Our results may reasonably be generalized to the high mountain ranges within the Rockies that lie between GLAC and ROMO, with projections on average wetter in GLAC. However, without further study we cannot reasonably extend our results to say whether or not snow refugia may persist in the Central Rockies below our study elevations (~1000m). Elevations below our study areas are where McKelvey indicates the greatest snowpack losses. Nor can we extrapolate to the Cascades with its very different maritime climate.
- While it is difficult to compare the McKelvey et al (2011) results directly to the present study due to differences in methodology and focus, the qualitative picture remains – projected warming has a larger effect at lower elevations whereas projected precipitation changes may dominate the Springtime snowpack in the high country.

1 Introduction

1.1 Motivation

This report responds to the United States Fish and Wildlife Service (FWS) need for information on potential climate impacts to snow persistence. The North American wolverine (*Gulo gulo luscus*) is currently being evaluated for listing as a threatened or endangered species under the Endangered Species Act (ESA) and climate change effects on snow persistence was identified as an important factor for the future viability of the wolverine. The species was considered for listing in 2014, but FWS concluded that it did not warrant listing. They further concluded that there is significant uncertainty about how the effects of climate change will affect wolverines and their habitat in the foreseeable future, and that this uncertainty includes information on how fine-scale changes in snowcover and persistence might affect denning site selection.

This report provides FWS with a finer scale assessment of snow extent and depth at which extends previous work by McKelvey et al. (2011). We believe the inclusion of finer scale analyses as well as additional snow processes such as slope and aspect (the compass direction that the slope faces) are critical to understanding high elevation snow persistence in a changing climate.

By design, our methods and models are chosen from the peer-reviewed, published literature. What we find, particularly with regard to the elevation dependence of snowpack change, is consistent with past research.

Funding was provided by the U.S. Fish and Wildlife Service, Region 6 and the NOAA/Earth System Research Lab/Physical Sciences Division. This effort builds on work underway by the project team at NOAA/ESRL/PSD, the NOAA-University of Colorado (CU) Cooperative Institute for Research in Environmental Sciences (CIRES), and CU Department of Civil, Environmental & Architectural Engineering. We are grateful for the feedback from the many USFWS Region 6 biologists and managers who provided feedback, and in particular to Kevin Swensen. We also acknowledge the World Climate Research Programme's Working Group on Coupled Modelling, and the modeling groups that supplied data to CMIP5. A glossary of terms is provided in Section 8. A complete set of snow projection data is available at ftp://ftp2.psl.noaa.gov/Projects/FAIR_paper_data/20200914_01/.

1.2 Project Objectives

Persistent spring snowpack has been described as an important factor in determining suitable habitat for the wolverine, including Northern boreal forests and subarctic and alpine tundra (Aubry et al, 2007, Peacock et al, 2011). This relationship was the basis for the analysis by Copeland et al. (2010) and McKelvey et al. (2011) used in the previous FWS decision. In both studies, climate change projections of snowpack were used to characterize potential future wolverine habitat.

The goal of this effort is to identify the depth and persistence of spring snow in the future. Our primary objective is to advance scientific understanding of the current spatial extent of spring snow retention on the landscape, and the future temporal and spatial extent of snow retention through a thirty-year period, 2041-2070, centered on the year 2055. We aim to advance snow analysis and modeling to better support assessment of snow-related species, in the following ways:

- Explicitly model the effects of slope and aspect, using fine-scale spatial models to analyze topographic effects on snow
- Better represent the range of plausible future changes (climate scenarios)
- Analyze extremes from the current year to year variability: we selected representative wet, dry, and near normal years from the main study period for detailed analysis and assessed how these would change under different future climate scenarios.

Our strategy was to build on previous methods where possible to be comparable to work by McKelvey et al. (2011) and Copeland et al. (2010). We departed from their methods where necessary to take advantage of analysis techniques not feasible at the large scales used in the studies done by those authors. These include new scientific data and tools that are now available, including the following:

- Use of a longer time series of satellite and in situ observations.
- Analysis of historic snowpack variability to investigate the influences of topography on snowcover
- Use of more recent climate model output and improved criteria for choice of climate change scenarios
- Use of hydrologic modeling at highly resolved (250m) spatial scale for simulation and future projection of snowcover and depth for two case study areas in Glacier National Park and Rocky Mountain National Park.

2 Project Overview and Background

2.1 Overview

We first reviewed the observed climate and variability, in order to provide context for future changes (Section 3). We next analyzed historic snow variability from satellite remote sensing of snow extent from the year 2000 to present to determine areas of greater and lesser sensitivity to climate drivers (temperature and precipitation), and identify possible snow refugia. Prior studies also show a relationship between terrain (slope and aspect) and persistence of snow (e.g. Lundquist and Flint, 2006) and thus this factor is potentially important under in a changed climate. (Section 4). We then did an intercomparison of the satellite observations of snow with that from the DHSVM hydrologic modeling study that includes a representation of slope and aspect (the compass direction that the slope faces) of the terrain and shading on the snowpack. Finally, the DHSVM hydrologic model was forced with five future scenarios of climate change for each of the two study regions (Section 5). These future climate scenarios were derived from the latest Coupled Model Inter-comparison Project Phase-5 runs (CMIP5, Taylor et al., 2012) which informed the latest Intergovernmental Panel on Climate Change (IPCC) report (IPCC AR5, 2013).

All methodologies were chosen to be consistent with those used in existing peer-reviewed work; a peer-reviewed publication based on this effort is in press (Barsugli et al. 2020).

2.2 Study Areas

High-resolution hydrologic modeling was needed to provide fine scale analysis of snow. However, given time, funding and computational constraints, it was necessary to limit the study domain to two areas of about 1,500-3,000km² for high-resolution analysis. Two study areas representing core and peripheral habitat regions in the northern and central Rocky Mountains were identified in consultation with FWS Region 6 personnel (Figures 2-1 and 2-2). We bracketed the extent of wolverine habitat conditions in the lower 48, because we were restricted to smaller areas for analysis. The two sites chosen included a high latitude, (relatively) low elevation area within Glacier National Park (GNP, Figure 2-1) that is currently occupied by wolverines and a lower latitude, high elevation area within Rocky Mountain National Park (RMNP, Figure 2-2) that has had recent documented wolverine occurrence and could be a potential reintroduction site for wolverines. Both model areas encompassed elevations from ~250m below treeline to maximum elevation in each domain (962 m – 3166 m in GLAC, and 2563 – 4253 m in ROMO).³ This elevation threshold was chosen for the analysis by FWS to represent the areas with known denning activities by wolverines. Note that we use the abbreviations GNP and RMNP to refer to the parks, vs GLAC and ROMO to refer to the study areas.

The analysis for the GLAC and ROMO study areas is presented in separate sections, repeating descriptions to make the material self-contained for the reader who may read about only one area; similarly, complete captions are given for each area.

³ The lowest elevation of each area was not a fixed elevation, but varied somewhat depending on the elevation of the lowest pixel in each hydrologic basin modeled, 962m for GLAC and 4253m for ROMO.

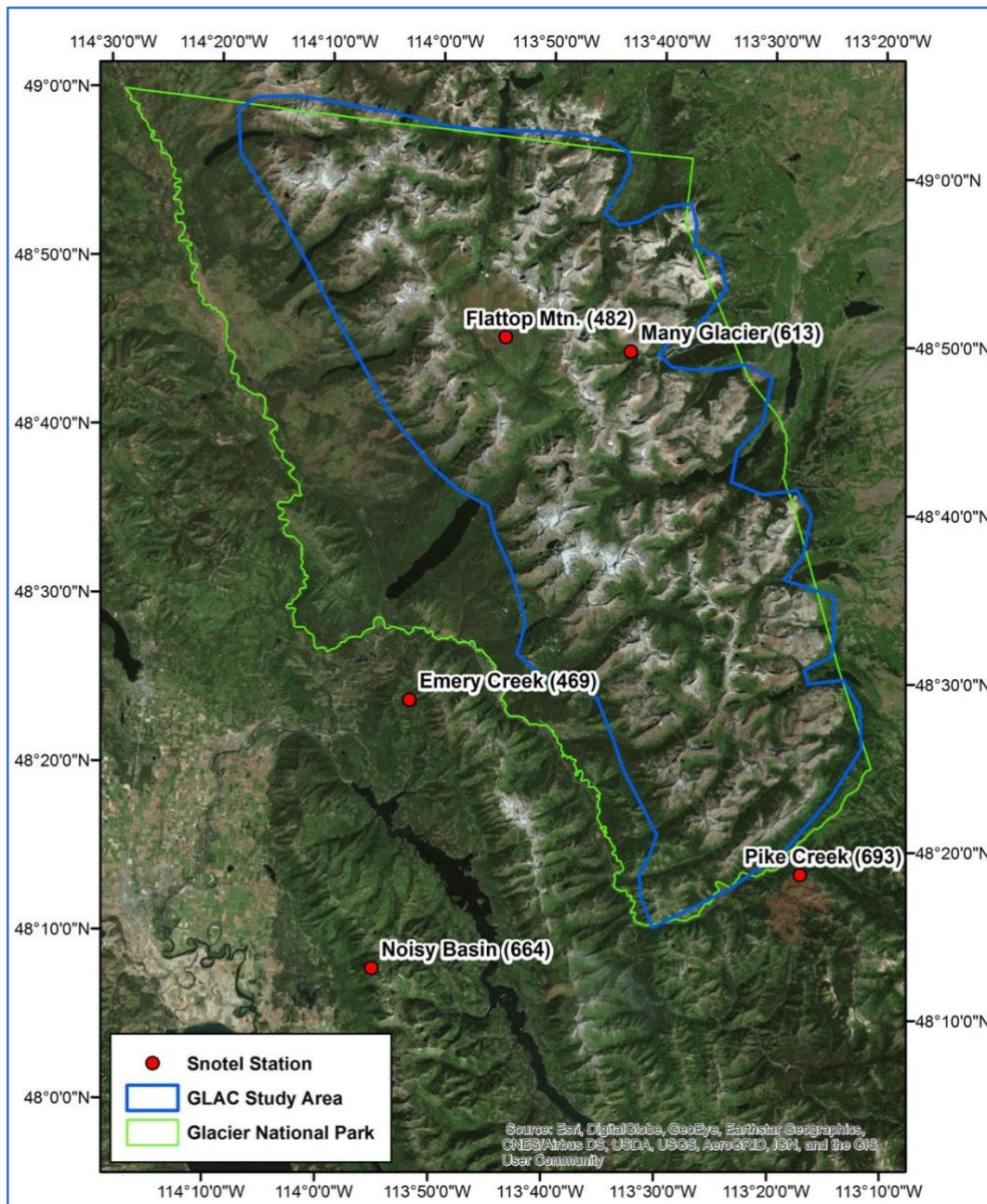


Figure 2-1. Glacier National Park (GLAC) Study Area. The high-resolution study area domain (blue outline) consists of high-elevation areas within and in the vicinity of Glacier National Park (GLAC) including the northern Rocky Mountains in northwest Montana, bordering Canada. SNOTEL stations indicated by red dots, and are also listed in Table 5-1. Study areas were chosen to encompass areas with elevations from the ridgetops down to ~200m below treeline and do not follow National Park boundaries. Tree line occurs at ~1800-2100 m in GLAC. Note that we use the abbreviation GNP to refer to the park, vs GLAC to refer to the study areas.

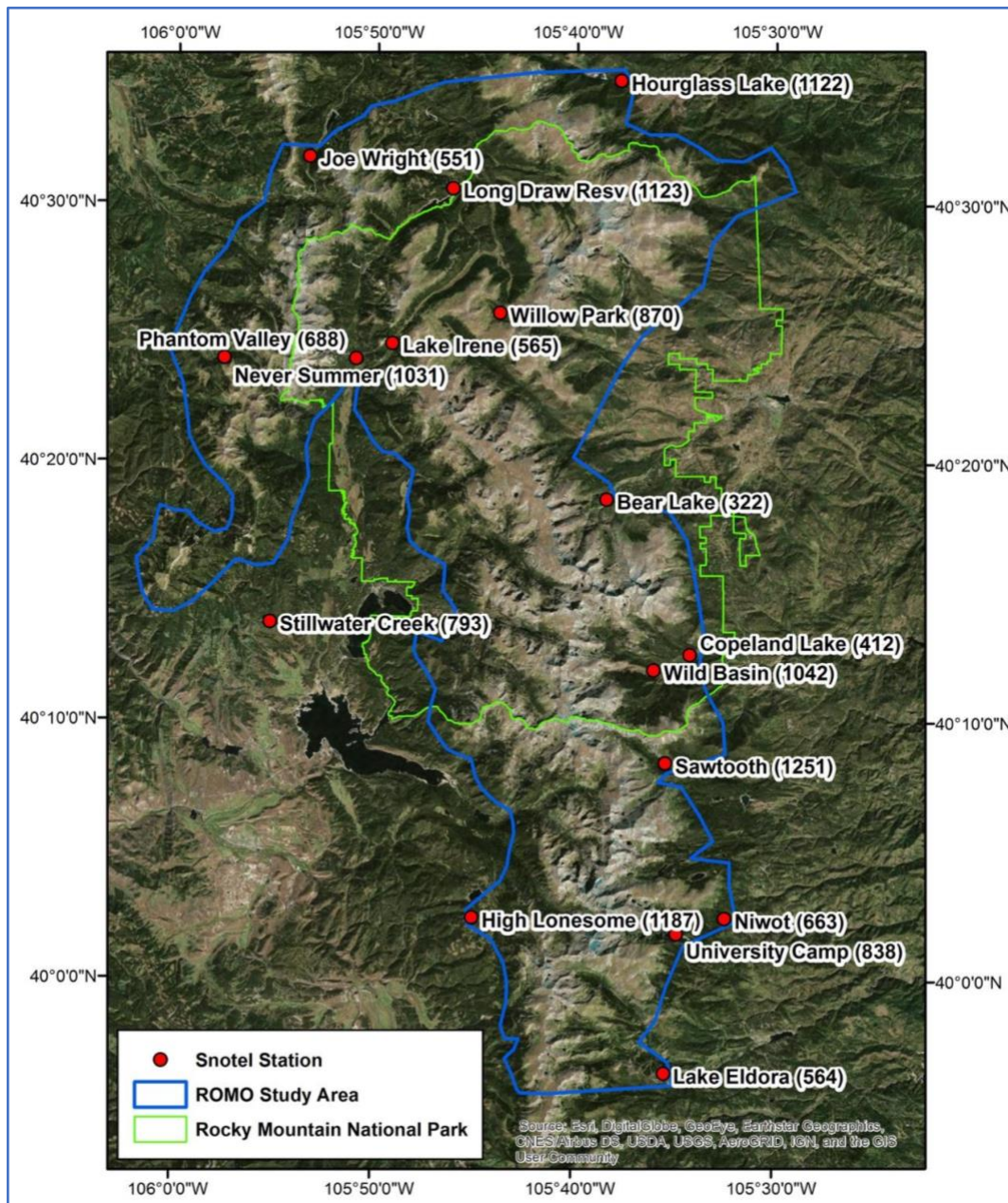


Figure 2-2. Rocky Mountain National Park (ROMO) Study Area. The high resolution domain (blue outline) consists of high-elevation areas within and in the vicinity of the Park (green outline) including the northern Colorado Front Range and Never Summer mountain ranges. SNOTEL stations indicated by red dots, and are also listed in Table 5-1. Study areas were chosen to encompass areas with elevations from the ridgetops down to ~200m below treeline and do not follow the National Park boundary. Tree line occurs at a higher elevation in ROMO (~ 3500 m) than GLAC (~1800-2100 m). Note that we use the abbreviation RMNP to refer to the park, vs ROMO to refer to the study area.

2.3 The West-wide context of future climate

Global climate models (GCMs) are the primary tools used by climate scientists to examine the nature of climate change during the 21st century. These models reveal both the uncertainty of climate projections as well as underlying regional patterns of change. This section provides a west-wide context for the specific choices of future climate scenarios that will be discussed later in the report.

Understanding the uncertainty of climate projections is commonly approached through comparison of the results from multiple climate models (e.g. IPCC, 2013). There are currently about 20 modeling centers worldwide that provide output from their best model or models to be considered in the Coupled Model Inter-comparison Project Phase-5 (CMIP5, Taylor et al., 2012), an international, coordinated modeling project which informed the most recent Intergovernmental Panel on Climate Change (IPCC) assessment report (IPCC AR5, 2013). When we quantify regional changes in climate variables such as temperature and precipitation by a particular time horizon in the 21st century, we find a large spread in the extent of warming and changes in precipitation, including both increases and decreases in precipitation, as shown in regional maps (Figure 2-4 and described further in Section 5). For temperature change, much of this spread (or uncertainty) is a result of the difference among the formulations of the GCMs (e.g., their climate sensitivities), whereas for precipitation it is both the differences among GCMs and internal climate variability. Some difference also comes out of the choice of future greenhouse gases (GHG) emission scenario. However, the differences among greenhouse gas emissions scenarios is less at mid-21st century compared to later in the century, and is much smaller than other sources of uncertainty at the regional scale (IPCC, 2013).

In addition to uncertainty, the CMIP5 climate models also reveal regional patterns of change. Figure 2-3 shows projected annual and seasonal temperature and precipitation changes by 2050 (2035–2064) over the western U.S., including the northern and central Rocky Mountains, from an ensemble of the 34 climate models used for this study under the RCP 8.5, a high-end emissions scenario. The large maps show the average change for all of the models (n=34) for that season, and the small maps show the average changes of the highest 20% and lowest 20% of the models, based on the statewide change for Colorado in temperature or precipitation. For much of the central and northern Rockies, all models show a substantial warming (+2.5°F to +5.5°F). While fewer models agree about the direction of precipitation change west-wide, even the lower (drier) 20% of the models show an increase in winter precipitation for the area around GNP, although there is less agreement for the central Rockies area including RMNP.

The uncertainty of climate change motivates the choice of several future climate scenarios for each study region. The regional patterns of change indicate that the range of the climate scenarios chosen will differ somewhat from region to region. The GCM output, and the specific selection of future climate scenarios for this study are discussed further in Section 5.

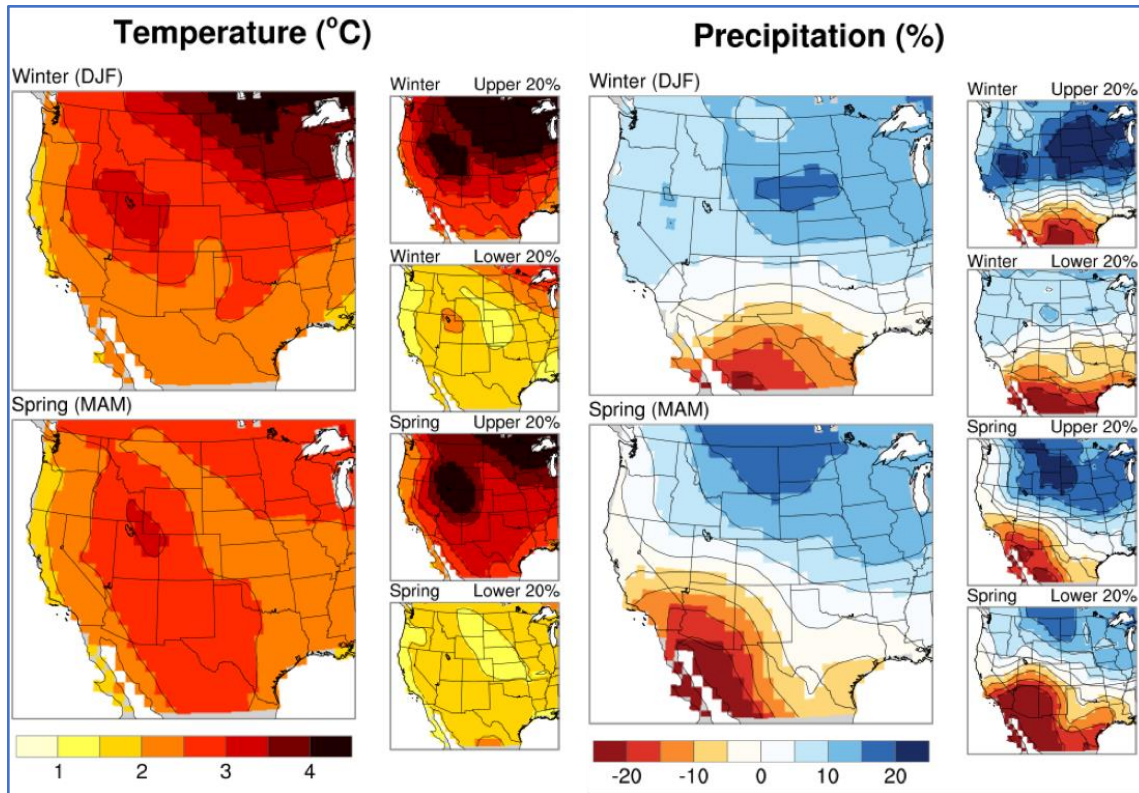


Figure 2-3. Projected changes in temperature (left) and precipitation (right) by 2050 over the western US for winter and spring. Climate projection data are from an ensemble of 37 CMIP5 GCMs under RCP 8.5. The large maps show the mean change of all models. Small maps show mean changes from upper 20% (n=8) and lower 20% (n=8) of the models based on statewide change in Colorado in temperature (note: figure originally from a report for Colorado). All anomalies are calculated based on 2035-2064 relative to 1971-2000. Adopted and modified from Lukas et al., 2014. (Data source: CMIP5 projections re-gridded to 1-degree grid, Reclamation 2013; <http://gdo-dcp.ucllnl.org/>).

2.4 Comparison between our analysis and that of Copeland and McKelvey

The Copeland et al. (2010) and McKelvey et al. (2011) studies were an integral part of the previous FWS decision process. Therefore, we present here a detailed comparison of their methodologies and ours, to establish both how our methodologies followed theirs when appropriate, and diverged where new data or updated methods were available. A summary of the most salient similarities and differences between our work and the studies used previously is presented in Table 2-1.

Table 2-1: Modeling Methods Compared to McKelvey

	McKelvey (Littell)	This Study
Spatial Resolution (modeling)	VIC model – 1/16 degree (~5km x 7 km, ~37km ² cell)	DHSVM model - 250m x 250m UTM grid (~0.0625 km ² cell)
Spatial Extent	Westwide except California and Great Basin	ROMO and GLAC study areas, ~300 m below treeline and above
Process differences	Slope and aspect were not modeled and the mountains were assumed to be flat from a solar radiation process, implicit elevation bands.	Slope, aspect, shading, explicit fine scale elevation effects.
Validation	None specific to snow	Comparison to SNOTEL (ground stations) and MODIS (satellite)
Future Scenarios	Delta Method; “2045”,”2085”; from 3 GCMs selected to span westwide temperature changes.	Delta Method: “2055” from 5 GCMs spanning regional changes in temperature and precipitation
Analysis	Changes in long-term mean snowpack only	Means and variability, including wet, near normal and dry years.
Snow representation	Binary snow/no snow at 13 cm snow depth	Analyzed snow depth at two thresholds: 5mm of SWE (‘light snow’) and 0.5m depth (‘significant snow’)

Both Copeland et al (2010; hereafter, simply Copeland or the Copeland study) and McKelvey present analysis based on satellite remotely-sensed snowcover from the MODIS. For example, Copeland calculated the number of years with snowcover on May 15th as detected in the MODIS snowcover dataset, by calculating a snow disappearance date. They found that most (45 of 75) North American den sites were in areas that snowcover persisted with 6 or 7 out of 7 years on May 15th. We also provide a historical analysis of remotely sensed snowcover from MODIS. We also investigated the of number of years of snow persistence for our study areas, however, the new MODIS product has two advantages over that available at the time of their study, 1) improved snow detection (snowcovered area, SCA), and 2) 17 years of MODIS data is now available vs the 7 available to Copeland and McKelvey. Furthermore, we investigated the relationships between snowcover persistence and both elevation and aspect (the compass direction of the slope face).

Both McKelvey et al. (2011) (hereafter, simply McKelvey or the McKelvey study) and the

present study investigate projections of snowcover using a distributed hydrologic model. The McKelvey study focused its' analysis on May 1st snow depth simulated by the Variable Infiltration Capacity hydrologic (VIC) hydrology model (1/16 degree, ~5km x 7 km), "flat" gridboxes, or cells, with no slope aspect dependence). The May 1st snow depth was then converted into a proxy for May 15th snow disappearance by applying a threshold of 13 cm – a procedure they refer to as "cross-walking". All subsequent calculations of theirs were done using the May 15th snowcover proxy. The VIC model runs were documented in Littell et al. (2011) and were based on meteorological inputs from Elsner et al. (2010). The present study uses the Distributed Hydrology Soil Vegetation (DHSVM) model, which was developed by the same group at the University of Washington for fine-scale simulations, and shares many model components with the VIC model. The primary output of DHSVM is snow water equivalent (SWE). We investigate several thresholds for converting SWE to "snowcover". Conversion of SWE to snow depth is done using empirically derived conversion factors relevant to Spring.

To generate future climate scenarios, Littell (on which McKelvey results are based) used the "delta method" (described later in Section 5) for the projected changes in climate compared to present day. This study also uses the "delta method," applied in a similar manner. The McKelvey study used a range of temperature change to select GCMs representing the range or spread of future scenarios. As shown below in Section 5.10 and Figure 5.7, their chosen future scenarios reflect a range of precipitation in GLAC, but in ROMO, the three scenarios have similar precipitation changes. This project selected a larger number of future scenarios based on changes in both temperature and precipitation, to be consistent with recommended strategies for incorporation of uncertainties into the assessment of impacts and developing adaptation strategies (e.g. Symstad et al, 2017, Fisichelli et al, 2016 a, b, Star et al, 2016, and Rowland et al, 2014, see Section 5-8).

Analysis metrics, including the time frames of the projections differ somewhat between the two studies. The McKelvey study calculated a metric for a historic period (1915-2005 average) and two futures, 30-year averages around "2045" and "2085." This study focused on a 30-year period around mid-century, "2055" to focus on FWS' time horizons for the wolverine and due to time and computational constraints given the project budget. Calculations for a later period using the CMIP5 climate models (e.g. ~2100) and our methods could easily be made, but were beyond the scope of this project.

We provide analysis for two thresholds of snow amount, a "light" snowcover (5 mm of snow water equivalent [SWE]), and significant, or "heavy" snowcover (equivalent to 0.5 m of snow depth). Because the Littell dataset that McKelvey used only includes May 1st snow depth simulation (and not May 15th), McKelvey's study chose a 13 cm snow depth on May 1st as a proxy for snow disappearance by May 15th. We instead chose to use a much lighter threshold for presence/absence of snow on May 15th itself. Our threshold of 13mm SWE was originally chosen to be comparable to McKelvey's snow depth. Our assumptions are discussed further in Sec. 5.6.

For the purposes of determining the presence or absence of snow we use a 5mm SWE threshold. It is common modeling practice to use a low threshold for snow disappearance rather than using a strict criterion of zero, due to peculiarities with the model's numerical accounting for snow (Ben Livneh, pers. comm.) In addition, the effect of small dustings of springtime snowcover on

previously bare ground were also minimized by this choice. The biologists we worked with also were concerned with analyzing the presence of “significant snow” which we defined as ≥ 0.5 m of snow depth. The value of ≥ 0.5 m was arrived at by an analysis of the modeled snow depth at known wolverine denning sites in Glacier National Park (see Section 5, Table 5-2). With the exception of one site that had melted out by May 15th, the other sites all have snowpack between 0.4 and 2.4 m. Note that SWE is a measure of the water content in the snowpack; to estimate depth, we assume a bulk density of the snowpack (see Section 5-5).

An important difference between this study and prior work by Copeland et al. (2010) and McKelvey et al. (2011) is the spatial scale of results. McKelvey and Copeland both presented results on a regular 1/16 degree latitude-longitude grid, in which each cell, or gridbox is ~ 5 -7 km on a side. These cells were assumed to be flat in the model-- that is they do not incorporate slope or aspect information in their surface energy balance. The result of this is north-facing slopes are treated identically to south-facing slopes. Our study uses the Distributed Hydrology Soil Vegetation Model (DHSVM) originally developed by Wigmosta et al. (1994)⁴ for simulating the snowpack at 250m x 250m resolution that incorporates other physical drivers of snowpack (a complete energy balance at the surface, a 2-layer snow model, and a 2-layer vegetation canopy model) and allows analysis of snow at different slopes and aspects (slope directions). The VIC modeling included the option for elevational snow bands within the VIC grid (Jeremy Littell, pers. comm.) but the snow band information was not explicitly used. Therefore, sub-grid scale elevational effects are implicit and approximate in the VIC model whereas it is explicitly modeled at the 250m-scale in DHSVM. A visual comparison of the gridbox sizes is shown in Figure 2-4 for further description of the terminology used to describe spatial resolution, see “resolution” in the Glossary (Section 9). Neither VIC nor DHSVM include the effects of wind or avalanche redistribution of snow (see section 5-10 for additional modeling caveats).

It should be noted there are tradeoffs between our strategies and the methods of Copeland and McKelvey. The finer scale analysis presented in this report integrates slope and aspect with respect to snow accumulation and retention that are thought to be important for maintaining snow refugia for denning sites (see Fig 2 in McKelvey et al 2011), and for elevations where wolverine dens have been observed. The disadvantage of this improvement in spatial resolution is that the high-resolution modeling is computationally intensive. We were only able to analyze two study areas due to these computational constraints and the short time to meet FWS deadlines. The Copeland and McKelvey projects analyzed a much larger domain, including most of the wolverine range in the continental US, but does not provide detailed analysis of any habitat area.

⁴ The most up-to-date documentation of the DHSVM model, including changes to the model subsequent to the original reference, is available from the following website:
<http://www.hydro.washington.edu/Lettenmaier/Models/DHSVM/documentation.shtml>

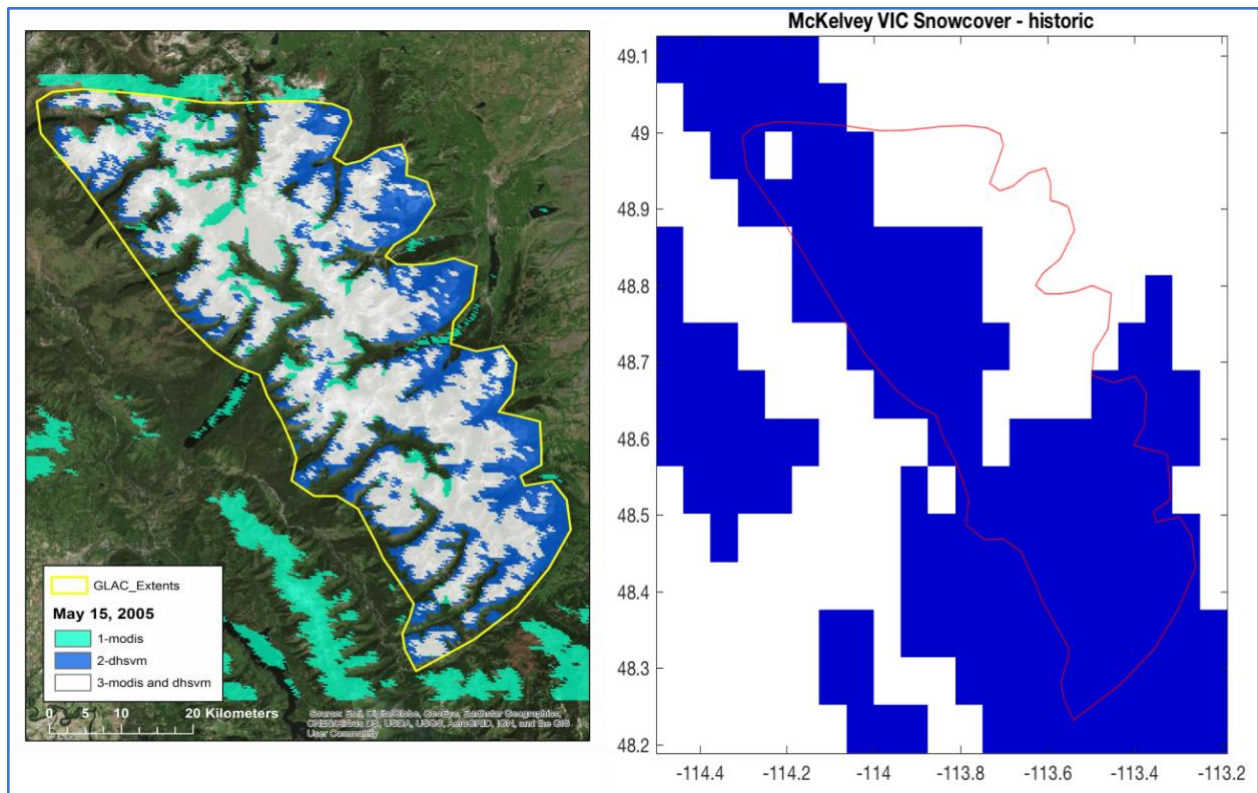


Figure 2-4. Visual comparison of resolution of our study (left) and the McKelvey study. Maps of the GLAC study area illustrate the differences in the resolution of the two studies, ours on the left and McKelvey on the right. Our case studies analyze two high elevation areas on a UTM grid, 250m x250 m, with the area of each gridbox analyzed is 0.0625 km² resolution (left) (0.0625 km²). The McKelvey study used data at 1/16° grid (right). At 48°N latitude, Glacier National Park, these gridboxes are slightly smaller than ~5km by 7 km (~37km²) resolution. Grid boxes at Rocky Mountain National Park (not shown, southern extent at ~40°N), are also ~5km by 7 km. Left image from John Guinotte. See also Table 2-1 for additional description of modeling methods compared to McKelvey.

3 Observed Climate and Variability

Key Points:

- Both study areas show upward trends in both temperature and freezing level
- Surface Air Temperature and Atmospheric freezing level are related, with a stronger relationship in ROMO (that is, a greater change in freezing level for a given surface air temperature change)
- There is year-to-year variability in historic temperature, precipitation, and hence the snowpack, leading to some extreme wet and dry years that were chosen for study:
 - Representative years chosen for GLAC: 2011 (wet), 2005 (dry), 2009 (near normal).
 - Representative years chosen for ROMO: 2011 (wet), 2002 (dry), 2007 (near normal).

3.1 Introduction

This section presents a historical analysis of the winter and spring climate variability for the two study regions, GLAC and ROMO, in order to provide context for future changes. This section includes a discussion of trends in temperature and freezing level; historical year-to-year variability in cool season (October – May) temperature and precipitation for the study areas, choice of representative years during the simulation period for cool/wet, warm/dry, and near normal conditions for the two areas; and a ranking of the representative years in a longer climate record. Later in the report, we will assess what the wet, dry and near normal years of the future may be like. A complete description of regional climate is beyond the scope of this project, but may be found in e.g. McWethy et al (2010), Garfin et al (2014), Lukas et al (2014), Shafer et al (2014), and citations therein.

3.2 Background Material: Trends in Surface Temperature and Freezing Level in the Study Areas

Temperature strongly influences hydrologic processes such as snowpack accumulation, and timing of snowmelt. Here we present some background material on observed trends in surface air temperature and on the freezing level in the atmosphere, and how these two quantities are related.

Both the Glacier and Rocky Mountain areas show a trend of increasing surface air temperature in the winter season (October-May, Figure 3-1), consistent with trends that have been observed west-wide (Garfin et al 2014; Lukas et al 2014; Shafer et al 2014). While winter season temperatures vary inter-annually, linear regression of these data (not shown) indicates about a 1.4 °C increase in temperature from 1948-2015 for an area around Glacier, and about a 1.2 °C increase around Rocky Mountain National Park.

Atmospheric freezing level height (FLH) represents the altitude in the free atmosphere (that is, away from the surface and its immediate influence) where the temperature is 0 °C. Above this level, the temperature of the air is typically below freezing. Freezing in the free atmosphere is indicative of the level above which precipitation falls as snow rather than rain. Freezing level height can have a strong influence on freeze-thaw processes in high-elevation regions (Bradley et al 2009). As with winter season temperatures, freezing level varies over time (Figures 3-2, 3-3), but linear regression (not shown) indicates about a 160m increase in the freezing level for Glacier (Fig 3-2), and about a 170 m increase in the freezing level for Rocky Mountain (Fig 3-3).

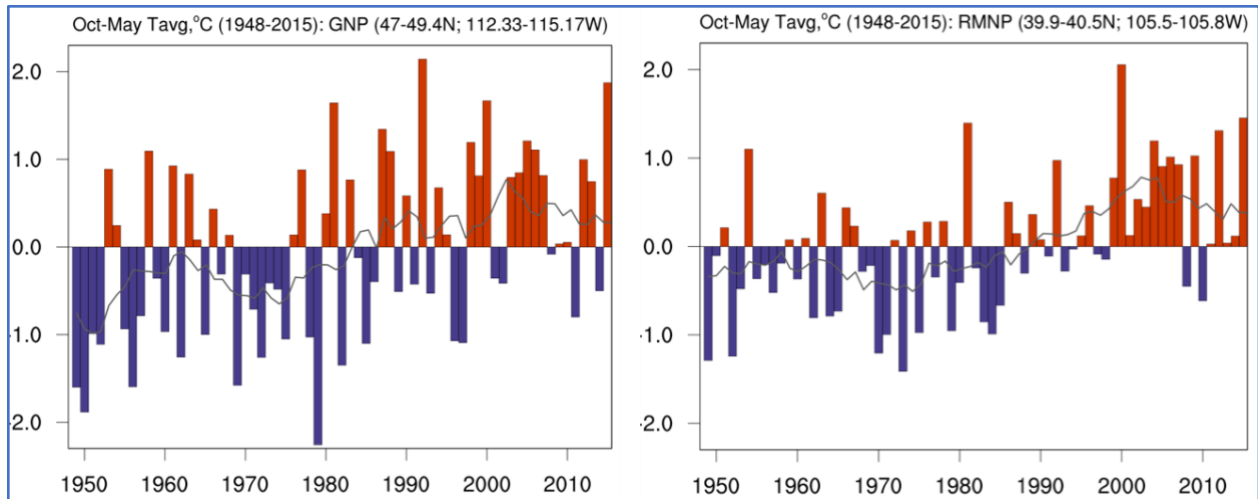


Figure 3-1. Historical trends in cold season (October-May) temperature for the Glacier National Park (GNP, left) and the Rocky Mountain National Park (RMNP, right). The plot shows year to year variability and anomalies in historic average October-May temperature between 1948-2015. Data is from the TopoWx 800m-resolution gridded dataset for a rectangular grid surrounding the GNP (47-49.4N; 112.33-115.17W) and RMNP (39.9-40.5N; 105.5-105.8W). Anomalies are relative to the 1971-2000 period. The grey curve shows a 10-year running mean trend. Linear regression (not shown) indicates about a 1.4 °C increase in temperature in GNP during this period, and about 1.2 °C increase in temperature in RMNP.

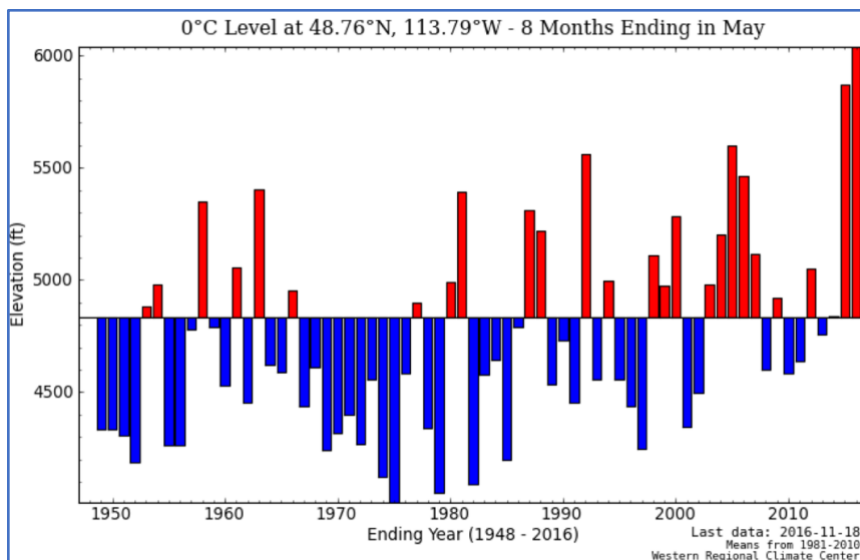


Figure 3-2. Historical trends in cold season (October-May) atmospheric freezing level for the Glacier National Park. Year to year variability in historic freezing level estimates. Data from the NCEP/NCAR Global Reanalysis 2.5° x 2.5° grid data from the North American Freezing Level Tracker, graphic provided in English units (NAFLT, <http://www.wrcc.dri.edu/cwd/products/>). The plot shows average October-May freezing level estimates for a broad atmospheric column in a gridbox centered over GNP (48.76N and 113.79W). Linear regression (not shown) indicates about 530 ft (160 m) increase in the freezing level over the period 1948-2015.

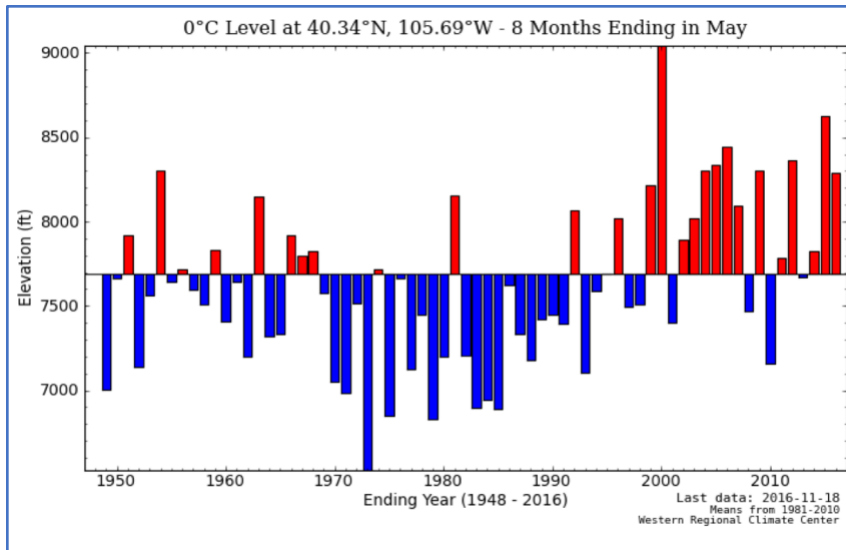


Figure 3-3. Historical trends in cold season (October-May) atmospheric freezing level for the Rocky Mountain National Park. Year to year variability in historic freezing level estimates based on NCEP/NCAR Global Reanalysis $2.5^\circ \times 2.5^\circ$ data from the NAFLT, graphic provided in English units, <http://www.wrcc.dri.edu/cwd/products/>). The plot shows average October-May freezing level estimations for a broad atmospheric column in a gridbox centered over RMNP (40.34N and 105.69W). Linear regression (not shown) indicates ~ 560 ft (170m) increase in the freezing level over the period 1948-2015.

Figure 3-4 illustrates a strong relationship between freezing levels and surface air temperature change for both regions in October-May with explained variance (R^2) close to 0.8. For GLAC (3-1, left), a 1°C anomaly in temperature equates to about a 115 m increase in the freezing level, over the period. For ROMO, for 1°C increase in temperature there has been about a 180 m increase in the freezing level (3-1, right). If these historical relationships hold in the future, the larger change in freezing level for the ROMO study area could indicate a greater sensitivity of snowcovered area to rising temperatures.

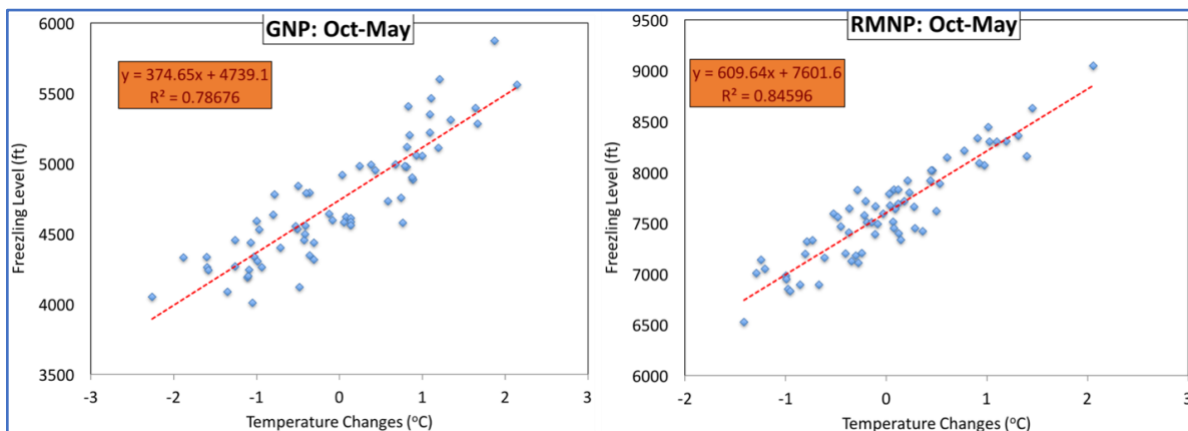


Figure 3-4. Relationship between temperature change and freezing level shifts for areas around Glacier (GNP, left) and Rocky Mountain (RMNP, right) National Parks. Note the difference in the y-axes due to the different Park elevations. There is a strong relationship between historic freezing levels and temperature change for both regions in Oct-May with R^2 close to 0.8. For GNP, there is about a 115 m (375 ft) increase in the freezing level for 1°C increase in temperature, whereas, for RMNP, there has been ~ 600 ft (180 m) increase in the freezing level for 1°C increase in temperature.

3.3 Exploring Year-to-Year Weather Variability through the Choice of Representative Years for Detailed Analysis

One of the primary study goals is to extend the analysis to include the effects of climate change on extreme years both for years with high- and low- spring snowpack. This is in contrast to McKelvey et al (2011) who studied only the effect of climate change on the *long-term average* snowpack. Our historical snowpack analysis (Section 4) was performed for the entire period 2000-2013 and the hydrologic modeling (Section 5) for 1998-2013, and then assessed how these wet, dry, and near normal years might change under several climate change scenarios. To capture the weather variability within these periods we focus some of our analysis in Sections 4 and 5 on a representative wet, dry, and near normal year for each study area. Nonetheless, results from all years were computed.

Table 3-1: Historical Percentiles of precipitation and temperature for the representative dry, near normal, and wet years for GLAC and ROMO study areas.

	Year Type	Year	Oct. - May Precipitation Percentile	Oct. - May Temperature Percentile
GLAC	Dry	2005	6	83
	Near Normal	2009	45	42
	Wet	2011	98	6
ROMO	Dry	2002	4	45
	Near Normal	2007	56	69
	Wet	2011	96	36

To drive our choice of representative years, we investigated historical cold-season (October-May) temperature and precipitation anomalies and MODIS-based snowcovered area for 2000-2013. Years were chosen within that range to represent a cool/wet year with high spring snowpack, a “near normal” year, and a “dry” year with low snowpack. Figure 3-5 shows scatterplots of the anomalous precipitation (as % of average) and temperature (degrees Celsius) for each year of the primary study period (2000-2013) for the two study areas. For both study areas, the 2011 winter stands out as a particularly large (cool/wet) anomaly.

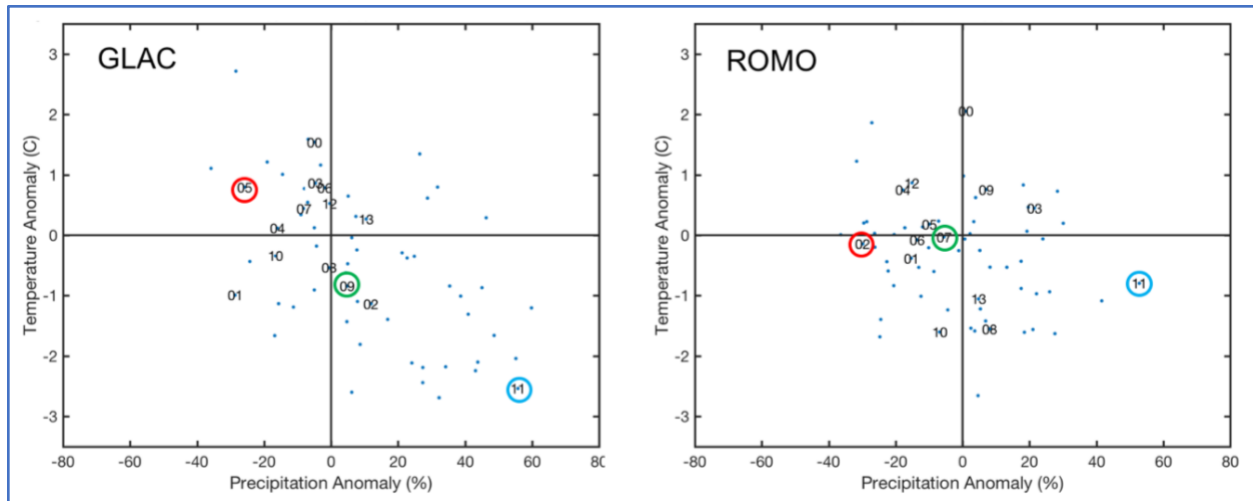


Figure 3-5. Cold Season (October – May) average temperature and precipitation anomalies compared to the 1981-2010 average for the GLAC (left) and ROMO (right) study areas. Relatively warm/dry winters are in the upper left quadrant, cool/wet in the lower right quadrant. Individual years are labeled (00=2000, 01=2001, etc); unlabeled dots represent data from 1951-1999 to illustrate the broader climatological range of year to year variability. Circles around the year show the representative case study years Warm/Dry (red, 2005 in GLAC, 2002 in ROMO), Near Normal (green, 2009 in GLAC, 2007 in ROMO) and Cool/Wet (blue, 2011 in both areas). Data is from the Livneh (2014) dataset. Average is taken over a rectangular area in latitude and longitude surrounding the study areas GLAC (48N-49N, 112W-114.5 W), and ROMO (39N – 41N, 105W-107W). The historical percentiles of precipitation and temperature for the representative dry, near normal, and wet years are provided in Table 3-1 (both areas), and Table 3-2 (GLAC) and Table 3-3 (ROMO.)

The choice a dry year for GLAC points to 2005. Examination of the time series of Snowcovered Area (SCA) derived from the MODIS satellite product (Figure 3-6) corroborates this choice. For ROMO the hot/dry year 2012 with exceptionally low snowcover was first chosen. However, modeling difficulties encountered in the model validation procedure described in section 5.4.2 led to the need to find an alternative “dry” year for ROMO. The scatter plot in Figure 3-5 indicates that 2004 or 2002 might both be good alternatives, and both of these years had adequate modeling success. Because 2002 had lower Spring snowcover (Figure 3-6), and because it was a widely agreed upon drought year in Colorado, we chose to use 2002 as the representative “dry” year for ROMO.

For the choice of near-normal year, 2007 is indicated for ROMO, as that is closest to the center of the scatterplot in Figure 3-5. A number of choices would seem plausible for GLAC, however as no one year stands out as “most normal.” To further guide our choices of representative years, we looked at the elevation profiles of SCA for the various years, and 2009 was chosen. We show the SCA as a function of elevation within the study areas (Figure 3-6cd) for the representative years. These plots indicate that the elevation profile of observed snowcover in our chosen near-normal years closely follow the median profile for 2000-2013.

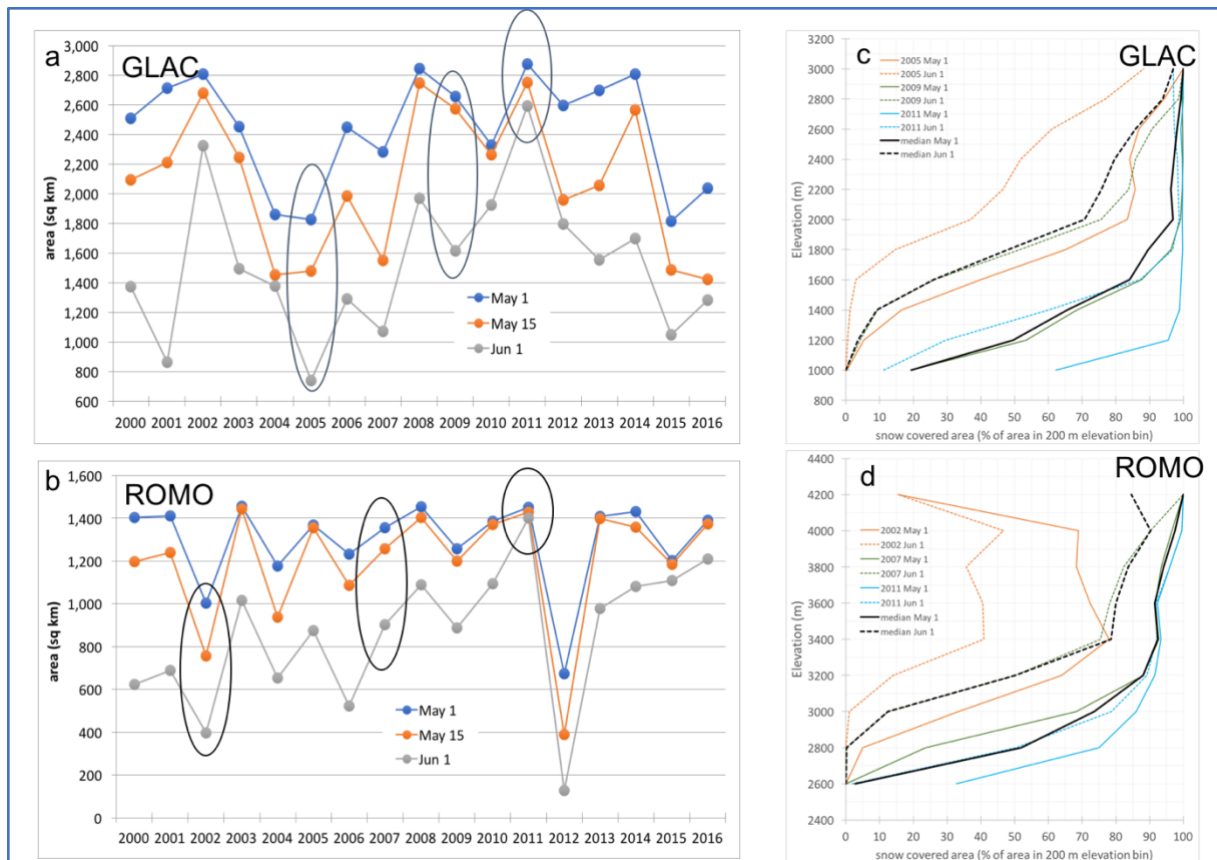


Figure 3-6. Snow covered area year to year variability (left) and elevation profiles (right). Left panels show SCA from MODIS by year for May 1 (blue), May 15 (red), and June 1 (gray), for GLAC (a) and ROMO (b). Dry, near normal, and wet representative years are circled for each study area. Right panels (c, GLAC) and (d, ROMO) show SCA as a function of elevation for May 1 and June 1. Note that the “near normal” study years (green lines) are close to the median profile (black lines).

3.4 The Study Period in the Longer Climate Record

Because the study period is 14 years long, the question arises as to how “extreme” the wet and dry years are in the longer climatological record. To address this question, we analyzed how often the temperature and precipitation anomalies for the study years are likely to occur in the longer (1950-2013) climatological record by computing their percentiles. Percentiles were calculated by ranking the data and using the following formula: $\text{percentile} = (\text{rank} - 0.5) / (\text{total number of years})$. Note that the exact rankings and percentiles may differ based on the underlying dataset and interpolation methods used, as the study areas have relatively few observing stations. However, percentiles calculated from the PRISM dataset (not shown) yield qualitatively similar results to those found below.

The percentiles of October – May precipitation and temperature averaged over the study areas are shown for the representative wet, near normal and dry in Table 3-1 for both study areas. The percentiles are calculated based on the 63 total years in the 1951-2013 period of the Livneh (2014) dataset. For GLAC, October – May 2011 was at the 98th percentile of precipitation and

the 6th percentile of temperature, while 2005 was at the 6th percentile of precipitation and 83rd percentile of temperature. For ROMO, 2011 was in the 96th percentile of October – May precipitation, but only the 36th percentile of temperature, and while anomalously cold was not extreme in temperature. 2002 was in the 4th percentile of precipitation, but only near the median in temperature.

For further reference, Tables 3-2 (GLAC) and 3-3 (ROMO) show the percentiles of precipitation and temperature for the entire study period, 2000-2013, as well as the percentiles for the April – June melt season. Even though the low precipitation was more extreme in 2002 than in 2012, the temperature was not. This is reflected in the MODIS spring snowcover (Figure 3-6), where 2002 was low, but not as nearly extreme as in 2012.

Table 3-2: Percentile of temperature and precipitation anomalies for GLAC study area based on the 1951-2013 period. Percentiles are shown for both the October – May cold season and for the April – June melt season.

GLAC	Percentile 1951-2013			
	Oct. - May Precipitation	Oct. - May Temperature	Apr. - June Precipitation	Apr. - June Temperature
2000	31	96	7	66
2001	2	37	47	58
2002	61	31	91	12
2003	33	87	13	69
2004	13	63	33	61
2005	6	83	80	47
2006	37	82	53	93
2007	21	72	6	75
2008	39	47	60	17
2009	45	42	12	34
2010	12	55	85	13
2011	98	6	87	4
2012	40	74	72	53
2013	60	66	56	29

Table 3-3: Percentile of temperature and precipitation anomalies for ROMO study area based on the 1951-2013 period. Percentiles are shown for both the October – May cold season and for the April – June melt season.

ROMO	Percentile 1951-2013			
	Oct. - May Precipitation	Oct. - May Temperature	Apr. - June Precipitation	Apr. - June Temperature
2000	45	98	40	98
2001	29	33	23	91
2002	4	45	2	96
2003	75	80	77	64
2004	21	91	75	77
2005	50	82	82	53
2006	28	74	4	94
2007	56	69	6	75
2008	80	12	45	13
2009	77	93	88	44
2010	48	13	87	37
2011	96	36	93	25
2012	10	94	7	99
2013	64	26	79	42

4 MODIS Observed Historic Snowpack Variability Analysis

Key points

- In GLAC, snowcovered area varies considerably by year, including “wet” years such as 2011 with very persistent snow, years with strong melt in early May, such as 2012, or in late May (2009, 2001), and “dry” years (2004, 2005; Section 4.3).
- Even in dry years, NE-facing slopes in GLAC tend to hold more snow and melt later in the season. There is > 80% snowcover above ~2000 m elevation on May 1 during dry years, and > 95% snowcover above ~1200 m during wet years (Figure 4-6).
- In ROMO, snowcovered area also varies considerably by year (Section 4-4).
- NW-facing slopes in ROMO tend to hold more snow even during dry years. In very dry years, snowcover peaks at intermediate elevations, suggesting that the high-altitude snowpack may be particularly vulnerable in this region under warm/dry conditions (Fig 4-13).

4.1 Introduction

In this section, we perform an analysis of the variability of snowcover in the historical period 2000-2016 using gridded snowcover data acquired by the Moderate Resolution Imaging Spectroradiometer (MODIS) on board the Terra satellite. The dataset and methodology of analysis is first described. The analysis for the GLAC and ROMO study areas are then presented in separate sections, repeating descriptions to make the material self-contained for the reader who may read about only one area. Each section consists of analysis of the following: a) total snowcovered area (SCA), b) SCA fractional area as a function of eight compass directions of slope aspect (octants), and c) elevation dependence.

4.2 Dataset and Methods

4.2.1 Data sub-setting and re-projection

We downloaded selected MODIS/Terra daily snowcover data on a 500m grid from the recently released version 6 (MOD10A1.006) (Hall and Riggs, 2016). All data from geographic tiles h09v04 (ROMO) and h10v04 (GLAC) were downloaded for days between March 1 and July 1 for all years from 2000 to 2016.⁵

The MODIS data are available in daily files, one for each tile, and georeferenced to an equal-area sinusoidal projection. Each tile covers 10° x 10° at the equator or approximately 1200 km by 1200 km, with a nominal pixel resolution of 500 m (actual resolution 463.313 m). To bring the data to the same grid as used in the hydrologic modeling necessitated re-projection of the data

⁵ Note that MODIS data was obtained for April, but FWS’ interest in April arose after completion of this part of the project, so June 1st but not April dates are shown in the graphics for this section.

onto a Universal Transverse Mercator Grid. We used the MODIS Reprojection Tool (https://lpdaac.usgs.gov/tools/modis_reprojection_tool) to subset the daily tiles to the areas of interest and re-project the subsetted areas to UTM grids with a pixel resolution of 250 m using nearest-neighbor resampling. The ROMO study area perimeter falls at the corner of tile h09v04, and extends slightly beyond the tile boundaries at its southern tip. We excluded this extension of the study from our analysis. Parameters for the MODIS data reprojection are provided in Table S4-1.

4.2.2 Converting Normalized Difference Snow Index to Binary (yes/no) Snowcover

To better align our analysis with that in Copeland and McKelvey's work we wanted to use a daily binary (yes/no) snowcover value. However, one main obstacle had to be overcome -- snowcover was characterized differently in the versions of the MODIS data that Copeland used and in the current version. The prior work by McKelvey and Copeland both used Collection 4 of the MODIS data which provided them with a binary snowcover classification for each pixel on each day (clouds permitting). Collection 4 data are only available for the years 2000-2007, necessitating the use of the more recent MODIS Collection 6 products for the present study. However, Collection 6 does not include a binary daily snowcover product. Instead, snowcover is identified using the Normalized Difference Snow Index (NDSI).

NDSI is reported as a ratio, with values ranging from 0.00 to 1.00 (scaled and reported as 0 to 100 in the data files). The NASA guidance on conversion was not definitive: "If a user wants to make a binary SCA [Snowcovered Area] from the C6 [Collection 6] product they can set their own NDSI threshold for snow using the NDSI_Snow_Cover or the NDSI data or a combination of those data." (NASA, 2016). In lieu of a prescription, we chose to follow the procedure used by NASA to produce the 8-day composite snowcover product; we applied a threshold of $NDSI > 0.1$ to the daily MODIS NDSI values to indicate the presence of snow in a pixel on a given day.

4.2.3 Snow disappearance date and snowcover on a given date

As in Copeland et al (2010), we calculate a snow disappearance date for each year at each pixel. We define the Snow Disappearance Date (SDD) as the first day after March 1 in which $NDSI/100$ was less or equal to 0.1 (Cite NASA). The SDD is denoted by the Day of Year value, in which January 1 is 1, February 1 is 32, March 1 is 60 (or 61 in leap years), etc. Once SDD was defined at each grid point for each year (resulting in 17 annual maps of SDD for the period of record), we were able to derive snowcover maps for any given date. For example, snowcover on May 1 was inferred by marking grid points as "snow-covered" if their SDD was equal or greater than 121 (or 122 for leap years). We repeated the process to infer snowcover maps for May 15 and June 1. This indirect method to infer snowcover allowed us to circumvent the reality of several missing data points due to cloud cover, and offered a conservative estimate of snow disappearance.

4.2.4 Snowcover by elevation and aspect

A 250-m digital elevation model (DEM) was created using bilinear interpolation from the National Elevation Dataset (NED) 10-m DEM products (USGS, 2009). Using this we obtained grids for elevation and aspect octants in both study regions. We reclassified the elevation values

into 200 m bins. The elevation bins range from 1000 to 3000 m in GLAC and 2600 to 4200 m in ROMO. Both the slope magnitude and the aspect of the slope (that is the compass direction that the slope faces) were analyzed using functionality in the open source Quantum GIS software. We reclassified the aspect grids into eight 45°-wide directional bins (hereafter, octants) centered on the points of the compass. In both types of analyses (elevation and aspect), we computed snowcovered area (SCA) on May 1st, May 15th, and June 1st, in terms of the total area in square kilometers and also in terms of the percentage of snowcovered area in several elevation bands and aspect octants.

4.3 MODIS analysis for GLAC

This section presents some summary statistics of snowcover, including total snowcovered area, and number of years during the period of study with snowcover on a given date. MODIS snowcover data was analyzed for March 1 – July 1 for all years 2000-2016. For more in-depth analysis including aspect and elevation-based analyses the report focuses on the years representative of year-to-year variability defined in Section 3: 2011 (“wet”), 2009 (“near normal”), and 2005 (“dry”).

4.3.1 Total Snowcovered Area

Total snowcovered area was the primary metric that was analyzed in McKelvey et al (2011) and provides an overall summary of availability of snow. Figure 4-1 presents maps of May 15 snowcover for the GLAC study area and vicinity from MODIS. These maps clearly depict the regional character of the year-to-year variations in snowcover. Figure 4-2 shows the total snowcovered area within the study area polygon, which is depicted in red on the previous figure. The year-to-year variations are shown for snowcover on three different dates during the melt season. The behavior in individual year varies considerably, including “wet” years such as 2011 with very persistent snow, years with strong melt in early May, such as 2012, or in late May (2009, 2001), and “dry” years (2004, 2005). It is worth noting that 2015 and 2016, the last two years of the MODIS record, show low snowcover, although the modeling study period ends in 2013 because the Livneh dataset ends in that year (Section 5). Both these years had near-normal precipitation, but had anomalously warm temperatures. These years would be good candidates for future analysis.

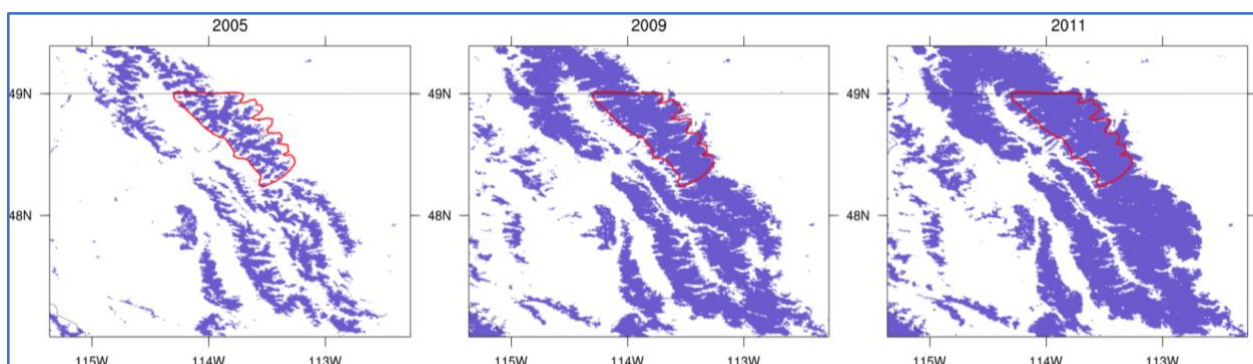


Figure 4-1. May 15 observed snow cover from MODIS for the GLAC study area (red outline) and vicinity. Maps of snowcover for a “dry” year (2005, left), “near normal year” (2009, middle), and “wet” year (2011, right). Snow cover is defined as NDSI > 0.1, and includes pixels with fractional snow cover (see text in 4.2.2 and 5.4.2. discussion).

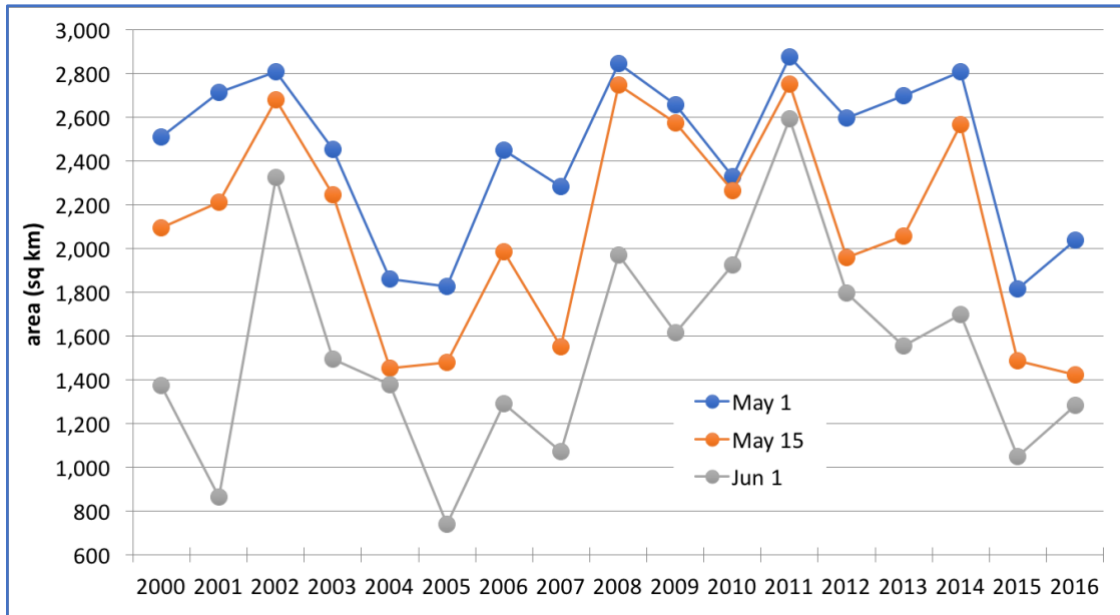


Figure 4-2. Year to year variability in total snow covered area (km²) on May 1 (blue), May 15 (red), and June 1 (gray) by year within the GLAC study area polygon. Snow cover is defined as NDSI > 0.1, and includes pixels with fractional snow cover (see text in 4.2.2 and 5.4.2. discussion). Data from MODIS.

To summarize all 17 years of the record, Figure 4-3 presents maps of the number of years with snowcover on April 1, April 15, May 1, May 15. These are similar to the analysis done by the Copeland and McKelvey studies. The primary difference is in the use of the newer MODIS products and the extension of the analysis from seven to seventeen years.

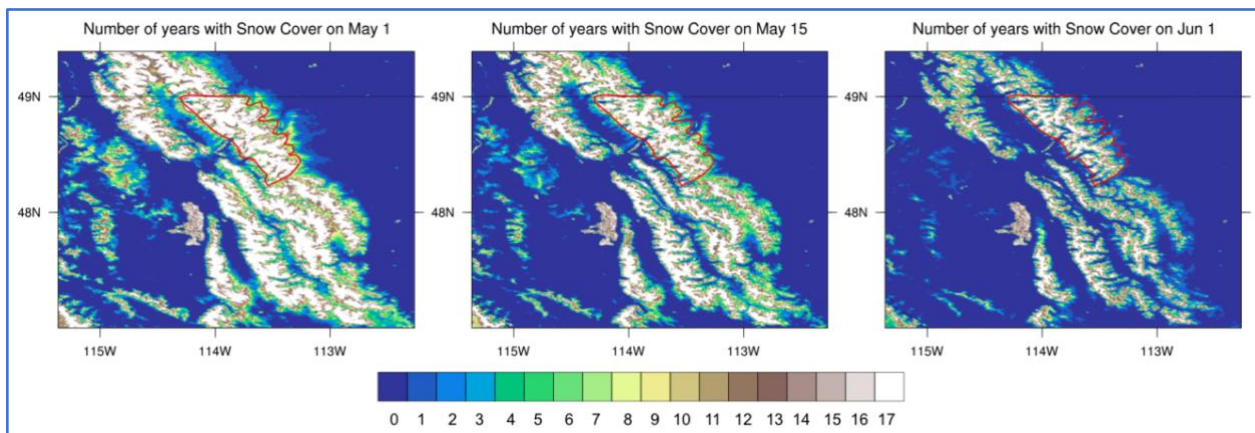


Figure 4-3. Number of Years out of 2000-2016 period with snow cover on May 1 (left), May 15 (middle), and June 1 (right) for the GLAC study area (red outline) and vicinity. Maps showing number of years out of 17 total for which snow cover is NDSI > 0.1, and includes pixels with fractional snow cover (see text in 4.2.2 and 5.4.2. discussion). Data from MODIS.

Figure 4-4 quantifies the maps in Figure 4-3, showing the area within the GLAC study area polygon with different numbers of years of snowcover. The three colored bars designate different days of the year. Because the study areas were chosen to be in the vicinity of tree line, it is no surprise that in the present climate there are large areas that see snow every year on May 1st.

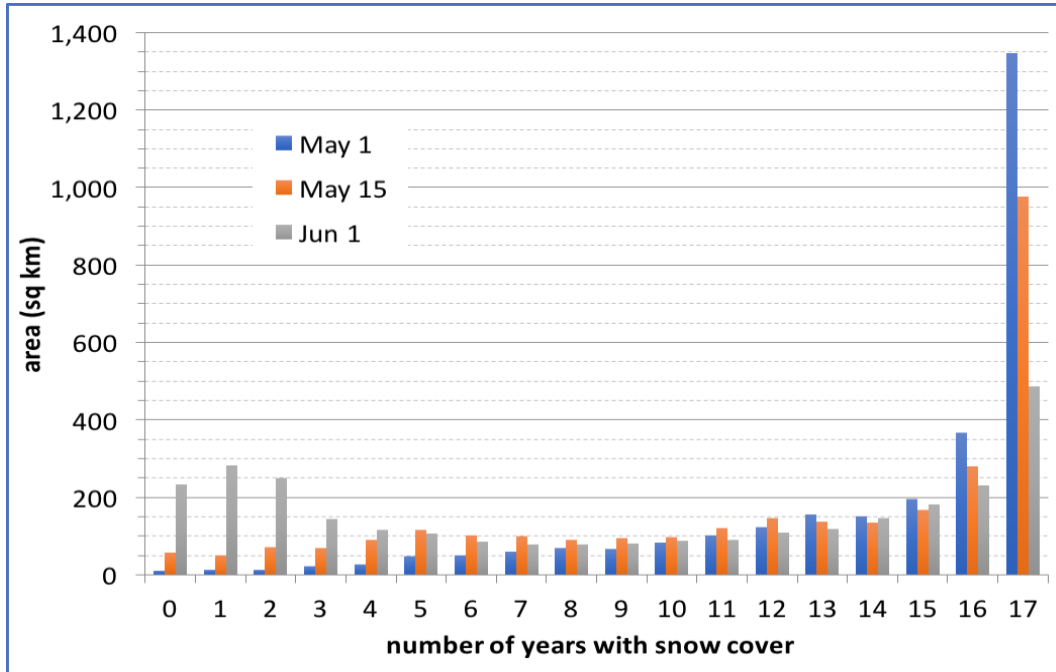


Figure 4-4. Snow covered area by number of years. Colored bars show the area within the GLAC study area polygon classified according to the number of years with snow cover NDSI > 0.1 (out of 17 total years) on May 1 (blue), May 15 (orange), and June 1 (grey). These bar plots quantify the maps in Figure 4-3, showing the area within the GLAC study area polygon with different numbers of years of snowcover. Snow cover data from MODIS.

4.3.2 Aspect Dependence of Snowpack: Fractional area

One of the primary goals of this study is to investigate topographic factors that influence the persistence of snow during the melt season. One such factor is the “slope aspect” or simply “aspect” – the compass direction that the slope faces. The total land area within each aspect octant varies due to the orientation of ridges and valleys in the study area. As a result, the analysis of total snowcovered area is dominated by the topography itself. These graphics are provided in the Supplementary Material.

To focus on the *relative* importance of the snow processes related to aspect, we calculated the fraction of the total land area within each octant that is snowcovered for each of the 17 years in the historical record (Figure 4-5), while in Figure 4-6 we focus on the representative wet and dry years. The asymmetric shape in Figure 4-5 clearly shows that in GLAC, the NE directions ranging from E to N have much larger fractional area covered by snow. Even in dry years, over 60 % of the NE facing slopes are snow-covered on May 15th (Figure 4-6).

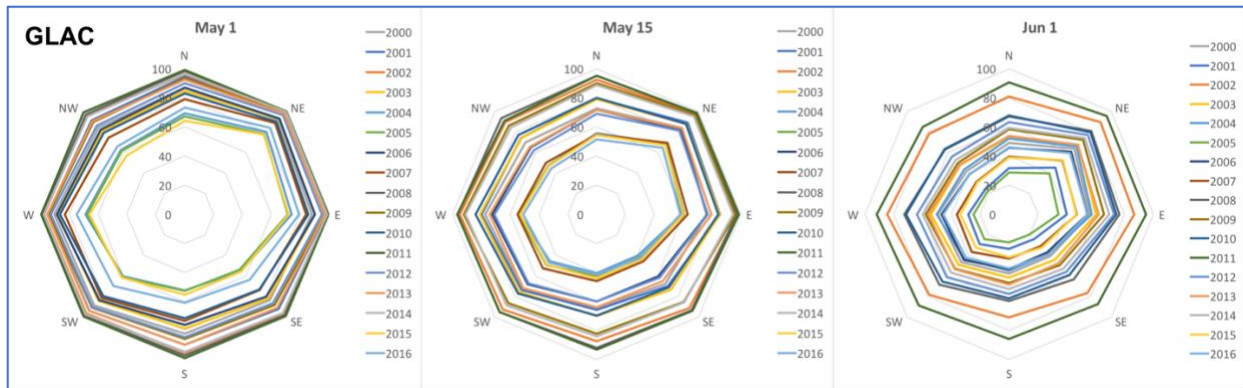


Figure 4-5. Snow covered area fraction (%) as a function of aspect for May 1, May 15, and June 1 for the GLAC study area. Eight-sided plots (octants, see glossary) show a separate colored line for each year, 2000-2016. Each of the eight apexes of the octant represents a direction of the compass. For example, the top apex represents north-facing slopes (N), the bottom apex represents south-facing slopes (S). Concentric octagons (gray) denote the magnitude scale ranging from 0% at the center to 100% for the outer octagon. The total snow covered area has been expressed as a percentage of the total land area in each aspect bin and includes pixels with fractional snow cover (see text in 4.2.2 and 5.4.2. discussion). Aspect of the slope is determined from a digital elevation model and is binned into eight octants according to the compass direction. For a different visualization of topographical aspect dependence, see Barsugli et al. (2020).

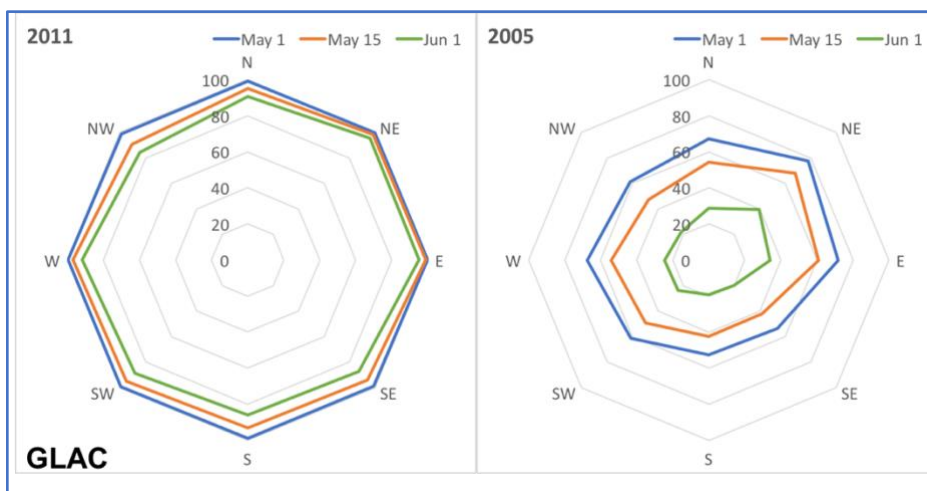


Figure 4-6. Observed snow covered area fraction (SCA %) as a function of aspect for representative wet (2011, left) and dry (2005, right) years in the GLAC study area. As in the previous figure, eight-sided plots (octants) show snow covered area fraction for May 1 (blue), May 15 (red), and June 1 (green) each year. The total SCA is expressed as a percentage of the total land area in each aspect octant, and includes pixels with fractional snow cover. Concentric octagons (gray) denote the magnitude scale ranging from 0 to 100%.

4.3.3 Elevation Dependence

Figure 4-7 shows the elevation dependence of MODIS snowcover for the wet, near-normal and dry years, with the median of all years as reference. The results are shown as a percentage of the total area within each 200-meter elevation band within the study area boundaries.

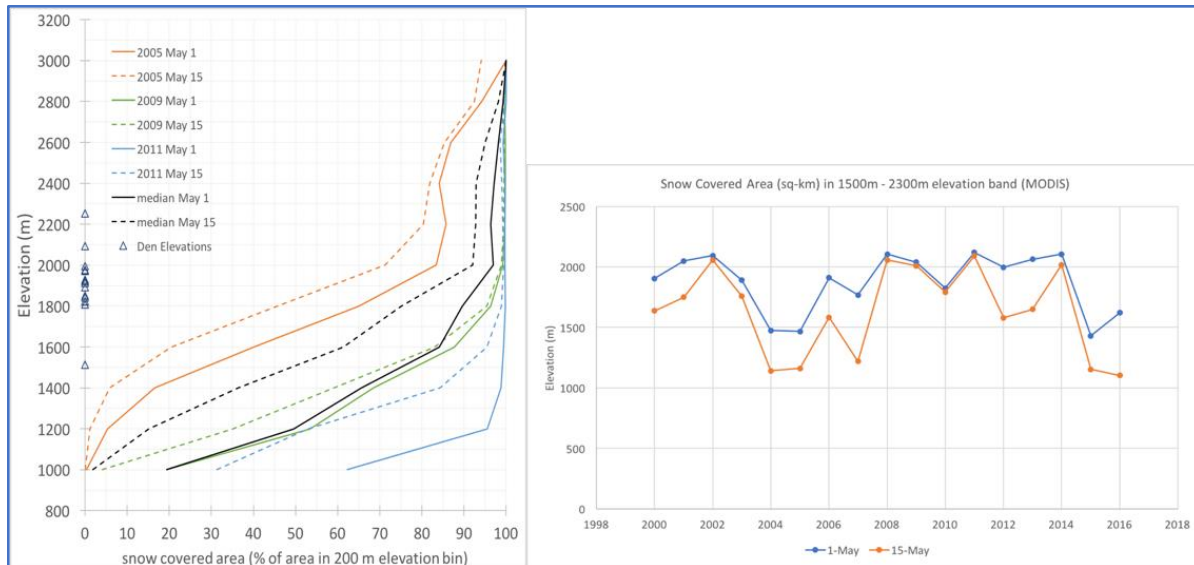


Figure 4-7. Analysis of observed Snow Cover versus elevation and wolverine dens in the GLAC study area. This figure shows the elevation dependence of MODIS snowcover for the wet, near-normal and dry years, with the median of all years as reference. Left Panel: Snow covered area (SCA) fraction (x-axis, 0-100%) as a function of elevation bands for representative wet (2011; blue lines), near normal (2009; green lines), and dry years (2005; red lines). Data from MODIS pixels were classified into 200-meter elevation bands. Snow covered area is shown as the percentage of area within each elevation band with snow cover on May 1 and May 15. Thick black lines show the median snow cover fraction for the given dates for 2000-2017. Triangles denote the elevations of wolverine dens in or near the study area, ranging from 1500- 2250 m. The right panel is similar to Fig 4.2, but analyzed for this 1500-2250 m elevation band that encompasses den elevations, showing year to year variability in historical total SCA (km²) on May 1 (blue), May 15 (red) from MODIS within the GLAC study area polygon. In both panels, snow cover is defined as NDSI > 0.1, and includes pixels with fractional snow cover. For known wolverine denning sites in Glacier National Park, see Section 5, Table 5-2.

4.4 MODIS analysis for ROMO

MODIS snowcover data was analyzed for March 1 – July 1 for the years 2000-2016. Data for all years was analyzed. We present here some summary statistics of snowcover, including total snowcovered area, and number of years during the period of study with snowcover on a given date. For more in-depth analysis including aspect and elevation-based analyses the report focuses on the representative years defined in Section 3: 2011 (“wet”), 2007 (“near normal”), and 2012 (“dry”).

4.4.1 Total Snowcovered Area

Total snowcovered area was the primary metric that was analyzed in McKelvey et al (2011) and provides an overall summary of availability of snow. Figure 4-8 presents maps of May 15 snowcover for the ROMO study area and vicinity from MODIS. These maps clearly depict the regional character of the year-to-year variations in snowcover. Figure 4-9 shows the total snowcovered area within the study area polygon, which is depicted in red on the previous figure. The year-to-year variations are shown for snowcover on three different dates during the melt season. The behavior in individual year varies considerably, including “wet” years such as 2011 with very persistent snow, years with strong melt in early May, such as 2004, or in late May (2001, 2013), and “dry” years (2012).

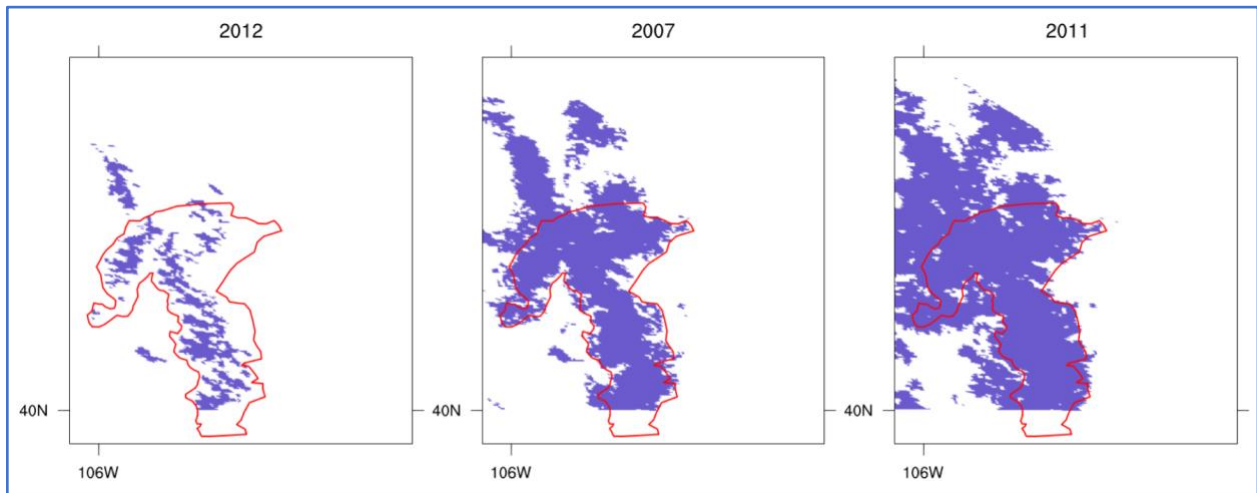


Figure 4-8. Maps of May 15 observed snowcover from MODIS for the ROMO study area (red outline) and vicinity. Representative Dry (2012, left), Near Normal year (2007, right), and Wet years (right, 2011). Snow cover is defined as NDSI > 0.1, and includes pixels with fractional snow cover (see text in 4.2.2 and 5.4.2. discussion). The data were taken from a single MODIS tile which does not include the southernmost tip of the study area.

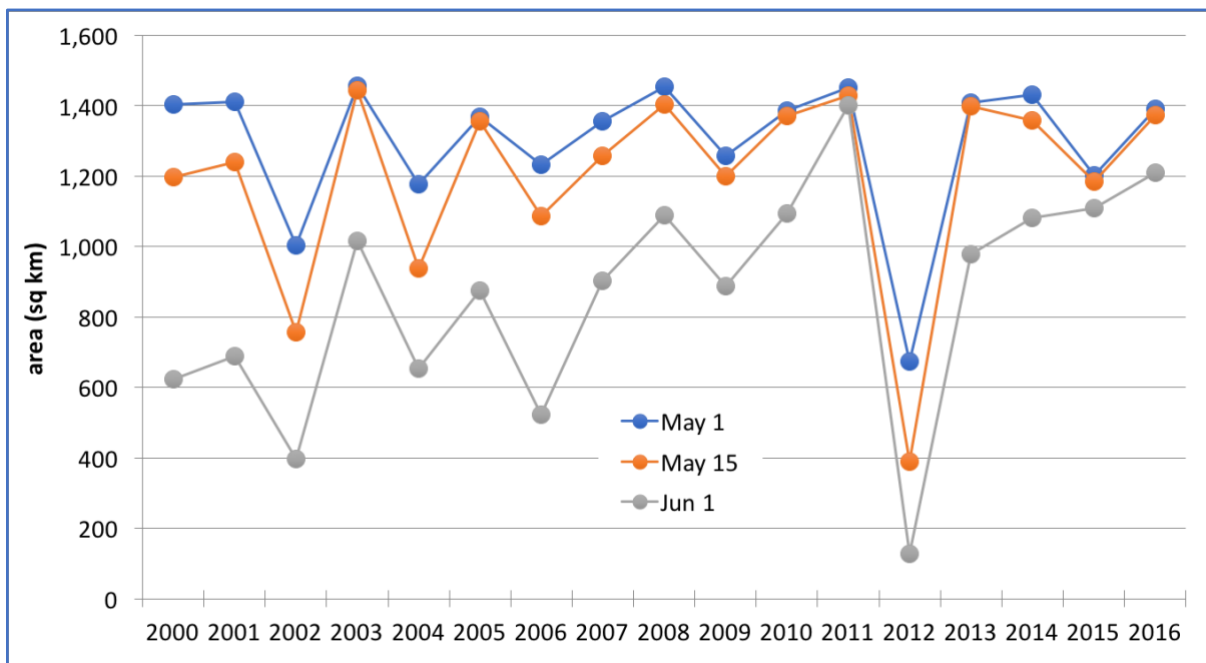


Figure 4-9. Year to year variability in total snow covered area (km^2) on May 1 (blue), May 15 (red) within the ROMO study area polygon. Snow cover is defined as NDSI > 0.1, and includes pixels with fractional snow cover. Data from MODIS.

To summarize all 17 years of the record, Figure 4-10 presents maps of the number of years with snowcover on May 1, May 15. These are similar to the analysis done by Copeland and McKelvey studies. The primary difference is in the use of the newer MODIS products and the extension of the analysis from seven to seventeen years.

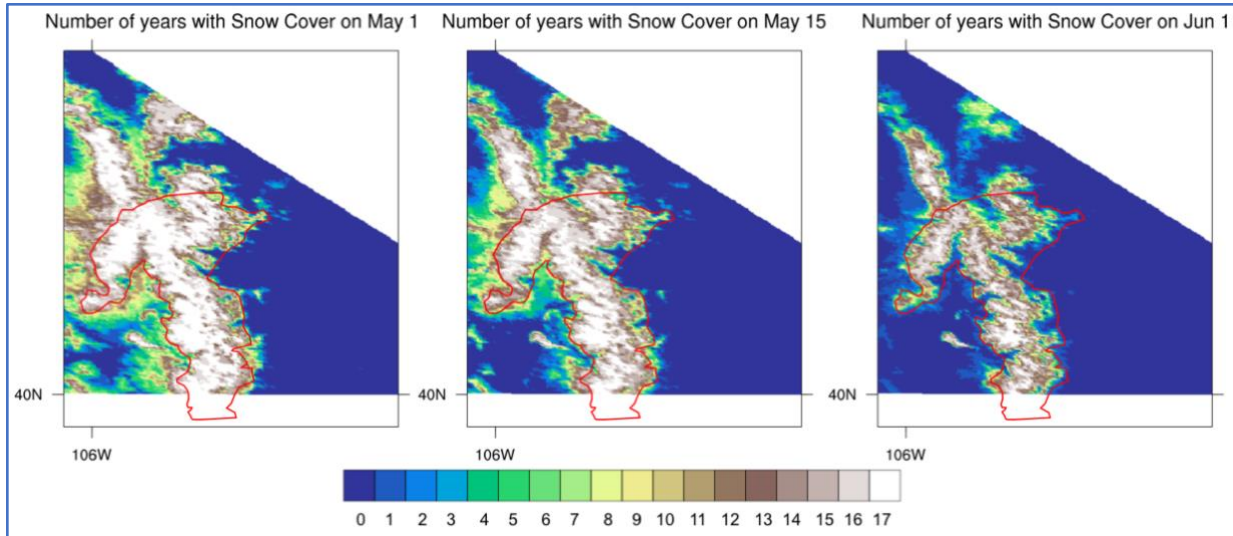


Figure 4-10. Number of Years 2000-2016 period with snow cover on May 1 (left), May 15 (middle), and June 1 (right) for the ROMO study area (red outline) and vicinity. Maps showing number of years out of 17 total for which snow cover is NDSI > 0.1, and includes pixels with fractional snow cover (see text in 4.2.2 and 5.4.2. for discussion). The data were taken from a single MODIS tile which does not include the southernmost tip of the ROMO study area. Data from MODIS.

Figure 4-11 quantifies the maps shown in Figure 4-10, showing the area within the GLAC study area polygon with different numbers of years of snowcover. The three colored bars designate different days of the year. Because the study areas were chosen to be in the vicinity of tree line, it is no surprise that in the present climate there are large areas that see snow every year on May 1.

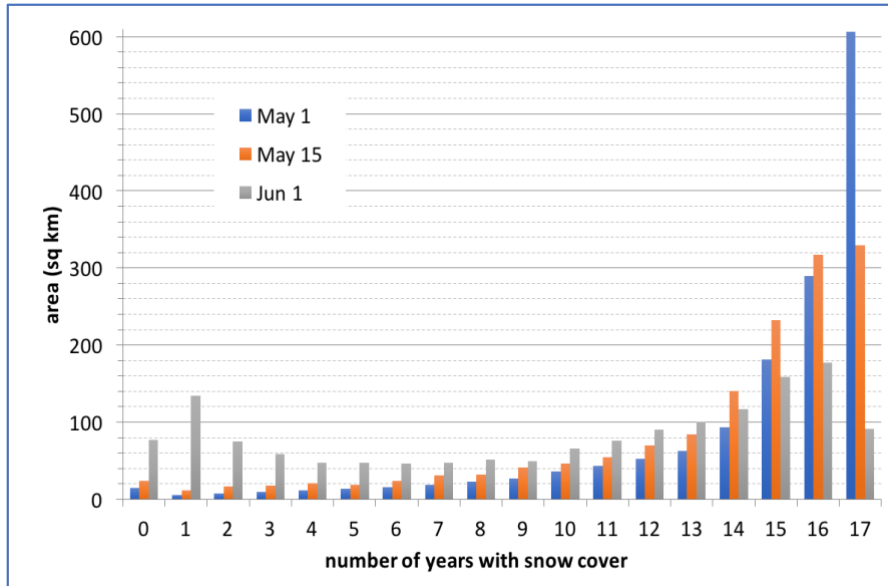


Figure 4-11. Snow covered area by number of years. Colored bars show the area within the ROMO study area polygon classified according to the number of years with snow cover NDSI > 0.1 (out of 17 total, 2000-2016) on May 1 (blue), May 15 (orange), and June 1 (grey). These bar plots quantify the maps in Figure 4-10, showing the area within the GLAC study area polygon with different numbers of years of snowcover. Snow cover data from MODIS.

4.4.2 Slope Aspect Dependence of Snowpack: Fractional Area

One of the primary goals of this study is to investigate topographic factors that influence the persistence of snow during the melt season. One such factor is the “slope aspect” or simply “aspect” – the compass direction that the slope faces. The total land area within each aspect octant varies due to the orientation of ridges and valleys in the study area. As a result, the analysis of total snowcovered area is dominated by the topography itself. These graphics are provided in the Supplementary Material.

The total land area within each aspect octant varies due to the orientation of ridges and valleys in the study area. As a result, the analysis of total snowcovered area is dominated by the topography itself. To focus on the *relative* importance of the snow processes related to aspect, Figure 4-12 presents an analysis of the fraction of the total land area within each directional “bin” that is snowcovered. The asymmetric shape shows that the NW-facing slopes have larger fractional area covered by snow. With the exception of 2012, even in dry years over 60 % of the NW facing slopes are snow-covered on May 15th. Figure 4-13 indicates that for the dry year 2012, snowcover was retained preferentially on NW-facing slopes.

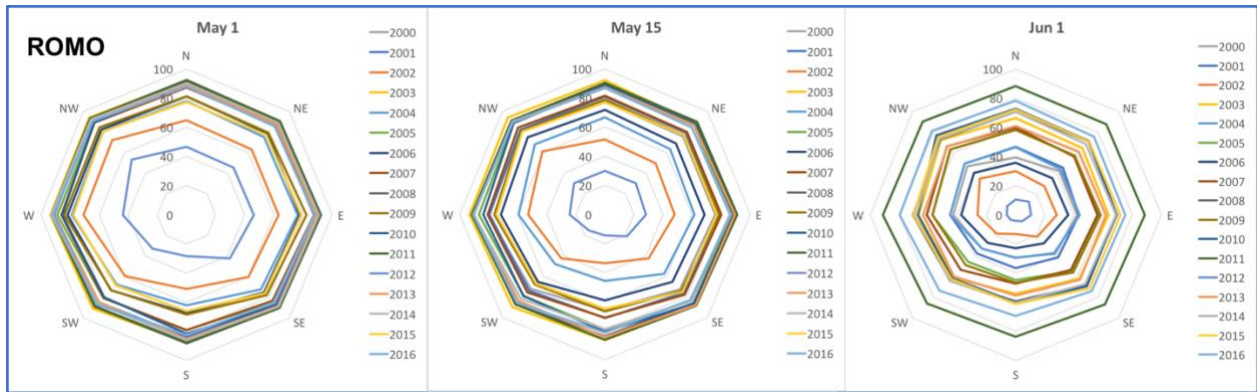


Figure 4-12. Snow covered area fraction (%) as a function of aspect for May 1, May 15, and June 1 for the ROMO study area. Eight-sided plots (octants) show a separate colored line for each year, 2000-2016. Each of the eight apexes of the octant represents a direction of the compass. For example, the top apex represents north-facing slopes (N), the bottom apex represents south-facing slopes (S). The total snow covered area has been expressed as a percentage of the total land area in each aspect bin. Aspect of the slope is determined from a digital elevation model and is binned into eight octants according to the compass direction. Concentric octagons (gray) denote the magnitude scale ranging from 0% at the center to 100% for the outer octagon. For a different visualization of topographical aspect dependence, see Barsugli et al. (2020).

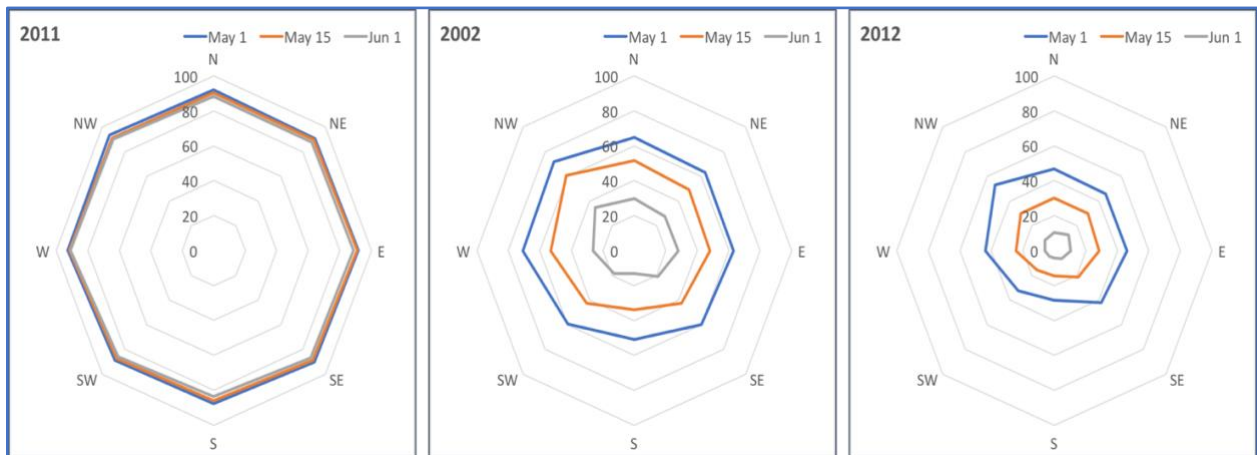


Figure 4-13. Observed snow covered area fraction (%) as a function of aspect for 2011 (“wet”) 2002 (near normal) and 2012 (“dry”) representative years in the ROMO study area. May 1 (blue), May 15 (red), and June 1 (green) are shown for each year. The total snow covered area has been normalized by the total land area in each aspect octant. Concentric octagons (gray) denote the magnitude scale ranging from 0 to 100%. Note that while 2012 had the least snow cover in late Spring, 2002 was adopted as a representative dry year due to modeling considerations discussed in in Section 5. We show both dry years here which exhibit similar dependence of fractional snow cover on aspect.

4.4.3 Elevation Dependence

Figure 4-14 shows the elevation dependence of MODIS snowcover for the wet, near-normal and dry years, with the median of all years as reference. The results are shown as a percentage of the total elevation within each 200-meter elevation band within the study area boundaries. The ROMO area shows that the dry year, 2002 (as well as the other very dry year during the period, 2012), was significantly different from the other two, with a fractional area declining with altitude above 3400m. This may indicate that the meteorology in this region interacts differently with the topography in extremely dry years than in wetter years. The high-altitude snowpack may be particularly vulnerable in this region if conditions like those in 2002 recur.

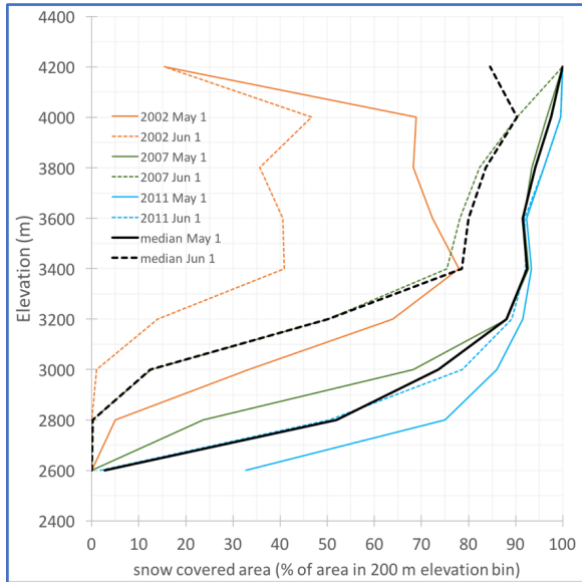


Figure 4-14. Snow covered area fraction as a function of elevation for the ROMO study area for representative wet (2011; blue lines), near normal (2007; green lines), and dry years (2002; red lines). MODIS pixels were classified into 200-meter elevation bands. Snow covered area is shown as the percentage of area (or fraction) within each elevation band with snow cover on May 1 and June 1. The median snow cover fraction for the given dates for the period 2000-2017 is shown in thick black lines. 2002 only is shown because it was ultimately used as a representative year in the scenarios analysis, not 2012. Note that 2012 also shows a decrease in snow covered area at the highest elevations. No dens have been documented in ROMO, however the elevation band for denning is estimated by FWS to be 2700-3600m (see Section 5).

5 Future Snowpack Projections: DHSVM Modeling

Key Points - Methods

- In order to simulate snowcover under future climate conditions, we use a high-resolution snow/hydrology model with inputs derived from historical observations and global climate model projections.
- The Distributed Hydrology Soil Vegetation (DHSVM) model was run for the historic period 1998-2013 and validated against available SNOTEL observing stations.⁶ The spatial patterns of snow were validated against MODIS satellite remotely sensed snowcover.
- Five scenarios of the future – for a thirty-year period, 2041-2070, centered on 2055 -- were selected from CMIP5 global climate model (GCM) projections based on a moderate (RCP 4.5) and high (RCP 8.5) emissions scenarios. These were chosen to represent a large fraction of the range of the CMIP5 ensemble projections in each study area in terms of precipitation and temperature changes. The scenarios differ somewhat between the two study areas to better represent the range of climate projections in each area.
- The selected GCM projections were downscaled using the “delta method” which applies change factors from the climate models to the historic temperature and precipitation that are used as inputs to the DHSVM model.
- Analysis is presented for light snowcover (Snow Water Equivalent > 5 mm) on May 15th for comparison with May 15th MODIS snowcover (as was used by McKelvey).
- To capture and assess year to year variability, Wet, Near Normal, and Dry representative case study years are shown for the historical simulations and how each of these years plays out under these five future scenarios.

Key Points – GLAC study area

- Projections for April 15th, May 1st, and May 15th Snowcovered Area and area with snow depth greater than 0.5 meters show declines on average in all scenarios, except for small increases in the Warm/Wet scenario and for almost all years (Section 5-11).
- For April 15th for the study area as a whole (Figure 2-1), there is a decline of 3-23 percent in snowcovered area with light snowcover (depth \geq 5 mm), and a 7-44% percent decline in area with significant snow (depth > 0.5 m) for the five scenarios considered, compared to the 2000-2013 historic average. For May 15th, the area with light snowcover declines 10-36 percent, and the area with significant snowcover declines 13-50 percent (Tables 5-4, 5-5)
- On April 15th, the Warm/Wet scenario shows the least change in average SCA (2121 Sq-km) compared to the historic snowcover (2609 sq-km, 7% decline) for significant (\geq 0.5 meter) snowcover. The largest decrease is the Hot/Wet scenario (1520 sq-km) with 44% decrease. Under the Hot/Wet scenario, the April 15th significant snowpack has been diminished below the level of the historic May 15th snowpack – a month shift (Fig. 5-14).

⁶ Some results are presented only for the 2000-2013 period determined by the overlap of the DHSVM simulations with the MODIS satellite record.

- All projections show declines in the number of years with significant snow. In each study domain, the areas with frequent availability (at least 14 out of 16 years) of significant snow (≥ 0.5 m) become concentrated in smaller high elevation areas, as seen in the maps in Figures 5-13, 5-14 (GLAC), and 5-20, 5-21 (ROMO). In contrast, lower elevation areas had the largest changes, or decreases in the number of years with significant snowcover.
- Most of the known den sites are located between 1800 and 2000m in GLAC. Below that elevation band large snow losses are predicted (40-70% decreases for two of the scenarios, 16-20% for the other three), above that elevation band there is little change in SCA for four of the five scenarios (2-8%) except in maximum warming scenario (-40%, Figure 5-22). In that 1800-2000m band, the snowpack change is sensitive to elevation and to the particular future climate scenario.
- This phenomenon of elevation-dependent snowpack change in the Western US is well supported in the literature. (Section 5-13)
- For representative wet years, the higher elevations of our study areas experience only 2-7% loss of snowpack under the scenarios with “least” change and the “central” change (Figure 5-8, 5-12), although for the dry years, losses range 18-57% (Table 5-5).
- Modest declines in SWE may occur without affecting the area with significant snow depth. On May 1st, for areas at 1800m and above in GLAC, losses of ~10-30% SWE (Figure 5-23) result in losses of only ~10% snowcover. The implication is that the wet, cold climate of the GLAC study area could act as a “buffer” to change in the area of 0.5 m deep snow on May 1st, at least at the elevations above 1800m.

Key Points – ROMO study area

- Projections of May 15th snowcovered area in ROMO declines on average in all scenarios, except for small increases in the Warm/Wet scenario, and for almost all years (Section 5-12).
- For April 15th for the study area as a whole (Figure 2-2), there is decline of 3-18% in area with light snowcover (depth ≥ 5 mm), and a change of -1 - +16 in area with significant snowcover (depth > 0.5 m) for the five scenarios considered, compared to the 2000-2013 historic average. For May 15th, the area with light snowcover declines 8-35 %, and the area with significant snowcover declines 6-38 percent (Tables 5-6, 5-7).
- Snowcovered Area in ROMO (≥ 0.5 m threshold on May 15) generally declines in wet years, shows a slight increase in (1-5%) in some years for the Warm/Wet scenarios with increased precipitation.
- One scenario with increased precipitation (Warm/Wet, giss) shows increases in April 15th SCA (Table 5-7). There are also slight increases in SWE for two scenarios at elevations at and above 3400m (Figure 5-25), but decreases in SWE for all scenarios below 3400m.
- Although no dens have been documented in ROMO, the elevation band for denning, modeled by regression analysis by FWS, is estimated to be 2700-3600m. On May 1st, modest declines in SWE of ~15% and less for areas at 3400m and above result in losses of only ~10% snowcover (Figure 5-24, 25). The implication is that the wet, cold climate of the higher parts of the ROMO study area could also act as a “buffer” to change in the area of 0.5 m deep snow on May 1st. Below that band losses in SWE of $\geq 35\%$ result in higher losses in SCA (20-65%), except in the scenario with least change (Warm/Wet, giss)

model). As in GLAC, the snowpack change in that 2700-3600m band is sensitive to elevation and to the particular future climate scenario.

- The phenomenon of elevation-dependent snowpack change in the Western US is well supported in the literature. Studies have found little historical change in snowpack in the Western United States above approximately 2500m elevation despite observed warming trends. Other literature on this topic is discussed in Section 5.13.
- ROMO exhibited more uncertainty in projections than GLAC, because compared to GLAC, the GCM climate projections for ROMO are more uncertain, i.e. have a larger spread, as to whether precipitation will increase or decrease (Figure 5-7).
 - For April 15th–May 15th, and for wet years, at the high elevations of the ROMO study area as whole, there is only modest loss of snowcover (<13%) under most scenarios of change (Table 5-7, see 2011 representative wet year). However even in wet years, the area of significant snowpack can decline by up to 26% for the Hot/Dry climate change scenario on May 15th (Table 5-7).

5.1 Introduction

In this section we describe the hydrologic model along with various modeling assumptions, validation of the model, the choice of risk-spanning future climate scenarios, and present results of historical and projected snowpack for the two study areas.

To determine the projected effects of a changing climate on snowpack we ran a physically-based hydrology model. The physical basis of the model – using a full energy and water balance of the snowpack rather than a simple temperature-index model -- is critical to evaluate change in a non-stationary climate. While ambient temperature is a critical factor in whether precipitation falls as rain or snow, the subsequent evolution of the snowpack, and in particular the melt season, is driven primarily by the energy balance at the surface. The energy balance is the result of several processes, including solar and longwave radiation, sensible and latent heat fluxes, and heat flux into the ground, as well as storage of heat in the snowpack. Therefore, including a realistic energy balance helps to understand how the perturbations to climate will affect the snowpack.

5.2 Model Description

The Distributed Hydrology Soil Vegetation Model (DHSVM) provides a physically-based simulation of land surface hydrology, including snowpack. The physical processes include a full surface water and energy balance model, a 2-layer canopy model, a multi-layer soil model, a 2-layer snowpack model (Wigmosta et al. 1994). It has been used in many studies that have provided realistic hydrologic simulations in topographically complex areas (e.g. Livneh et al. 2015). The model has explicit treatment of topographic slope, and aspect (the compass direction that the slope faces).

The model was selected for developing snowpack projections because it can be run at a fine spatial scale (250 m x 250m pixels) yet is able to be run over extensive domains. There are both finer-scale snow models, for which it would have been impractical to simulate such a large

domain, and coarser-scale models, such as the 1/16 degree grid of the VIC model that the McKelvey study used (see section 2.3). Coarser-scale models do not explicitly model the effects of slope and aspect, which is one of the primary goals of this study. Both DHSVM and VIC were primarily developed at the University of Washington, and are available as open-source community models. The two models share many components in common, including similar snow and canopy models. As such it supports the project goal of building on McKelvey study by modelling at a finer scale and treating slope and aspect explicitly.

The model was set up for both study domains on a 250m grid in Universal Transverse Mercator (UTM) coordinates within the modeling domain defined within the polygons shown in Section 2. Soil properties and vegetation type as well as a digital elevation model (DEM) were adapted to the model grid. A soil hydraulic routing network was also determined from the DEM, though in this project we do not investigate the runoff. The effect of slope and aspect on incoming solar radiation is implemented through a computation of the degree of shading for each 250-m pixel that was variable throughout the day and differed from month to month based on the solar angle in the sky and from the DEM. The model requires inputs of time-varying meteorological fields on sub-daily time scales. Snow water equivalent was output on the 1st and 15th of the month from March 1st to June 1st for every year of the simulation and projections.⁷ As noted below, snow depth was estimated using a typical snowpack density for late Spring.

5.3 Meteorological Inputs

The DHSVM model inputs were derived in a multi-step process. First, values of daily minimum temperature, daily maximum temperature, and precipitation were extracted from the Livneh (2015) dataset, which has a grid resolution of 1/16th degree in latitude and longitude. These daily values were disaggregated in time. Other forcing variables needed by the model, solar radiation, downwelling longwave radiation, specific humidity were derived from empirical relationships using the MTCLIM algorithms which were evaluated by Livneh et al. (2014) finding small overall biases. The Livneh et al (2015) data was then interpolated to the 250m DHSVM grid using an inverse-distance weighting algorithm along with assumed lapse rates (elevation dependence) in temperature and in precipitation. More details of the Livneh 2015 dataset are included in the Section 5 Supplementary Material.

5.4 DHSVM Historical Validation

The goal of the model validation is to assess the overall magnitude, temporal, and spatial aspects of the modeled snowpack in the Spring and how these differ from observational estimates. Observational estimate of snow depth or snow water equivalent at the scales that we simulated are not available, leading to uncertainty about the “true” snowpack. For the overall magnitude and temporal aspects of the snow simulation, we compared the historical model simulation to point observations at the few available SNOTEL sites, focusing on the duration and melt-out

⁷ All data has been provided to FWS, and is available at:
ftp://ftp2.psl.noaa.gov/Projects/FAIR_paper_data/20200914_01/

date of the snowpack. The spatial aspect of bias was evaluated by comparing the model output to the observed spatial patterns of snowcover obtained from the MODIS analysis (see Section 4), qualitatively for GLAC and quantitatively for ROMO. When interpreting the projections, future model biases are typically assumed to be similar to historical biases. With this assumption, the calculation of, for example, percentage change is less sensitive to biases and uncertainties in the historical simulation.

5.4.1 Comparison to SNOTEL

The DHSVM historical simulation was compared against the snow data from nine SNOTEL sites in the ROMO study area that were in operation during the full time-period of interest, and the 3 SNOTEL sites in and adjacent to the GLAC study area (Table 5-1). Validation against SNOTEL snow data was performed by running the DHSVM model in “point” mode so that it simulated the conditions at the SNOTEL locations only. Because the SNOTEL stations are deliberately sited in clearings, the canopy was assumed to be open for the validation runs, while the actual 250m grid canopy values were used for the production runs. Two metrics were chosen: the meltout day of year (defined as the date when SWE fell to less than 1mm), and the duration of snowcover (total number of days during the water year (October-September) when SWE > 10cm). Figure 5-1a shows the modeled and observed meltout dates for the GLAC and ROMO SNOTEL sites, and Figure 5-1b shows the duration of snowpack. One does not expect exact reproduction of the snowpack at the SNOTEL sites, but rather a scatter about the 1-to-1 line, which is seen. The Copeland Lake SNOTEL site, and to some extent the Many Glacier SNOTEL sites are outliers, with the model retaining snowpack significantly longer than in observations. Both these sites are at relatively low elevations, and are quite sensitive to potential temperature biases in the input data. The Livneh (2015) dataset is known to have a cool bias relative to other datasets, which may influence these sites disproportionately.

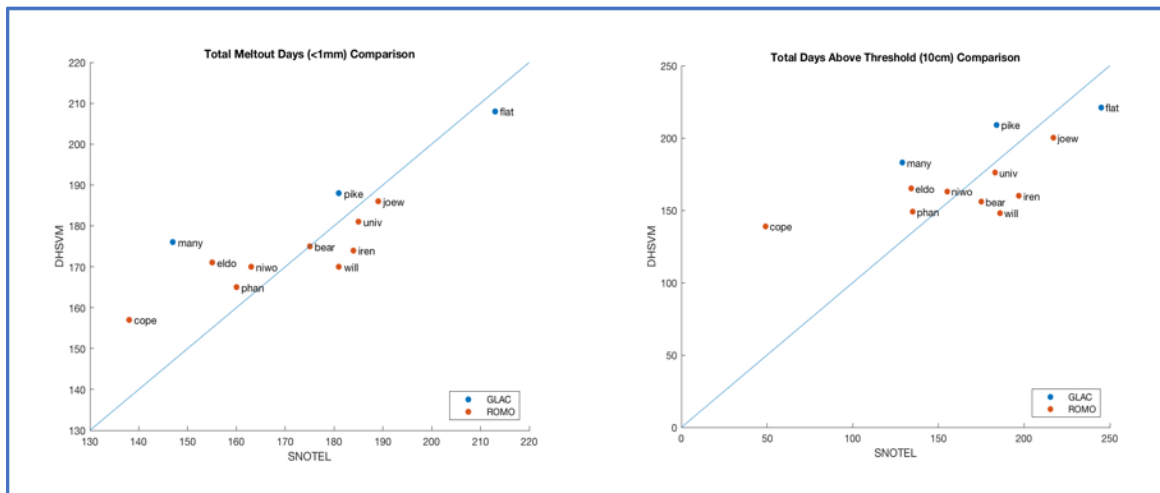


Figure 5-1. Validation of DHSVM Historical Simulation at SNOTEL sites in ROMO and GLAC using two metrics. Left panel shows observed total meltout date (Julian day of year) vs. simulated date for 12 SNOTEL stations in GLAC (blue circles) and ROMO (red filled circles). Total meltout date is defined as the first day in Spring when SWE was less than 1mm. Right panel shows observed vs simulated observed snowpack days above threshold, defined as number of days with greater than 10cm of SWE for the same stations. SNOTEL station abbreviation codes are provided in Table 5-1.

Table 5-1 SNOTEL Sites at Study Areas. Maps with SNOTEL sites are shown in Figs 2-1 and 2-2. Note that sites installed after 1997 were not used due to their short record.

SNOTEL SITE NAME (Site Number, Abbreviation)	
Glacier Study Area	Flattop Mountain (482, flat), Many Glacier (613, many), Pike Creek (693, pike)
Rocky Mountain Study Area (used for Validation)	Bear Lake (322, bear), Copeland Lake (412, cope), Joe Wright (551, joew), Lake Eldora (564, eldo), Lake Irene (565, iren), Niwot (663, niwo), Phantom Valley (688, phan), University Camp (838, univ), Willow Park (870, will)
Rocky Mountain Study Area (not used - installed after 1997)	Never Summer (1031), Wild Basin (1042), Hourglass Lake (1122), Long Draw Reservoir (1123), High Lonesome (1187), Sawtooth (1251)

The year-to-year variations of peak snowpack at the GLAC SNOTEL sites are well captured, as illustrated in Figure 5-2 that shows simulated and observed time series of SWE at these stations. Figure 5-3 shows selected SNOTEL sites in the ROMO area. As can be seen in Figure 5-2, the Copeland Lake site is less well simulated than other sites. We attribute this to being located at a lower elevation than other sites, and hence susceptible to small biases in temperature in the meteorological inputs. Other sites in ROMO are well simulated. Based on this evaluation of DHSVM performance, the standard set of model parameters was adopted for the GLAC domain without modification.

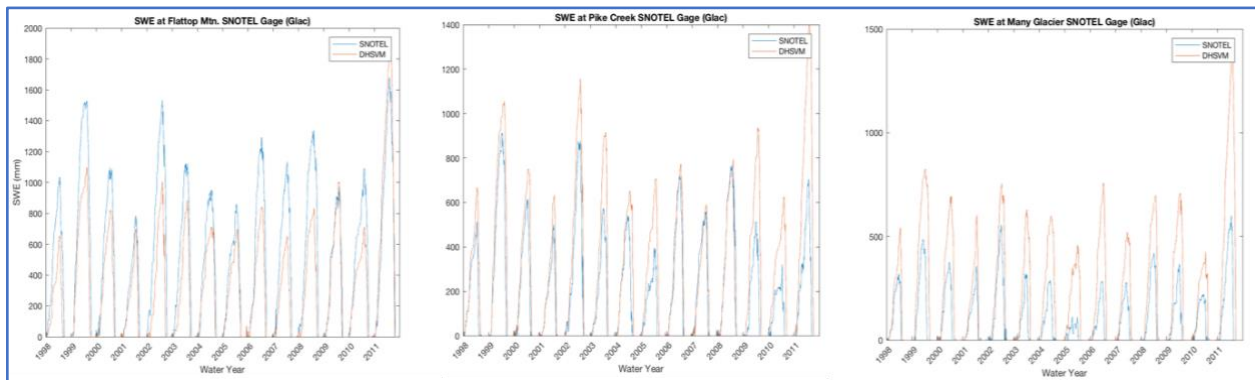


Figure 5-2. Time series comparing observed (blue) and simulated (red) Snow Water Equivalent (mm) for the GLAC study area. Flattop Mountain (left), Pike Creek (center), and Many Glacier (right) SNOTEL stations. See Table 5-1 for SNOTEL stations.

The question arises of the independence of the SNOTEL data from the Livneh et al. (2015) forcing data. The primary observing station data they used for interpolation did not include SNOTEL. However, a monthly adjustment factor was applied to the interpolated precipitation to reproduce the 1981-2000 climatology of PRISM. The Livneh et al (2015) temperature data were entirely independent of SNOTEL data. Therefore, we expect that the errors revealed at the SNOTEL sites should be representative of errors at other, unobserved sites in the domain.

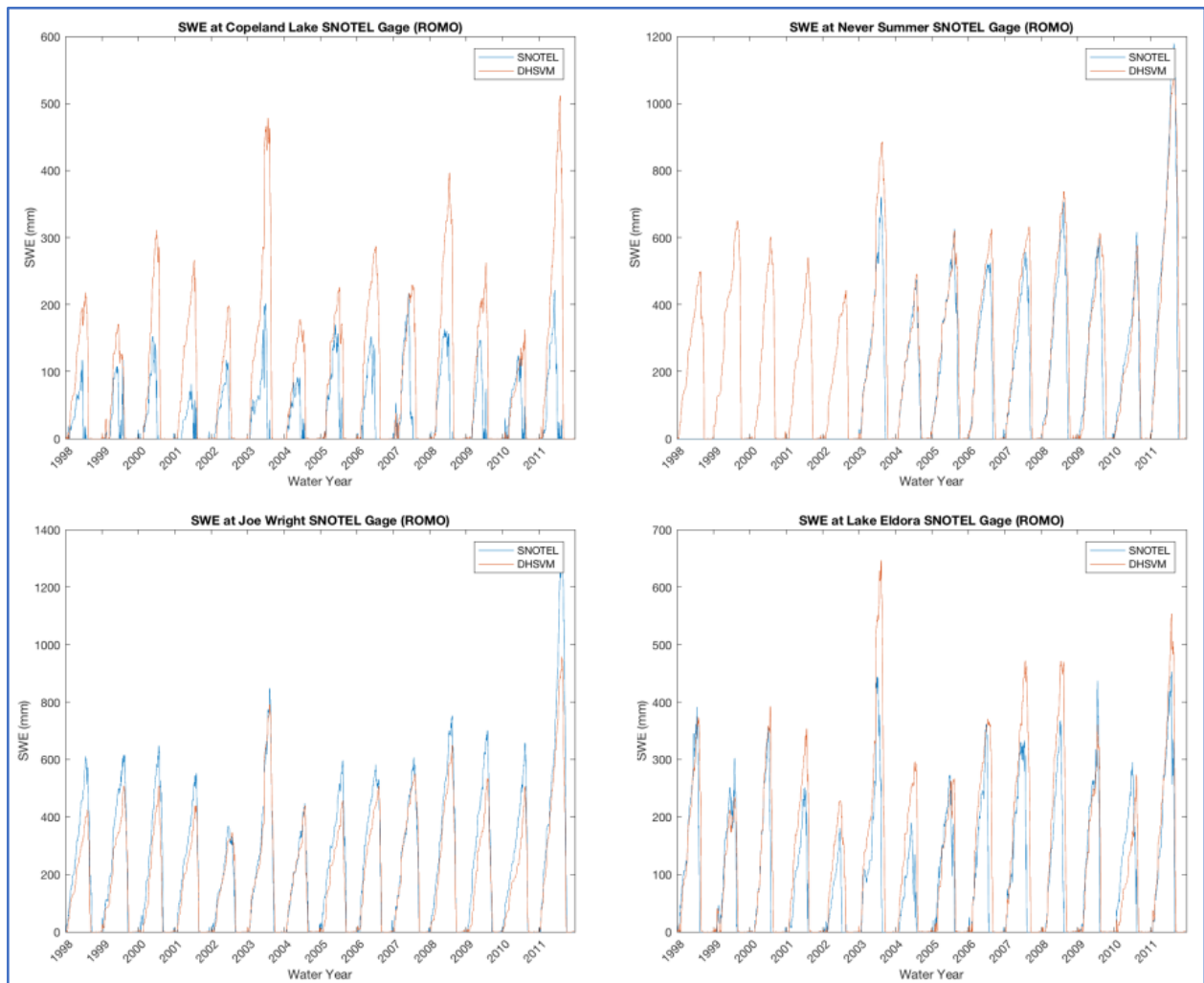


Figure 5-3. Time series comparing observed (blue) and simulated (red) snow water equivalent (SWE, mm) for the ROMO study area. Copeland Lake (upper left), Never Summer (upper right), Joe Wright (lower left), and Lake Eldora (lower right) SNOTEL stations. See Table 5-1 for SNOTEL stations.

5.4.2 Comparison to MODIS Snowcover

The spatial distribution of snowcover was assessed by comparison with MODIS data. Some care must be taken to compare observed NDSI, which indicated fractional snowcover within pixels, with modeled SWE, which does not account for fractional snowcover within a pixel. For this evaluation, a threshold to determine “snowcovered ground” was chosen for both the MODIS (NDSI ≥ 0.1) and for the DHSVM (SWE ≥ 5 mm). Figures 5-4 and 5-5 show spatial overlays of the DHSVM simulated snowcover and the MODIS observed snowcover for the representative dry years in ROMO and GLAC. In terms of snowcover, dry years were more difficult to simulate than wet years, however, the spatial agreement is good for these two examples.

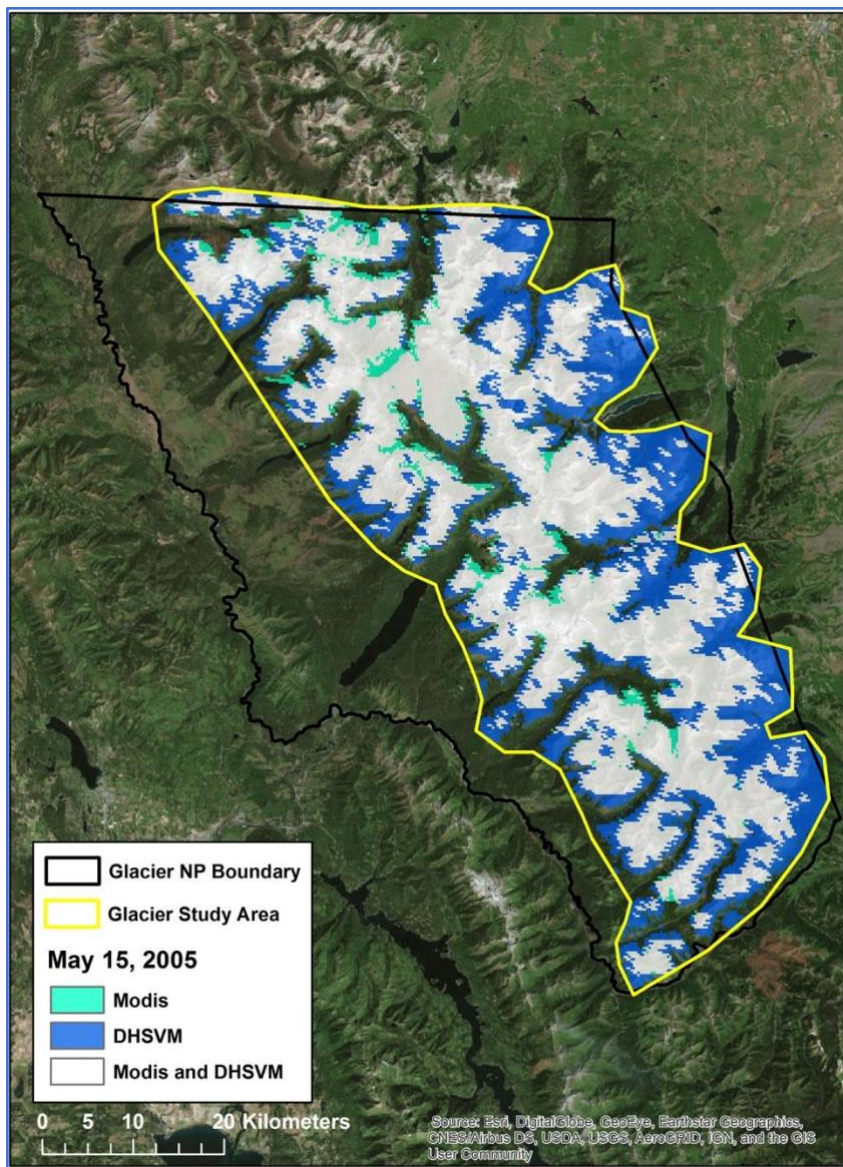


Figure 5-4. MODIS snow cover compared to DHSVM snow cover for May 15, 2005 for the GLAC study area (yellow outline). Spatial overlay of shows areas of agreement (white) between MODIS and DHSVM snow cover, areas where only MODIS indicated snow cover (green), and areas where only DHSVM model indicated snow cover (blue). 2005 is a representative dry year for GLAC. Graphic courtesy of John Guinotte, FWS.

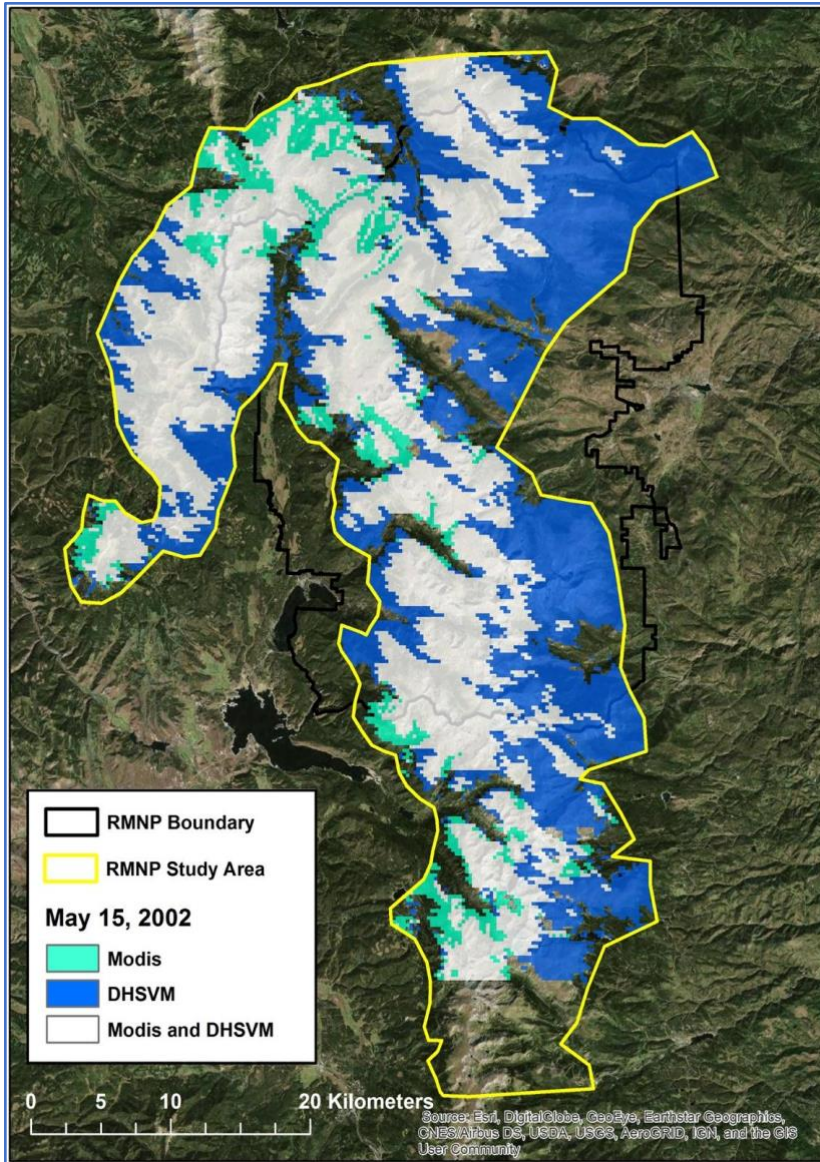


Figure 5-5. MODIS snow cover compared to DHSVM snow cover for May 15, 2002 for the ROMO study area (yellow outline). Spatial overlay of shows areas of agreement (white) between MODIS and DHSVM snow cover, areas where only MODIS indicated snow cover (green), and areas where only DHSVM model indicated snow cover (blue). 2002 is a representative dry year for ROMO. Graphic courtesy of John Guinotte, FWS.

However, initial attempts to model ROMO indicated biases in the spatial patterns of snowcover compared to MODIS. To overcome model errors at ROMO, an adjustment of two DHSVM snow parameters was conducted. The representative values of the physical quantities of these parameters can span a fairly large range, and hence an experiment was conducted to evaluate the appropriate settings of the model for ROMO based on minimizing differences between simulated and MODIS SCA for the historical period, as well as reducing biases with SNOTEL SWE.

The first parameter modified was the snow-surface roughness (SR), which affects the amount of turbulent heat fluxes that occur between the snow and the atmosphere, whereby a small number corresponds to a smoother snowpack that has less heat exchange with the overlying air, while the opposite is true for a large value. The second parameter was the liquid water capacity (LWC) that describes the volume of water that the snowpack can hold before water will leach out of the snowpack. This parameter is important, since it is common for snow to melt during the day and then for liquid water to refreeze at night.

Adjustments were made to SR and LWC within reasonable physical ranges and the DHSVM simulated SCA was compared with MODIS via a threat score. The threat score used, referred to as the Critical Success Index (CSI) by Zappa (2010), is defined as:

$$CSI = \frac{a}{a + b + c}$$

Where a indicates a snow-covered pixel in both the simulation and observed data, b indicates a snow-covered pixel in the simulation but a bare pixel in the observed (“false positive”), and c is a bare pixel for the simulation and a snow-covered pixel shown by the observed data (“false negative”). The objective was to maximize the threat score. Approximately ten unique parameter settings were tested. Additionally, for each parameter setting the mean bias in meltout day and duration of snowcover between DHSVM simulated and SNOTEL SWE was calculated with the objective being a minimization of the bias between the two (bias = simulated – observed). The final DHSVM settings for ROMO were identified by the parameter values that corresponded with a combination of a high threat score and a low bias. The Supplementary Material provides the parameter settings (Table S5-1) and ensuing performance metrics (Figure S5-1).

5.5 Determination of Snow Depth from DHSVM model output

DHSVM does not compute snow depth as a separate quantity, but instead returns snow water equivalent (SWE). To estimate the snow depth from SWE we adopt a uniform value of 2.5:1 for the SD:SWE ratio, corresponding to a snow density of 0.4 for May 1st and May 15th. For April 15th conditions, we adopt a bulk density of 0.33 which yields a conversion factor of 3.0:1. Further discussion can be found in the Section 5.5 Supplementary Material. Several lines of evidence point to the reasonableness of this assumption. First, SNOTEL stations where both depth and SWE are measured show similar ratios for the two study areas. Second, we investigated the ratio of density from the SNODAS (Snow Data Assimilation System) product from the NOAA National Operational Hydrologic Remote Sensing Center, which points to a very narrow range around 2.6-2.7 for the ratio. Finally, for comparison with the McKelvey et al (2011) work we compared the May 1 Snow Depth and SWE products from the Littell et al (2011) hydrologic model runs (obtained separately from <https://cig.uw.edu/datasets/wus/>). These all point to an approximate value consistent with a density between 0.35 and 0.4. The results of this study do not depend on a precise value for snow density. The conclusions of the report are not sensitive to the choice of conversion factor within the ranges indicated by the above analysis.

5.6 Choice of thresholds for analysis

While the McKelvey study analysis was for the presence or absence of snowcover, this modeling effort produces results in terms of SWE. This allows greater flexibility in evaluation of the depth of the snowpack, but presents a problem in comparison. To compare the model-generated SWE with both the McKelvey study results and our own MODIS historical snowcover analysis we used a threshold of 5mm SWE to define presence/absence of snowcover, also called “light snow”. We also were concerned with analyzing the presence of “significant snow” which we defined as ≥ 0.5 m of snow depth. The value of ≥ 0.5 m was arrived at by an analysis of the modeled snow depth at known wolverine denning sites in Glacier National Park (Table 5-2). With the exception of one site that had melted out by May 15th, the other sites all have snowpack between 0.4 and 2.4 m.

Table 5-2: Modeled Snow Depth on May 15 at reported den sites in the Glacier Study Area.

There are no documented den sites have been reported in RMNP. (source: John Guinotte, FWS)

Den site	Date observed (month-yr)	Meltout Date (MODIS)	April 15 snow depth dhsvm (m)	May 01 snow depth dhsvm (m)	May 15 snow depth dhsvm (m)	Notes
1	Apr-03	5/25/2003	1.32	1.07	1.04	Natal Den
2	May-03	5/25/2003	1.32	1.07	1.05	Maternal Den
3	Apr-04	6/4/2004	1.96	1.46	1.13	Natal Den
4	Apr-04	6/29/2004	1.0	0.75	0.54	Maternal Den
5	May-04	6/29/2004	1.07	0.83	0.65	Maternal Den
6	Mar-05	6/11/2005	1.6	1.11	0.58	Maternal Den
7	Apr-05	6/11/2005	1.6	1.11	0.58	Natal Den
8	May-05	6/11/2005	1	0.76	0.47	Maternal Den
9	Mar-06	5/25/2006	3.05	2.56	2.44	Unknown-maternal or natal
10	Apr-06	5/14/2006	0.68	0.26	0	Meltout occurred before May 15 Unknown-maternal or natal
11	Apr-06	6/7/2006	2.83	2.4	2.38	Unknown-maternal or natal
12	May-06	5/31/2006	1.14	0.79	0.61	Maternal Den
13	May-06	5/31/2006	1.14	0.79	0.61	Natal Den
14	May-07	6/4/2007	1.82	1.28	0.68	Natal Den

5.7 Delta Method for Future Scenarios

The advantages and disadvantages of the delta method have been discussed extensively in the literature (e.g. Sofaer et al, 2016, for a recent review). The primary advantages of this method are its long history of use, its simplicity, and its use of the historical observed weather as the baseline. The simplicity allowed for the study to be completed in a short time-frame, while still reaching our primary objectives of finer spatial scale and a more complete exploration of future climate scenarios. The use of the historical baseline allows us to explore how wet, near normal, and dry “representative years” would play out under the different climate futures. However, it is important to keep in mind that we are “parameterizing the future variability in terms of the historical variability.” This treatment of daily variability also leads to the primary disadvantage of the delta method: the assumptions that the changes in extremes follow the changes in the means, and that the pattern of daily weather is simply shifted without changing the sequences of weather (Sofaer et al, 2016). This aspect is less of a concern for this study, as snow accumulation and ablation are cumulative processes, so that the daily sequences of storms is less critical to simulate than the monthly and seasonal totals. Another assumption of the delta method is that the large-scale changes in temperature and precipitation apply uniformly to the study area. Equivalently we assume that change factors in ambient (free-air) temperature and precipitation will not depend on the small scale spatial detail. Because we explicitly compute the surface energy balance, we are able to simulate surface temperature differences that depend on fine-scale terrain, mitigating to some extent this limitation of the delta method.

Following McKelvey (2011), we use the “delta method” to downscale the climate model data to the 250m modeling grid. The steps in this method are as follows:

- Start with historical daily meteorological forcings (inputs to the DSHVM model) for the historical baseline period (1998-2013)
- Run DHSVM with the historical forcings to produce the simulated historical snow and hydrology.
- From climate model output, compute the change in 30-year average temperature for each calendar month over the time frame of interest. Do the same for the percent change in precipitation
- Apply these change factors to the historical daily meteorological inputs to DHSVM to generate future scenarios of meteorological inputs.
- Run DHSVM with these new inputs to generate the projected snow and hydrology.
- Compare the projected snow to the historic DHSVM model simulations to infer changes in snowpack.
- Repeat for a set of change factors from different climate models that adequately sample the uncertainty in climate projections.

The result of the delta method is a continuous-in-time simulation of the historical period (1998-2013), and an equal length simulation of how this sequence of years would play out in the future under five different scenarios of climate change. Figure 5-6 illustrates typical DHSVM model output using the delta method. Figure 5-6a shows a map of May 15, 2011 Snow Water Equivalent for the Glacier Study Area from the historical simulation, while Figure 5-6b shows a single projected future for what that year’s SWE would look like under a particular scenario of climate change. The future scenario represents a year similar to 2011, that is, a

relatively wet and cool year compared to other years in the future. However, in this example, the temperature and precipitation have been adjusted to be consistent with the 2041-2070 projected climate from the MIROC climate model, the model with the highest temperature increase and about 10% increase in precipitation.

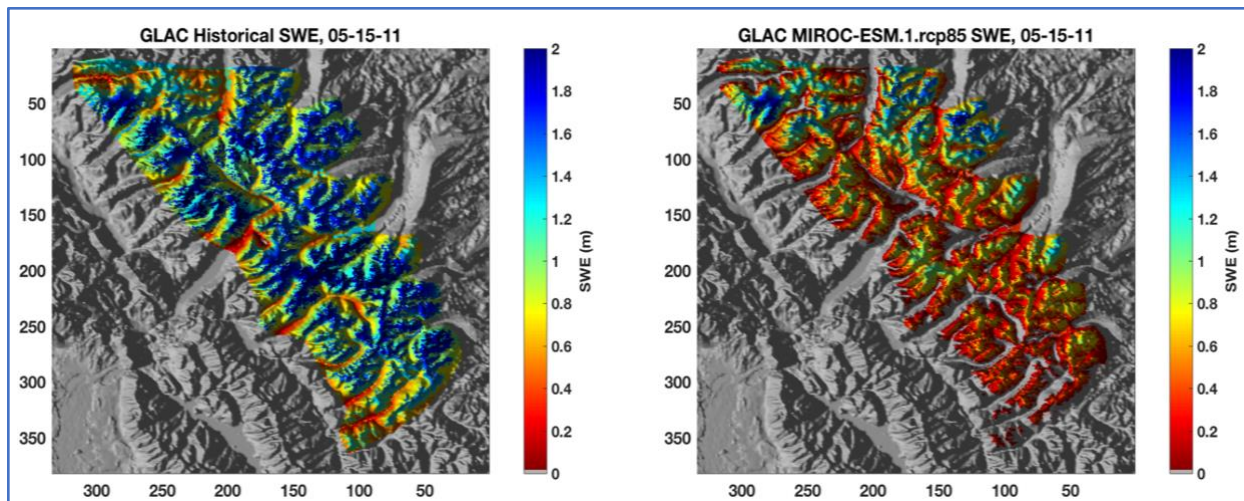


Figure 5-6. Example of DHSVM model output for historical SWE (May 15, 2011) and a future scenario for GLAC. a) left: historical simulation for 2011 and b) right, for the Hot/Wet future scenario (#3, miroc) applied for the period 2041-2070 derived from the MIROC climate model projections. The future scenario represents a year similar to 2011, that is, a relatively wet and cool year, but the temperature and precipitation adjusted to be consistent with the 2041-2070 projected climate from the MIROC climate model. Numbering on the axes indicates the regular grid of 250m x 250m gridcells on a Universal Transverse Mercator map projection – these grid numbers are not shown in subsequent figures. North is up; for distance scale see Figs. 2-2, 5.5. Simulation with the DHSVM model was only performed within the study area polygon, surrounding area provided for context.

5.8 GCM Uncertainty and Scenario Planning Approach

As noted in Section 2, global climate models (GCMs) are our primary tools to examine the nature of climate change during the 21st century. There are currently about 20 modeling centers worldwide which provided output from their best model(s) to be considered in the Coupled Model Inter-comparison Project Phase-5 (CMIP5, Taylor et al., 2012) the basis for the latest Intergovernmental Panel on Climate Change (IPCC) report (IPCC, 2013). Figure 5-7 shows the changes in temperature and precipitation for the two study areas for the 2041-2070 period, centered on 2055, for a rectangular latitude/longitude area around each park. We find a large spread in the extent of warming (1-4 °C) and changes in precipitation, including both increases and changes in precipitation (-5% to +20%) for these regions by 2055. The McKelvey study chose GCMs based on the range of temperature change (see Sec 2.2, and Figure 5-7). For temperature, much of this spread (or uncertainty) is a result of the difference between GCMs (e.g., their climate sensitivities), whereas for precipitation it is both the difference between GCMs and internal climate variability. Some difference also comes from the choice of future greenhouse gases (GHG) emission scenario. However, these differences among mid-21st century climate responses are limited compared to later in the century (Hawkins and Sutton, 2011, 2012, and see discussion in Ray et al., 2010, section 4).

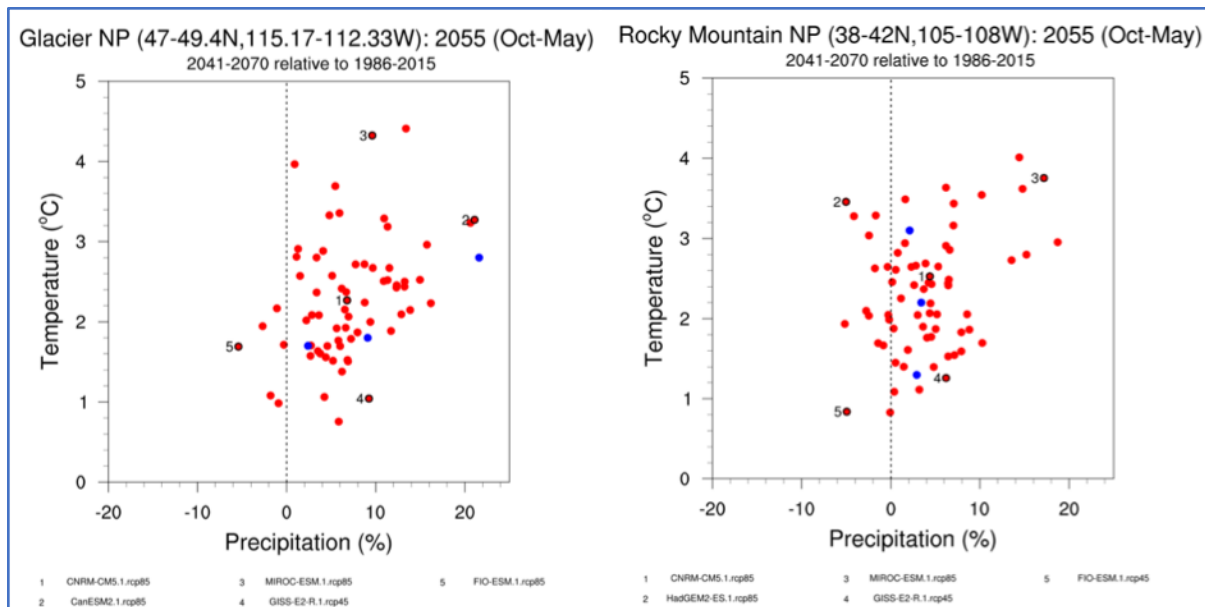


Figure 5-7. Projected Changes in Cold Season (October-May) Temperature and Precipitation by 2055 for GLAC Study Area (left) and ROMO study area (right). Solid red circles show changes in temperature and precipitation for a nominal 2055 climate, i.e. 2041-2070 period relative to 1986-2015, from 68 global climate model experiments, 34 models each from RCP 4.5 and 8.5 emissions scenarios. This plot illustrates how the five divergent climate scenarios selected for each area (black circles around the red) span the different parts of this projection space (see section 5.9). Four of the same GCMs are used as future scenarios for both areas (#1, and 3-5); different GCMs are used for #2 in order to represent a range of futures in each area. The models and future scenario names, and relative changes compared to other scenarios are shown in Table 5-3. The blue circles indicate the three scenarios considered in the McKelvey et al. study for the 2030-2059 period.

For more robust planning and climate adaptation, experts recommend incorporation of these uncertainties into the assessment of impacts and developing adaptation strategies. The scenario planning approach is a method that has been recommend and promoted by different entities and experts (National Park Service, 2013; Rowland et al., 2014; Maier et al., 2016; Murphy et al. 2016; Star et al., 2016, Fisichelli et al, 2016 a,b). Therefore, we adopted a strategy of selecting multiple divergent future scenarios challenging to the system of interest, following that in Rowland et al (2014), Fisichelli et al (2016 a, b), Star et al (2016) and Symstad et al. (2017).

5.9 Climate Projections Evaluation and Scenarios Selection

We compiled output for temperature and precipitation projections for 34 CMIP5 GCMs from the Reclamation (2013; <http://gdo-dcp.ucllnl.org/>) archive of 1-degree regrided GCM dataset for Representative Concentration Pathways (RCP) 4.5 and 8.5 (IPCC, 2013), which are respectively the moderate and high GHG emissions scenarios --- for a total of 68 GCM projections (see Table S5-3 in the Supplementary Material) These data were then analyzed to quantify broad-scale projections for the two study regions by 2055 (i.e. a mid-point centered on the 2041-2070 period) – primarily changes in the cold season (Oct-May) temperature and precipitation by 2055 relative to the 1986-2015 period. Figure 5-7 (above) shows these changes for Rocky Mountain and Glacier National Parks, respectively. As mentioned earlier, we found a large range in

temperature increases (1-4 °C) and changes in precipitation (-5% to +20%) for these regions by 2055. Table 5-3 shows GCM names, numbers and colors coded in later figures, and relative changes in temperature and precipitation. To incorporate the large range in climate projections, we worked with the ensemble of 68 CMIP5 temperature & precipitation projections, described by the red filled-circles in Figure 5-7, to select five future climate scenarios (black circles) that span the different parts of this projection space. Five GCMs representing these scenarios were identified for both RMNP and GNP. For each of these GCMs, we calculated changes in temperature and precipitation by 2055 for each month of the year, which we call the “monthly delta”. These monthly deltas were used to perturb the hydrological models to simulate snow response in RMNP and GNP by 2055.

Some processes which may be of relevance not represented in the model include wind and avalanche re-distribution of snowpack. Snow depth is not explicitly modeled, and must be inferred (Section 5-5). The meteorological forcing does not take into account cold air pooling or how this may change in the future. Cold air pooling – the anomalously cold air that can collect in valley bottoms, particularly in Winter, could also act to prolong the duration of snowcover in those locations. While Curtis et al (2014) identify this as a potential process, they do not physically model cold air pooling, but merely include it in their present-day climatology as a simple “offset” from their unadjusted data. Nonetheless their work provides a complementary approach to the identification of potential snow refugia, though more work would need to be done to study the geographic and seasonal aspects for the study areas.

Table 5-3. The future climate scenarios (five for each area) with changes in temperature and precipitation relative to other scenarios (See also Fig 5-7 for an alternate visualization of these changes), and the GCM used as the basis for the deltas for this scenario. More details on the GCMs are in the Glossary.

Future Scenario Name and #	Scenario Change in GLAC relative to other scenarios	Scenario Change in ROMO relative to other scenarios	Code and color for GCM used for this scenario
Central (#1)	+~2.2 °C increase in temperature (close to the ensemble mean) and +~5% increase in precipitation	+~2.5 °C increase in temperature (close to the ensemble mean) and +~8% increase in precipitation	cnrm, red
GLAC: Hot/Very Wet (#2)	relatively higher increase in temperature (+~3.2 C) and the highest increase in precipitation (+20%) for the GLAC scenarios	N/A	canesm, green
ROMO: Hot/Dry (#2)	N/A	relatively higher temperature increase (+~ 3.5 °C) and ~5% decrease in precipitation. This scenario results in the greatest change (reduction) in snow pack and snowcover.	hadgem, green
Hot/Wet (#3)	the highest temperature increase of the GLAC scenarios (+~4.2 °C) and +~10% increase in precipitation	the highest temperature increase of the ROMO scenarios (+~3.7 °C) and the highest increase in precipitation (+~18%).	miroc, purple
Warm/Wet (#4)	relatively lower temperature increase (+~1 °C) and +~10% increase in precipitation	relatively lower temperature increase (+~1.3 °C) and +~7% increase in precipitation that appears to partially offset the impacts of the temperature increase. This scenario results in the least change in snow pack and snowcover.	giss, aqua
Warm/Dry (#5)	relatively lower temperature increase (+~1.6 °C) and ~5% decrease in precipitation	relatively lower temperature increase (+~0.8 °C) and ~5% decrease in precipitation	fio, orange

5.10 Modeling Caveats

Some processes which may be of relevance not represented in the model include wind and avalanche re-distribution of snowpack. Snow depth is not explicitly modeled, and must be inferred (Section 5-5). The meteorological forcing does not take into account cold air pooling or how this may change in the future. Cold air pooling – the anomalously cold air that can collect in valley bottoms, particularly in Winter, could also act to prolong the duration of snowcover in those locations. While Curtis et al (2014) identify this as a potential process, they do not physically model cold air pooling, but merely include it in their present-day climatology as a simple “offset” from their unadjusted data. Nonetheless their work provides a complementary approach to the identification of potential snow refugia, though more work would need to be done to study the geographic and seasonal aspects for the study areas.

5.11 GLAC Study Area Results

This section presents SWE and SCA for representative years, area and number of years with snow depth threshold ≥ 0.5 m. The elevation dependence of snow for GLAC is discussed in Section 5-13. **On average, the GLAC study area exhibits a 7 – 44 % decline in the area of snow depth ≥ 0.5 meters on April 15th, and a 13-50 % decline in the area on May 15 for the scenarios considered.**

5.11.1 SWE and Snowcovered Area for representative years

Figures 5-8 shows DHSVM model simulated snow water equivalent (SWE) on May 15 for the wet (2011) representative year. Maps of snowcover derived from SWE by applying a threshold of 5 mm are available in the Supplementary material. Results for thresholds of 1 mm of SWE were also investigated and show similar patterns. Snowcovered area with a “light snowcover” threshold was computed primarily for comparison with both the MODIS results from Section 4, and with McKelvey. In Figure 5-8, the historical simulation is shown along with three of the five future scenarios, chosen to represent the central scenario (cnrm), the greatest change in snowpack on average (Hot/Wet (miroc) scenario) and the least change (Warm/Wet (giss) scenario). The projected snow maps answer the question “what would the snowpack in a wet year like 2011 look like in the 2040’s through 2070’s under these scenarios of climate change.”

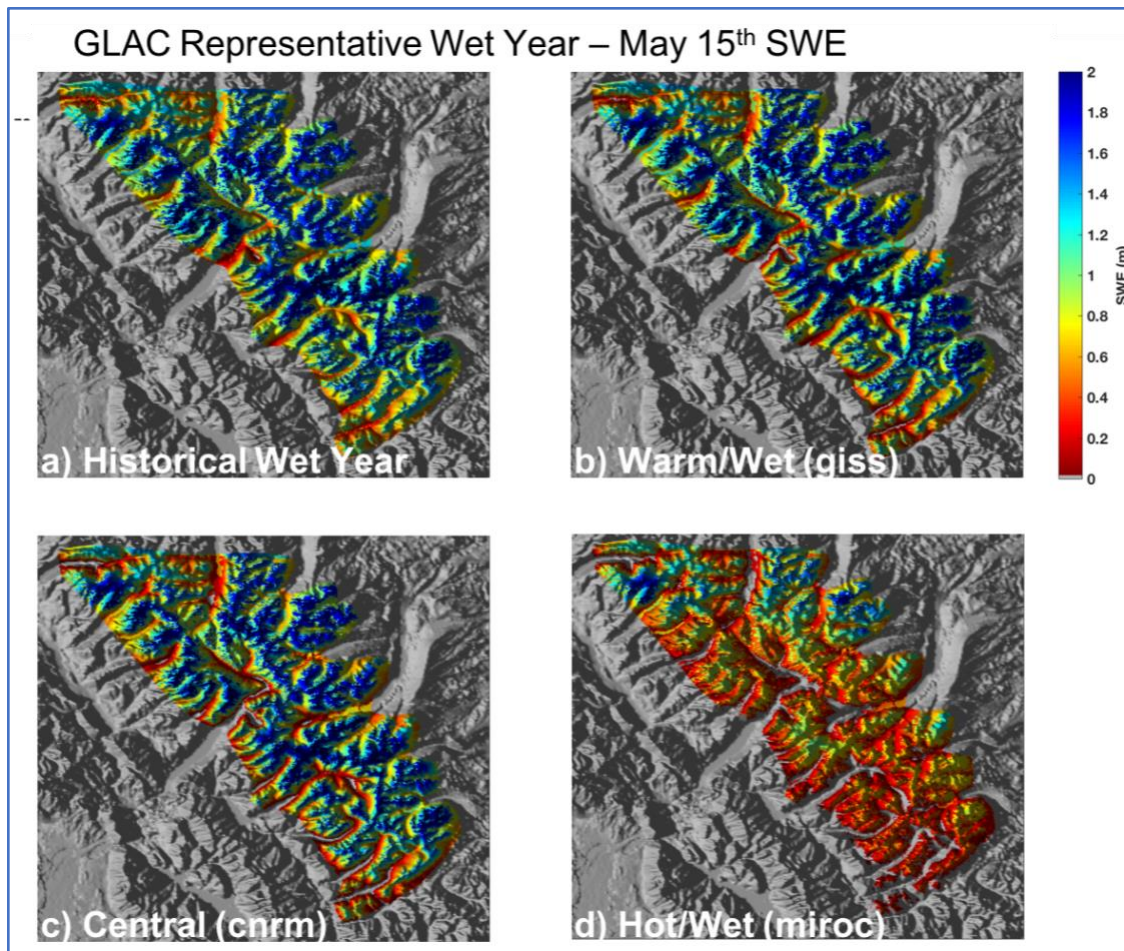


Figure 5-8. Historical and projected May 15th Snow Water Equivalent (m) for a Representative Wet Year in GLAC. Historical simulation year 2011 (wet year, top left), and for three future scenarios applied to 2011: b) the warm/wet (giss) scenario results in the lowest change in SWE (top right), c) the central scenario (cnrm) results in a moderate change in SWE (bottom left), and the, d) hot/wet scenario (miroc) results in the greatest change in SWE (bottom right). These projected snow maps illustrate what the snowpack in a wet year like 2011 would look like in the 2040's through 2070's under these scenarios of climate change. Scenarios are listed in Table 5-3 and shown in Figure 5-7, maps for additional scenarios are provided in the Supplementary Material (S5-7 and 8). Table 5-4 provides numerical values for (SWE historical average (2000-2013) and five future scenarios.

Figures 5-9 and 5-10 show SWE for the Near Normal (2009) and Dry (2005) representative years. The historical simulation and future scenarios are as in Figure 5-8. Figure 5-11 summarizes the results for snowcovered area in terms of the total snowcovered area (km^2) within the study area polygon. The numerical values of snowcovered area for all years in the simulation, as well as percent changes for these quantities are shown in Table 5-4. Table 5-4 indicates that the snowcovered area decreases for all scenarios. On average, the GLAC study area exhibits a 7 – 44 % decline in the area of snow depth ≥ 0.5 meters on April 15th, and a 13-50 % decline in the area on May 15th for the scenarios considered.

The following points stand out:

- Comparing the Wet and Dry representative years we see that dry years are more vulnerable to climate change in terms of percent loss of snowcovered area.
- For the Wet year, the high elevations of the study area result in little loss of snowpack in the study areas under most scenarios of change.
- However, in Figures 5-10 and 5-11 we notice an anomaly – for the dry year, the Hot/Wet (miroc) scenario does not have the greatest loss of snowcovered area. The increase in precipitation in this scenario has somewhat compensated for the loss of snowpack due to warming. Instead the Hot/Very Wet (cnsm) scenario, with its even larger warming shows the greatest loss of snowcovered area.
- Snow changes at the elevations of known dens are discussed later in Section 5.13 and Figures 5-22 and 5-23.

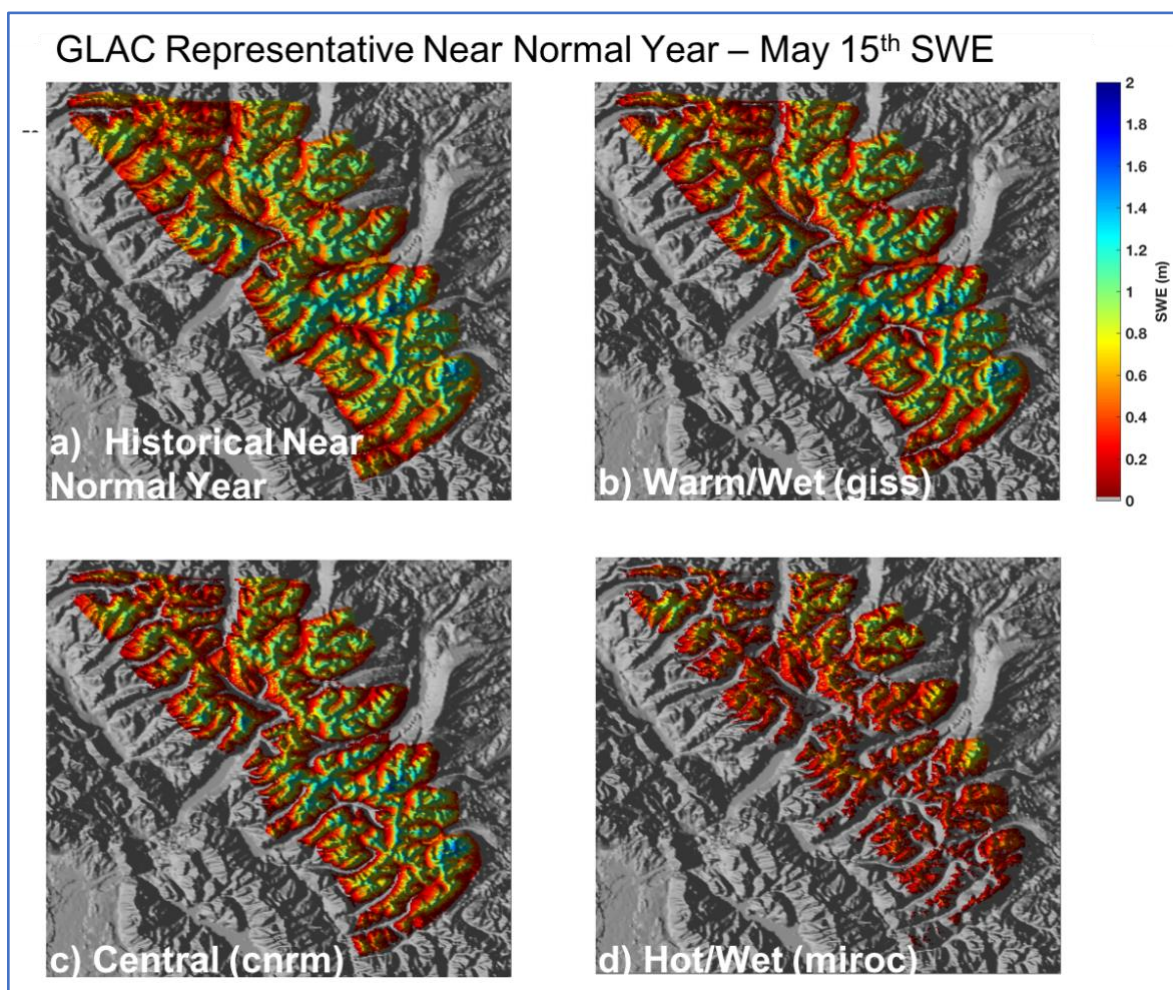


Figure 5-9. Historical and projected May 15th Snow Water Equivalent (m) for a Representative Near Normal Year in GLAC. Historical simulation year 2009 (wet year, top left), and for three future scenarios applied to 2009: b) the warm/wet (giss) scenario results in the lowest change in SWE (top right), c) the central scenario (cnrm) results in a moderate change in SWE (bottom left), and the, d) hot/wet scenario (miroc) results in the greatest change in SWE (bottom right). These projected snow maps illustrate what the snowpack in a near normal year like 2009 would look like in the 2040's through 2070's under these scenarios of climate change. Scenarios are listed in Table 5-3 and shown in Figure 5-7, maps

for additional scenarios are provided in the Supplementary Material (S5-7). In May, snow depth = 2.5 x SWE. Table 5-4 provides numerical values for SWE historical average (2000-2013) and five future scenarios.

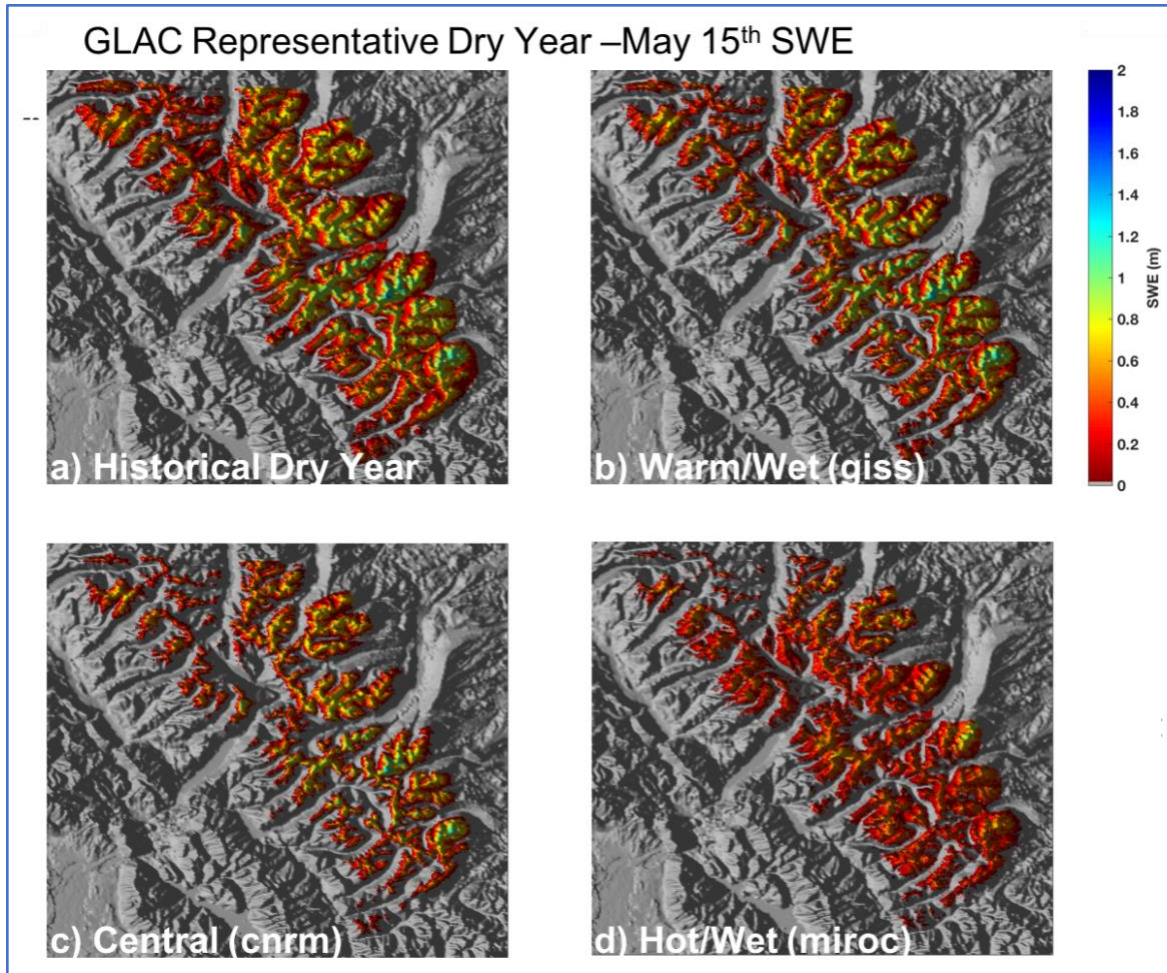
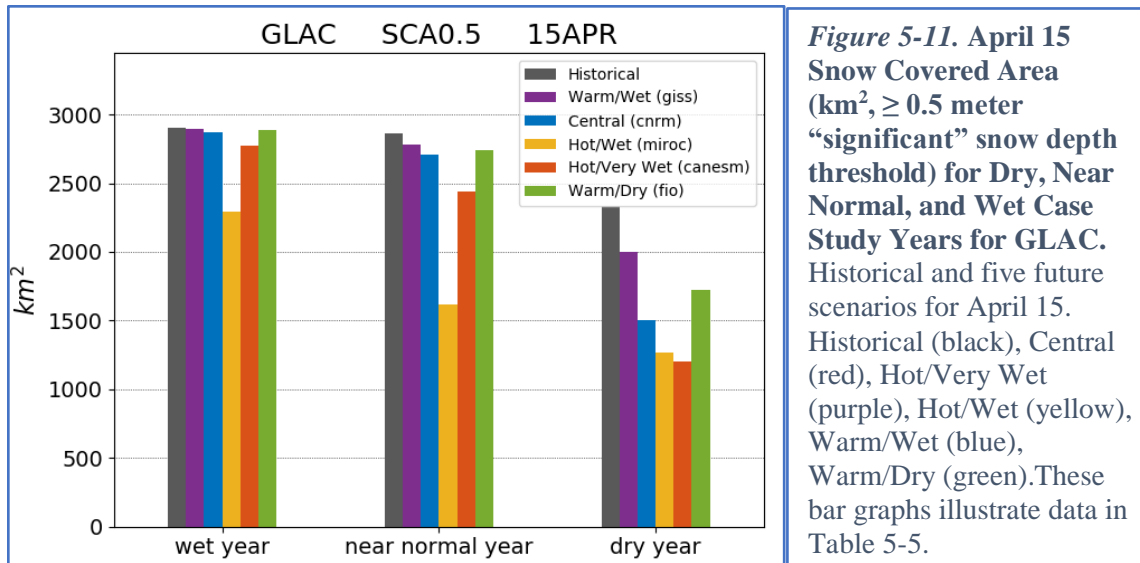


Figure 5-10. Historical and projected May 15th Snow Water Equivalent (m) for a representative Dry year in GLAC. Historical simulation year 2005 (wet year, top left), and three future scenarios applied to 2005: b) the warm/wet (giss) scenario results in the lowest change in SWE (top right), c) the central scenario (cnrm) results in a moderate change in SWE (bottom left), and the, d) hot/wet scenario (miroc) results in the greatest change in SWE (bottom right). A color ramp indicates SWE 0-2m at each model gridcell. These projected snow maps illustrate what the snowpack in a dry year like 2005 would look like in the 2040's through 2070's under these scenarios of climate change. In May, snow depth = 2.5 x SWE. Scenarios are listed in Table 5-3 and shown in Figure 5-7, maps for additional scenarios are provided in the Supplementary Material (S5-8). Table 5-4 provides numerical values for (SWE historical average (2000-2013) and five future scenarios.



5.11.2 Area and Number of years with ≥ 0.5 m Snow Depth

Because of interest in wolverine denning sites, we analyze snow depth ≥ 0.5 m, which we will also refer to as “significant snow” to contrast with the emphasis on light snow in McKelvey et al (2011) and in the previous section. Figure 5-12 shows the area with snow depth ≥ 0.5 m on April 15th and May 15th in the study area for the dry, near normal, and wet years. Because of the higher threshold for snow, the effects are somewhat larger than for the light snow threshold. This is particularly evident in the dry year, which has a 50% decline on May 15 for four of the future scenarios. The numerical values of snowcovered area at the ≥ 0.5 m threshold are shown in Table 5-5 for all years, as well as percent changes for these quantities.

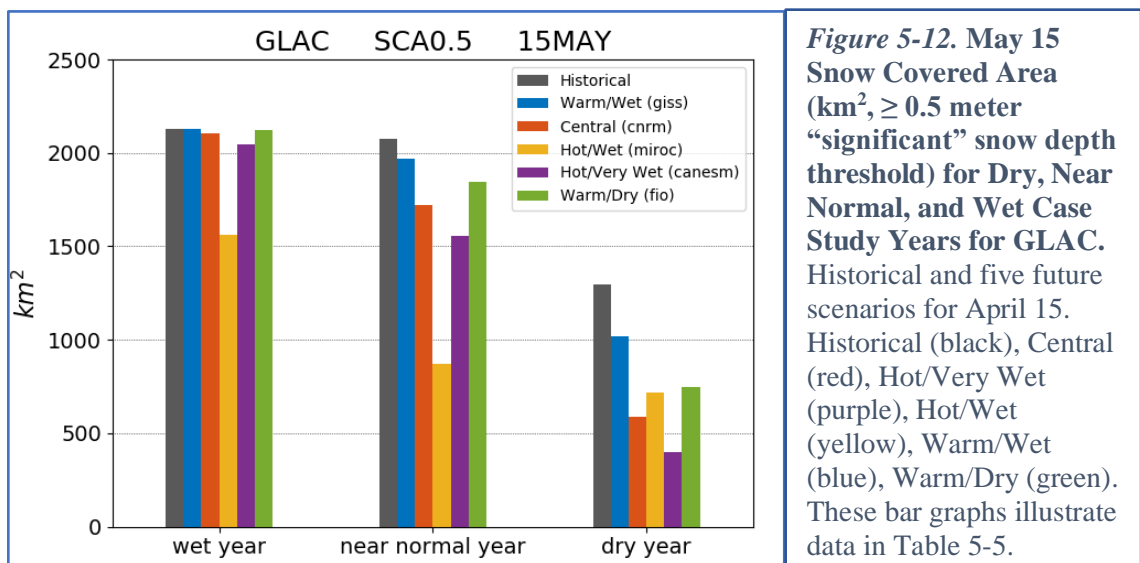


Figure 5-13 shows a map of the number of years (out of 16 possible) where each model pixel had ≥ 0.5 m of snow depth on May 15. This number-of-years statistic is analogous to that used by the Copeland study, except that there are more years of data, and these maps use a much higher threshold of snow. The projections show declines in the number of years with significant snow. The areas with frequent (14-16 years) availability of significant snow become concentrated in smaller, relatively higher elevation areas within the study domains.

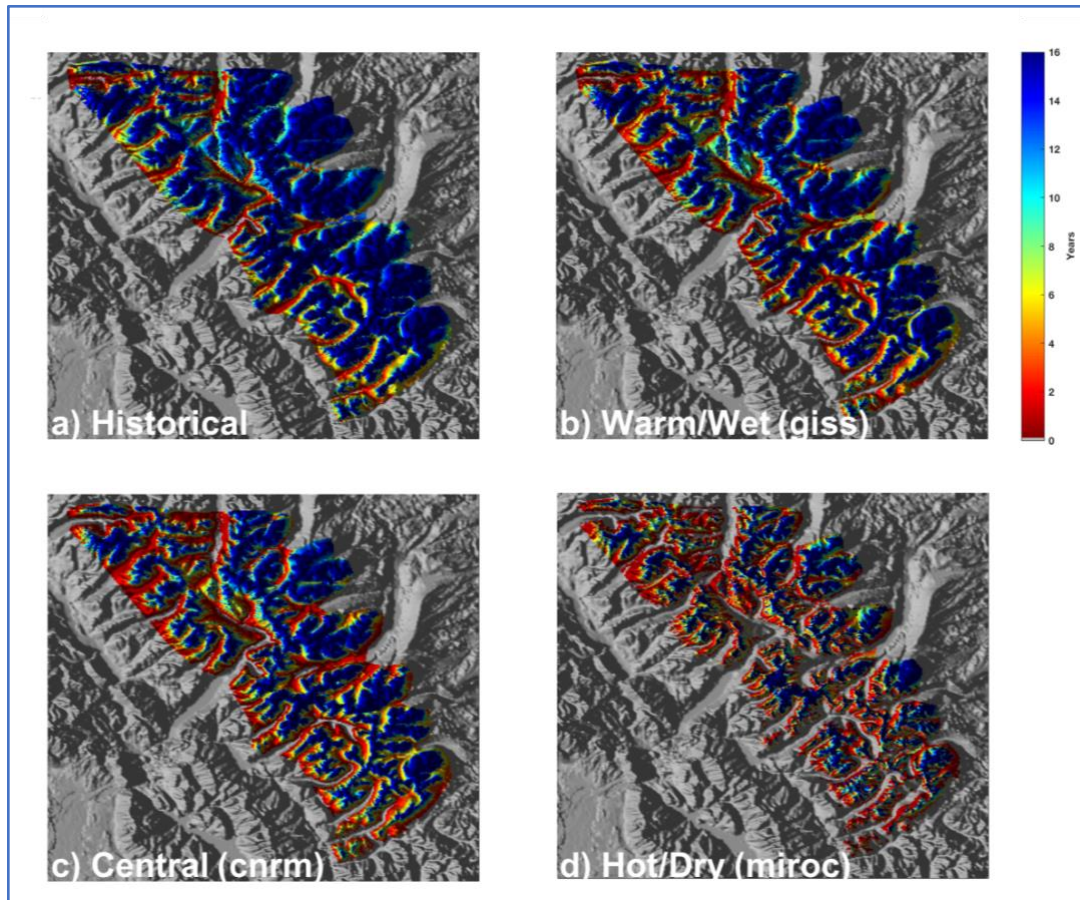


Figure 5-13. Number of years (out of 1998-2013) with Snow Depth ≥ 0.5 m on May 15th for GLAC. Historical simulation compared to the Warm/Wet (giss), Central(cnrm), and Hot/Wet(miroc) future scenarios at each model gridcell. Scenarios are described in Table 5-3. In May, snow depth = 2.5 x SWE.

The effects of climate change on snow melt have been presented as analogous to a “time shifting” of the melt season earlier in the year. For example, McKelvey used the May 31 vs. May 15 snowcovered area as a proxy for a 2-week shift in the melt season. Figure 5-14 contrasts the evolution of the snowpack with respect to the number of years with significant snow from April 15th to May 15th in the historical simulations (Top Row) with the Warm/Wet scenario (Middle Row) and Hot/Wet (Bottom Row) scenarios. We see that the Warm/Wet scenario, shows the least change in the number of years compared to the historic snowcover in terms of the availability of significant snow. In contrast, under the Hot/Wet scenario, the number of years that significant snowpack occurs on April 15th has been diminished well below the level of the historic May 15th snowpack – more than a month shift (Figure 5-14).

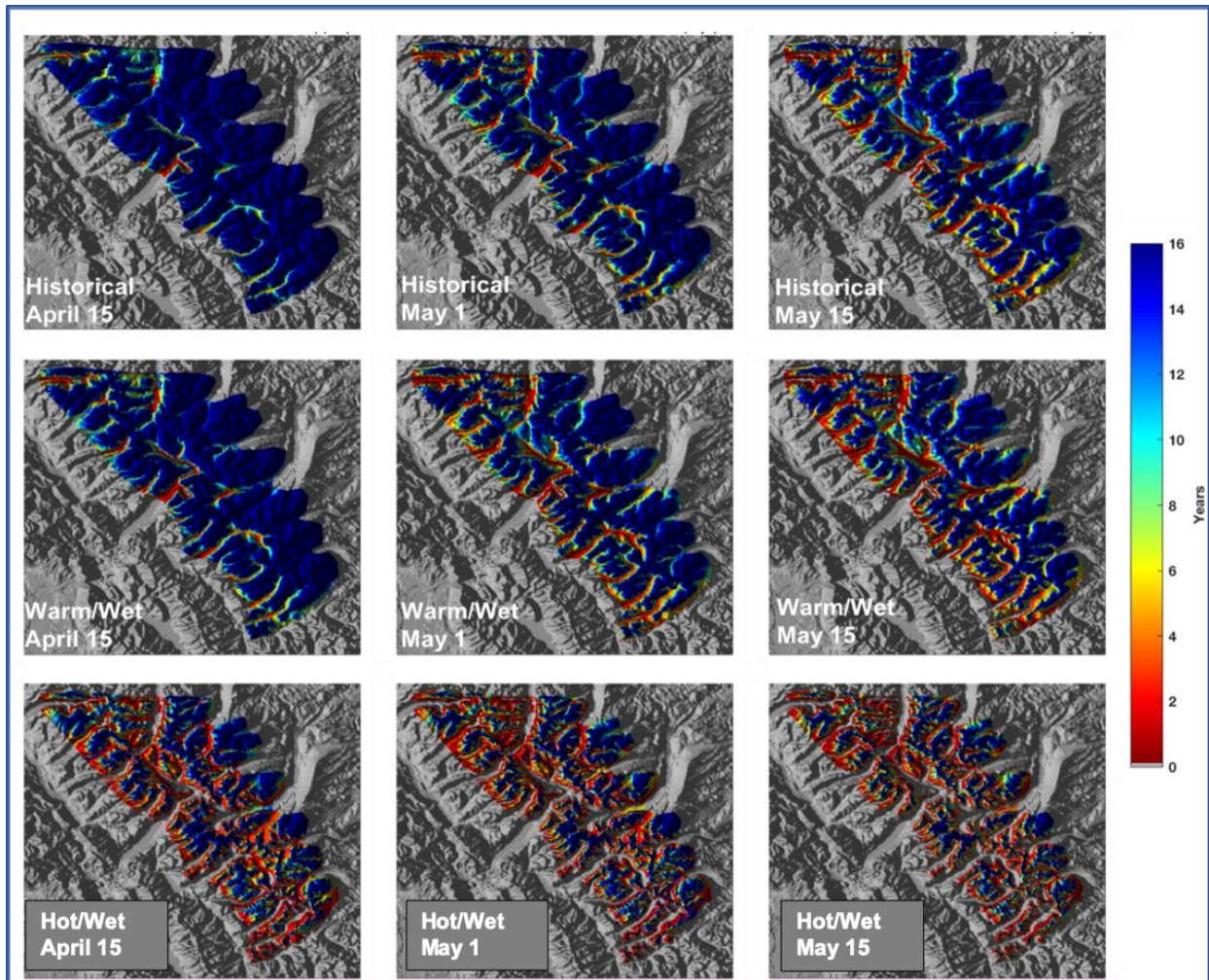


Figure 5-14. Number of years (out of 1998-2013) with Snow Depth ≥ 0.5 m on April 15, May 1 and May 15 for historic and two future climate scenarios for GLAC. The “number of years” indicates the yearly availability of deep snow at each model gridcell across all years in the DHSVM simulations, including wet, dry, and near normal years. The three columns are for three dates: April 15th(left column), May 1st(middle column), and May 15th(right column). Middle Row: Warm/Wet future scenario (giss, “Least Change”) at the same dates, Bottom Row: Hot/Wet future scenario (miroc, “Greatest Change”) at the same dates. The reduction in the number of years on May 1 for each future scenario can be compared to the historical simulation at a later calendar date, showing a < 2 week shift for the Warm/Wet scenario and a > 1 month shift for the Hot/Wet scenario. Scenarios are listed in Table 5-3.

GLAC		Snow Covered Area sq-km (5 mm SWE threshold)																	
Scenario	1998	1999	2000	2001	2002	2003	2004	2005	2006	2007	2008	2009	2010	2011	2012	2013	Average	Median	
15-Apr	historical	2838	2876	2901	2886	2901	2869	2772	2615	2836	2784	2899	2900	2853	2901	2892	2890	2851	2881
	Central (cnrm)	2301	2732	2901	2804	2879	2708	2278	2067	2500	2297	2849	2870	2604	2897	2748	2743	2649	2737
	Hot/Very Wet (cansm)	2080	2342	2900	2589	2748	2288	1784	1630	1972	1714	2610	2695	2177	2839	2215	2405	2312	2315
	Hot/Wet (miroc)	2043	2069	2210	2326	2161	2419	1489	1993	2087	2020	2753	2245	2200	2591	1766	2700	2192	2181
	Warm/Wet (giss)	2697	2819	2901	2840	2887	2769	2578	2361	2677	2572	2881	2885	2706	2901	2827	2828	2758	2823
Warm/Dry (fio)	2604	2735	2901	2839	2887	2808	2469	2176	2634	2490	2867	2883	2712	2900	2848	2785	2721	2797	
1-May	historical	2625	2814	2707	2818	2892	2608	2494	2694	2563	2888	2901	2598	2901	2775	2861	2745	2782	
	Central (cnrm)	1978	2433	2160	2505	2820	2405	1657	2072	1917	2773	2882	2008	2887	2202	2619	2327	2303	
	Hot/Very Wet (cansm)	1578	2039	1815	1985	2580	1899	1400	1287	1633	1271	2499	2792	1419	2813	1730	2249	1938	1857
	Hot/Wet (miroc)	1828	1865	1806	1843	1731	2214	1324	2354	1721	1727	2655	2129	1845	2542	1374	2319	1955	1844
	Warm/Wet (giss)	2327	2653	2482	2647	2861	2556	2293	2142	2416	2204	2854	2896	2276	2901	2529	2739	2548	2543
Warm/Dry (fio)	2256	2522	2301	2634	2832	2628	2214	1906	2337	2172	2824	2892	2257	2900	2531	2697	2494	2526	
15-May	historical	1658	2756	2516	2413	2875	2383	2211	2460	1865	2825	2838	2488	2900	2595	2597	2505	2555	
	Central (cnrm)	918	2232	1832	1814	2664	2156	1572	1296	1652	1105	2457	2534	1813	2818	1816	1844	1908	1824
	Hot/Very Wet (cansm)	859	1948	1568	1409	2434	1703	1197	1007	1381	749	2241	2261	1259	2684	1468	1664	1614	1518
	Hot/Wet (miroc)	1414	1611	1223	1305	1476	2070	1053	1597	1396	1266	2391	1781	1731	2373	1119	1960	1610	1537
	Warm/Wet (giss)	1342	2562	2220	2109	2810	2413	2068	1829	2099	1455	2693	2714	2152	2883	2250	2342	2246	2235
Warm/Dry (fio)	1166	2378	2045	1994	2729	2456	1870	1564	1953	1338	2588	2659	2073	2866	2171	2053	2119	2063	
GLAC		Snow Covered Area % change (5 mm SWE threshold)																	
Scenario	1998	1999	2000	2001	2002	2003	2004	2005	2006	2007	2008	2009	2010	2011	2012	2013	Average	Median	
15-Apr	Central (cnrm)	-12	-5	0	-3	-1	-6	-18	-21	-12	-17	-2	-1	-9	0	-5	-5	-7	-5
	Hot/Very Wet (cansm)	27	19	0	10	5	20	36	38	30	38	10	7	24	2	23	17	-19	-20
	Hot/Wet (miroc)	-28	-28	-24	-19	-25	-16	-46	-24	-26	-27	-5	-23	-23	-11	-39	-7	-23	-24
	Warm/Wet (giss)	-5	-2	0	-2	0	-3	-7	-10	-6	-8	-1	-1	-5	0	-2	-2	-3	-2
	Warm/Dry (fio)	-8	-5	0	-2	0	-2	-11	-17	-7	-11	-1	-1	-5	0	-2	-4	-5	-3
1-May	Central (cnrm)	26	14	20	11	2	14	25	34	23	25	4	1	23	0	21	8	-15	-17
	Hot/Very Wet (cansm)	-40	-27	-33	-30	-11	-32	-46	-48	-39	-50	-13	-4	-45	-3	-38	-21	-29	-33
	Hot/Wet (miroc)	-30	-34	-33	-35	-40	-21	-49	-6	-36	-33	-8	-27	-29	-12	-50	-19	-29	-34
	Warm/Wet (giss)	-11	-6	-8	-6	-1	-8	-12	-14	-10	-14	-1	0	-12	0	-9	-4	-7	-9
	Warm/Dry (fio)	-14	-10	-15	-7	-2	-6	-15	-24	-13	-15	-2	0	-13	0	-9	-6	-9	-9
15-May	Central (cnrm)	45	19	27	25	7	20	34	41	33	41	13	11	27	3	30	29	-24	-29
	Hot/Very Wet (cansm)	-48	-29	-38	-42	-15	-37	-50	-55	-44	-60	-21	-20	-49	-7	-43	-36	-36	-41
	Hot/Wet (miroc)	-15	-42	-51	-46	-49	-23	-56	-28	-43	-32	-15	-37	-30	-18	-57	-25	-36	-40
	Warm/Wet (giss)	-19	-7	-12	-13	-2	-10	-13	-17	-15	-22	-5	-4	-13	-1	-13	-10	-10	-13
	Warm/Dry (fio)	-30	-14	-19	-17	-5	-9	-22	-29	-21	-28	-8	-6	-17	-1	-16	-21	-15	-19

Table 5-4: GLAC Snowcovered Area (5 mm SWE threshold) Top: Area (km²) in historical average (2000-2013) and five future scenarios. Bottom: percent change in future simulations compared to historical. Average and Median values also shown. The representative dry year is 2005, wet is 2011, and near normal is 2009.

GLAC	Scenario	Snow Covered Area sq-km (0.5 m depth threshold)													2013 Average	Median			
		1998	1999	2000	2001	2002	2003	2004	2005	2006	2007	2008	2009	2010			2011	2012	
15-Apr	historical	2628	2801	2708	2826	2876	2733	2532	2338	2650	2484	2830	2866	2380	2901	2833	2797	2699	2765
	Central (cnmm)	2047	2444	2202	2577	2753	2387	1889	1502	2077	1933	2574	2705	1858	2871	2454	2414	2293	2400
	Hot/Very Wet (canesm)	1730	2121	1904	2081	2153	1922	1403	1263	1674	1339	2365	2437	1298	2774	1932	2047	1922	1927
	Hot/Wet (miroc)	1406	1171	1339	1530	1265	1989	1078	1265	1354	1439	2349	1619	1176	2290	1280	1569	1520	1422
	Warm/Wet (giss)	2402	2647	2525	2683	2829	2530	2251	2004	2405	2197	2732	2785	2152	2899	2660	2633	2521	2581
	Warm/Dry (fio)	2269	2445	2279	2647	2730	2584	2084	1720	2278	2072	2588	2745	1874	2890	2662	2499	2398	2472
1-May	historical	1970	2638	2380	2468	2855	2537	2235	2062	2324	1906	2704	2777	2011	2901	2544	2680	2437	2503
	Central (cnmm)	1296	2045	1744	2058	2588	1976	1481	1265	1569	1332	2371	2523	1393	2856	1791	2118	1900	1884
	Hot/Very Wet (canesm)	1139	1783	1470	1535	2313	1494	1056	970	1325	852	2152	2191	995	2725	1418	1811	1577	1482
	Hot/Wet (miroc)	1159	1142	1175	1089	1015	1767	922	1181	1037	1077	1826	1581	1056	2229	888	1582	1295	1150
	Warm/Wet (giss)	1621	2399	2060	2187	2726	2168	1845	1709	1941	1510	2537	2626	1707	2893	2167	2449	2159	2167
	Warm/Dry (fio)	1491	2153	1880	2105	2645	2249	1698	1435	1790	1446	2402	2560	1455	2880	2103	2237	2033	2104
15-May	historical	1043	2593	2152	1708	2778	2360	1922	1670	2035	1224	2479	2625	1956	2886	2274	2227	2121	2189
	Central (cnmm)	496	1927	1457	1231	2377	1690	1160	927	1236	648	1882	2101	1312	2710	1459	1401	1501	1429
	Hot/Very Wet (canesm)	521	1724	1283	963	2151	1321	870	724	1116	450	1838	1922	975	2556	1179	1339	1308	1231
	Hot/Wet (miroc)	899	1046	761	706	908	1655	634	1035	818	770	1572	1208	1161	1975	748	1215	1069	972
	Warm/Wet (giss)	833	2346	1819	1455	2619	1990	1577	1374	1646	932	2270	2418	1683	2838	1861	1950	1851	1840
	Warm/Dry (fio)	623	2077	1611	1284	2506	2002	1382	1096	1437	778	2003	2361	1398	2785	1752	1528	1658	1570
GLAC	Scenario	Snow Covered Area % change (0.5 m depth threshold)													2013 Average	Median			
		1998	1999	2000	2001	2002	2003	2004	2005	2006	2007	2008	2009	2010			2011	2012	
15-Apr	Central (cnmm)	-22	-13	-19	-9	-4	-13	-25	-36	-22	-22	-9	-6	-22	-1	-13	-14	-15	-13
	Hot/Very Wet (canesm)	-34	-24	-30	-26	-13	-30	-45	-49	-37	-46	-16	-15	-45	-4	-32	-27	-29	-30
	Hot/Wet (miroc)	-47	-58	-43	-46	-56	-27	-57	-46	-49	-42	-17	-44	-51	-21	-55	-44	-44	-49
	Warm/Wet (giss)	-9	-6	-7	-5	-2	-7	-11	-14	-9	-12	-3	-3	-10	0	-6	-6	-7	-7
	Warm/Dry (fio)	-14	-13	-16	-6	-5	-5	-18	-26	-14	-17	-9	-4	-21	0	-6	-11	-11	-11
1-May	Central (cnmm)	-34	-22	-27	-17	-9	-22	-34	-39	-32	-30	-12	-9	-31	-2	-30	-21	-22	-25
	Hot/Very Wet (canesm)	-42	-32	-38	-38	-19	-41	-53	-53	-43	-55	-20	-21	-51	-6	-44	-32	-35	-41
	Hot/Wet (miroc)	-41	-57	-51	-56	-64	-30	-59	-43	-55	-43	-32	-43	-47	-23	-65	-41	-47	-54
	Warm/Wet (giss)	-18	-9	-13	-11	-5	-15	-17	-17	-16	-21	-6	-5	-15	0	-15	-9	-11	-13
	Warm/Dry (fio)	-24	-18	-21	-15	-7	-11	-24	-30	-23	-24	-11	-8	-28	-1	-17	-17	-17	-16
15-May	Central (cnmm)	-52	-26	-32	-28	-14	-28	-40	-44	-39	-47	-24	-20	-33	-6	-36	-37	-29	-35
	Hot/Very Wet (canesm)	50	34	40	44	23	44	55	57	45	63	26	27	50	11	48	40	-38	-44
	Hot/Wet (miroc)	-14	-60	-65	-59	-67	-30	-67	-38	-60	-37	-37	-54	-41	-32	-67	-45	-50	-56
	Warm/Wet (giss)	-20	-10	-13	-15	-6	-16	-18	-18	-19	-24	-8	-8	-14	-2	-18	-12	-13	-16
	Warm/Dry (fio)	-40	-20	-25	-25	-10	-15	-28	-34	-29	-36	-19	-14	-29	-4	-23	-31	-22	-28

Table 5-5: GLAC Snowcovered Area (0.5 m snow depth threshold) Top: Area (km²) in historical average (2000-2013) and five future scenarios. Bottom: percent change in future simulations compared to historical. Average and Median values also shown. Figures 5-11 and 5-12 illustrate these quantities in bar graphs. The representative dry year is 2005, wet is 2011, and near normal is 2009.

5.12 ROMO Study Area

This section presents SWE and SCA for representative years, area and number of years with snow depth threshold ≥ 0.5 m, with figures and tables analogous to those for GLAC. The elevation dependence of snow for ROMO is discussed in Section 5-13. On average, the ROMO study area exhibits a change of +1% to -16% in the area with significant snowcover (depth > 0.5 m) on April 15th compared to the 2000-2013 historic average, and a decline of 6-38 percent for May 15th for the scenarios considered (see Tables 5-6, 5-7).

5.12.1 SWE and Snowcovered Area for representative years

Figure 5-15 shows DHSVM model simulated SWE on May 15th for the wet representative year (2011). The historical simulation is shown along with three of the five future scenarios, chosen to represent the central scenario (cnrm), the greatest change in snowpack (Hot/Dry, hadgem2) and the least change (Warm/Wet, giss). The future scenarios answer the question “what would the snowpack in a wet year (like 2011) look like in the 2040’s through 2070’s under these scenarios of climate change.” Note that the “greatest snowpack change” scenario is different for ROMO than for GLAC. We have included Hot/Dry as well as a Warm/Dry scenario in the choice of scenarios for ROMO because a significant number of climate models project drying conditions in ROMO, whereas in GLAC, the vast majority of climate models predict a wetter future (see Fig 5-7).

Figures 5-16 and 5-17 shows SWE for the “Near Normal” (2009) and “Dry” (2002) year. One can see that in the dry year, the snowcover is already very low even in the historical simulation with maximum SWE in the domain approximately of ~ 0.5 m on May 15th compared to values of ~ 1.0 m for the wet year.

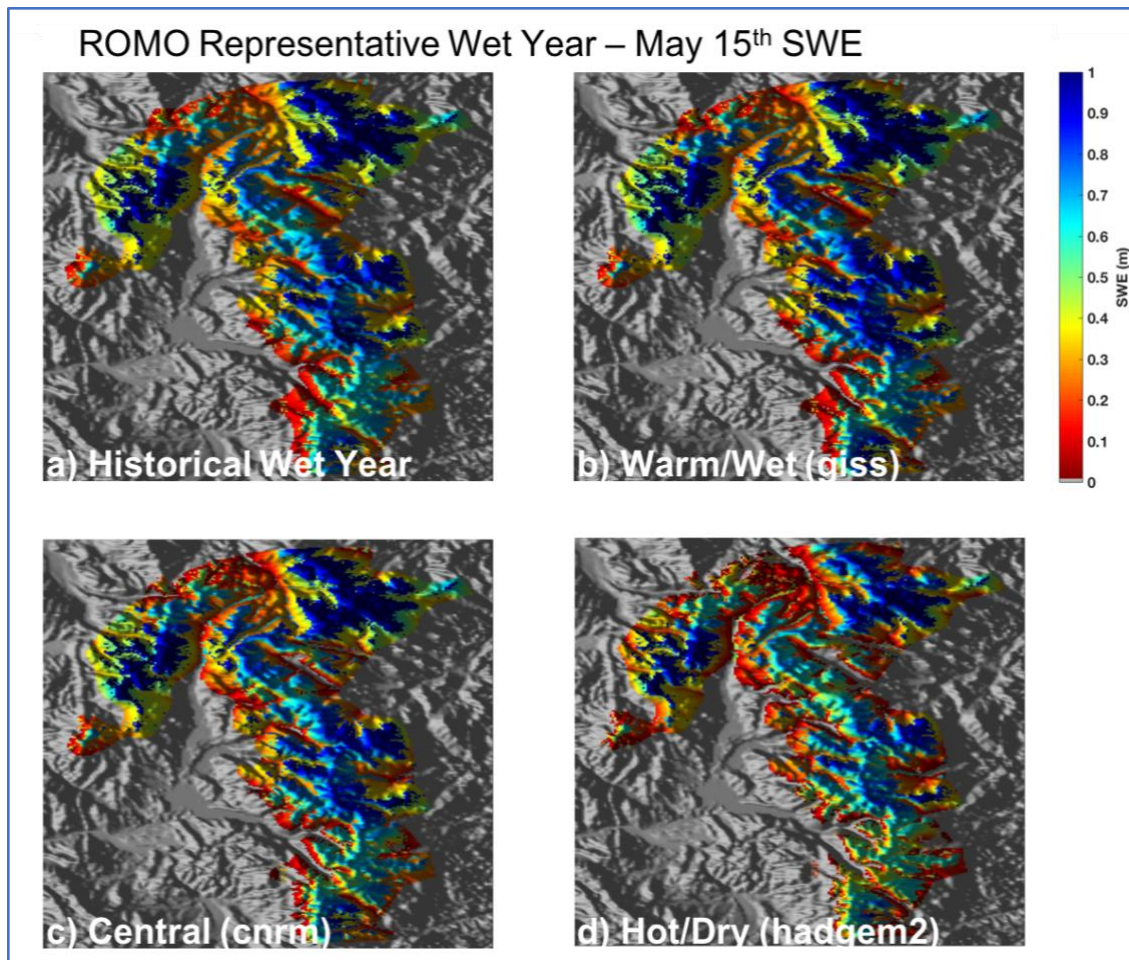


Figure 5-15. Historical and projected May 15th Snow Water Equivalent (m) for a Representative Wet Year in ROMO. Historical simulation year 2011 (wet year, top left), and for three future scenarios applied to 2011: b) the warm/wet (giss) scenario results in the least change in SWE of all six scenarios considered (top right), c) the central scenario (cnrm) results in a moderate change in SWE (bottom left), and the, d) hot/wet scenario (hadgem2) results in the greatest change in SWE (bottom right). A color ramp indicates 0-2m at each model gridcell. In May, snow depth = 2.5 x SWE. Note that while the GCMs for warm/wet and central are the same in GLAC and ROMO, the GCM for the hot/dry scenario is different (hadgem2 vs miroc), to better represent the range of the GCMs (see Fig 5-7 and section 5-8). The GCM for the hot/dry scenario is also different (hadgem2 vs miroc), to better represent the range of the GCMs. These projected snow maps illustrate what the snowpack in a wet year like 2011 would look like in the 2040's through 2070's under these scenarios of climate change. Scenarios are listed in Table 5-3 and shown in Figure 5-7. See S5-8 in the Supplementary Material for maps with additional scenarios. Table 5-4 provides numerical values for SWE historical average (2000-2013) and five future scenarios.

ROMO Representative Near Normal Year – May 15th SWE

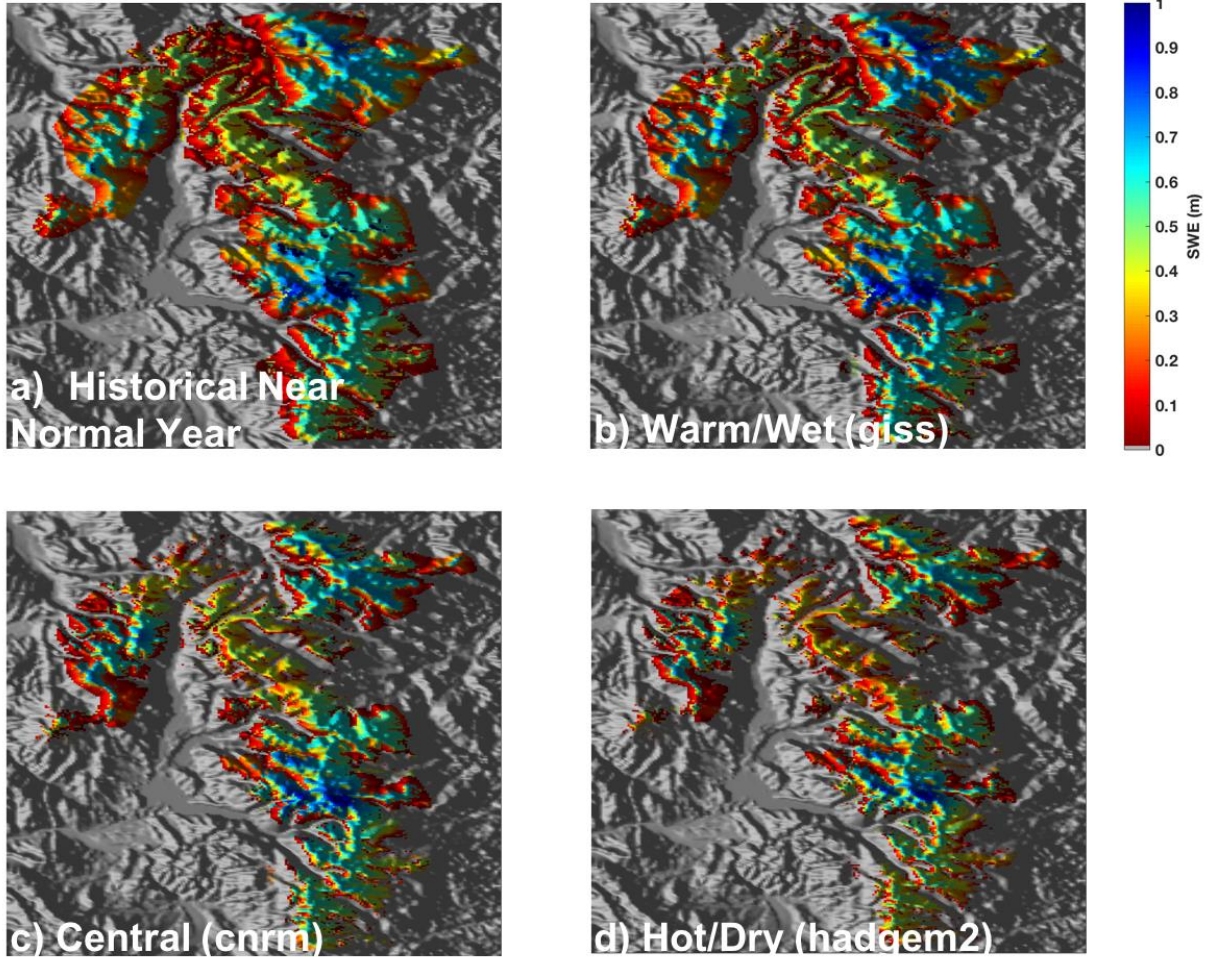


Figure 5-16. Historical and projected May 15th Snow Water Equivalent (m) for a Representative Near Normal Year in ROMO. Historical simulation year 2011 (wet year, top left), and for three future scenarios applied to 2011: b) the warm/wet (giss) scenario results in the least change in SWE of all six scenarios considered (top right), c) the central scenario (cnrm) results in a moderate change in SWE (bottom left), and the, d) hot/wet scenario (hadgem2) results in the greatest change in SWE (bottom right). Note that while the representative wet year is the same in GLAC and ROMO, the representative dry and near normal years differ based on climatology (see section 3-3). These projected snow maps illustrate what the snowpack in a near normal year like 2011 would look like in the 2040's through 2070's under these scenarios of climate change. Scenarios are listed in Table 5-3 and shown in Figure 5-7, maps for additional scenarios are provided in the Supplementary Material. Table 5-4 provides numerical values for SWE historical average (2000-2013) and five future scenarios.

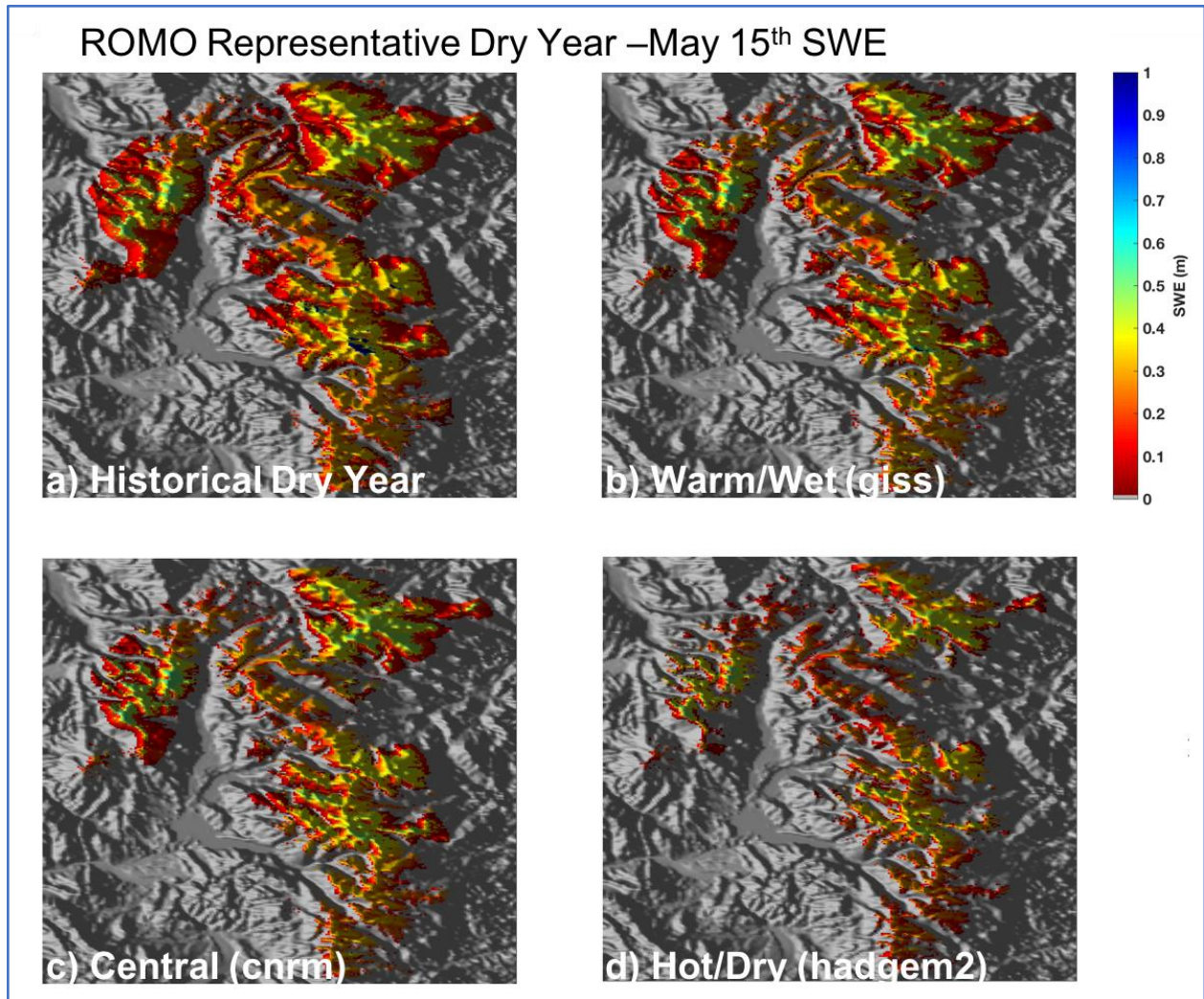


Figure 5-17. Historical and projected May 15th Snow Water Equivalent (m) for a Representative Dry in ROMO. Historical simulation year 2002 (wet year, top left), and for three future scenarios applied to 2002: b) the warm/wet (giss) scenario results in the least change in SWE of all six scenarios considered (top right), c) the central scenario (cnrm) results in a moderate change in SWE (bottom left), and the, d) hot/wet scenario (hadgem2) results in the greatest change in SWE (bottom right). Note that while the representative wet year is the same in GLAC and ROMO, the representative dry and near normal years differ based on climatology (see section 3-3). These projected snow maps illustrate what the snowpack in a dry year like 2002 would look like in the 2040's through 2070's under these scenarios of climate change. Scenarios are listed in Table 5-3 and shown in Figure 5-7, maps for additional scenarios are provided in the Supplementary Material. Table 5-4 provides numerical values for SWE historical average (2000-2013) and five future scenarios.

Figure 5-18 summarizes the results in terms of the total snowcovered area (km^2) within the study area polygon. In this case, the threshold used is 5mm of SWE, representing a light snowcover, and for May 15th, comparable to the results in McKelvey. Comparing the Wet and Dry years we see a more complicated pattern emerge. As in GLAC the wet year (2011) is less vulnerable to climate change in terms of percentage of area lost. Unlike GLAC, the near normal year (2007) shows large percentage declines, comparable to those of the dry year 2002. The numerical values of snowcovered area for all years, as well as percent changes for these quantities are shown in Table 5-7. **On average, the ROMO study area exhibits a change of +1% to -16% in area with significant snowcover (depth > 0.5 m) for April 15th compared to the 2000-2013 historic average, and a decline of 6-38 percent for April 15th for the scenarios considered (Tables 5-6, 5-7).**

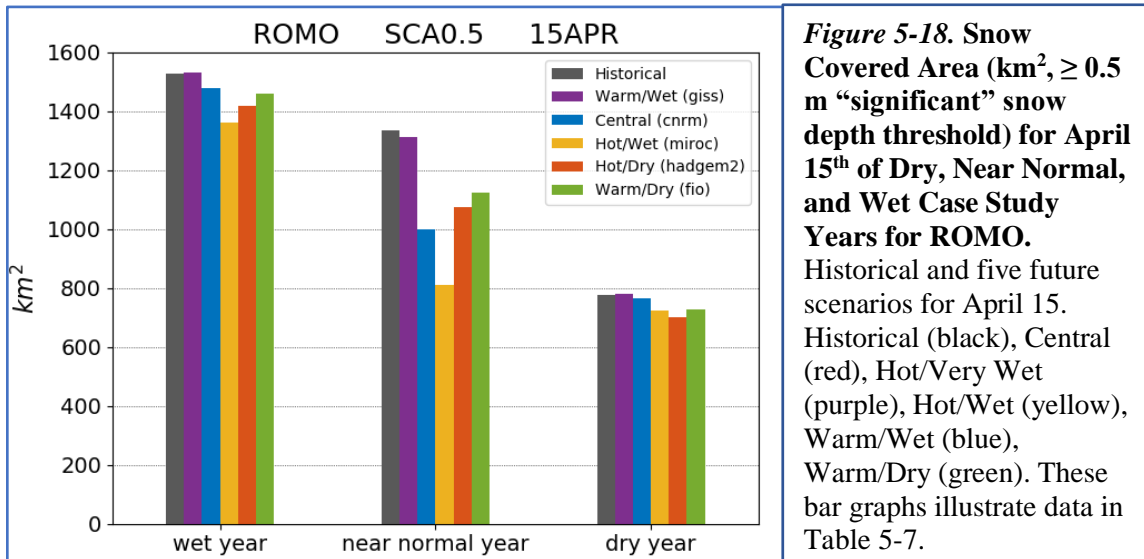


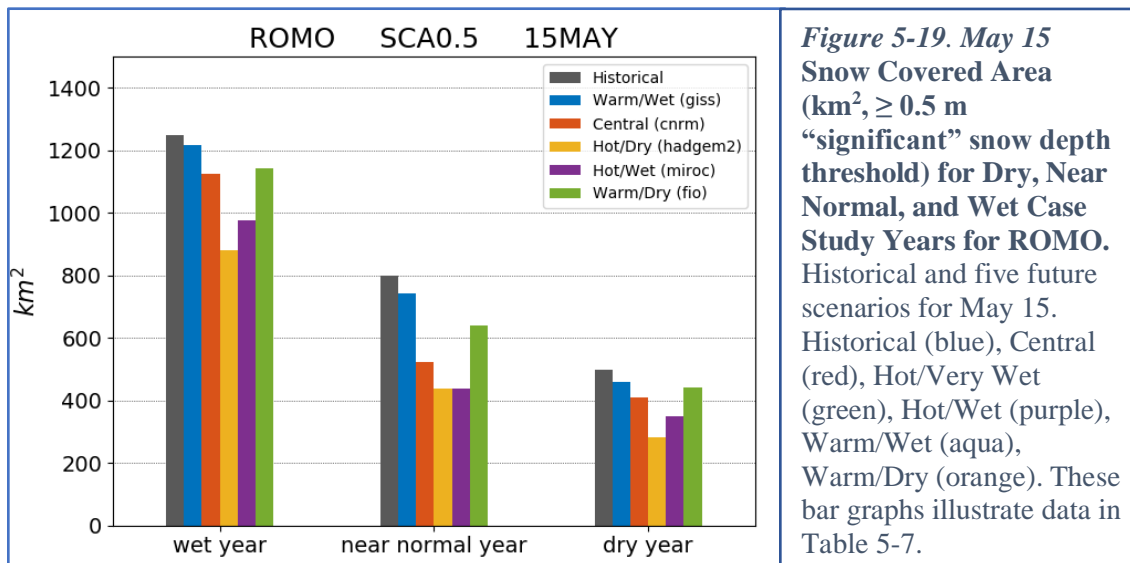
Figure 5-18. Snow Covered Area (km^2 , ≥ 0.5 m “significant” snow depth threshold) for April 15th of Dry, Near Normal, and Wet Case Study Years for ROMO. Historical and five future scenarios for April 15. Historical (black), Central (red), Hot/Very Wet (purple), Hot/Wet (yellow), Warm/Wet (blue), Warm/Dry (green). These bar graphs illustrate data in Table 5-7.

ROMO		Snow Covered Area sq-km (5 mm SWE threshold)																	
Scenario	1998	1999	2000	2001	2002	2003	2004	2005	2006	2007	2008	2009	2010	2011	2012	2013	Average	Median	
15-Apr	Historical	1575	1522	1575	1593	1564	1596	1433	1593	1590	1587	1597	1583	1594	1583	1595	1561	1587	
	Central (cnrm)	1442	1348	1486	1519	1428	1590	1026	1550	1536	1447	1596	1495	1526	1582	1105	1590	1454	1507
	Hot/Dry (hadgem2)	1317	1199	1405	1491	1246	1575	917	1496	1530	1475	1595	1463	1485	1569	806	1578	1384	1480
	Hot/Very Wet (miroc)	1123	944	1248	1360	1208	1528	1478	1439	1486	1094	1586	1275	1351	1505	1010	1589	1282	1313
	Warm/Wet (giss)	1539	1486	1555	1585	1507	1595	1253	1584	1586	1576	1597	1573	1582	1593	1251	1594	1528	1579
Warm/Dry (fio)	1509	1438	1552	1572	1508	1593	1122	1579	1580	1552	1597	1557	1557	1591	1206	1594	1507	1557	
1-May	Historical	1557	1519	1537	1546	1417	1592	1368	1596	1564	1568	1596	1573	1542	1594	1058	1593	1514	1560
	Central (cnrm)	1367	1274	1380	1256	1125	1559	957	1569	1394	1296	1590	1441	1387	1576	735	1538	1340	1384
	Hot/Dry (hadgem2)	1180	1073	1135	1096	900	1486	829	1306	1230	1265	1577	1341	1172	1547	570	1491	1201	1215
	Hot/Very Wet (miroc)	1058	873	1075	1030	928	1449	726	1555	1238	979	1563	1172	1217	1494	475	1457	1143	1124
	Warm/Wet (giss)	1496	1442	1459	1460	1233	1583	1154	1584	1515	1520	1595	1549	1496	1591	887	1587	1447	1505
Warm/Dry (fio)	1460	1429	1486	1448	1262	1577	1055	1591	1516	1494	1594	1536	1452	1590	830	1582	1431	1490	
15-May	Historical	1463	1452	1173	1281	1245	1587	1041	1536	1507	1481	1590	1512	1516	1591	915	1574	1404	1494
	Central (cnrm)	1122	1148	895	906	926	1327	667	1316	1133	1047	1553	1185	1302	1535	612	1424	1145	1151
	Hot/Dry (hadgem2)	840	912	565	679	661	1376	479	982	945	922	1410	891	1039	1431	427	1144	919	917
	Hot/Very Wet (miroc)	885	751	700	779	754	1371	484	1117	1032	816	1485	943	1163	1424	403	1304	963	914
	Warm/Wet (giss)	1306	1335	993	1109	1040	1570	841	1420	1380	1355	1579	1401	1441	1580	762	1542	1291	1367
Warm/Dry (fio)	1290	1316	1023	1084	1063	1562	817	1433	1385	1317	1582	1410	1444	1578	723	1534	1285	1351	
ROMO		Snow Covered Area % change (5 mm SWE threshold)																	
Scenario	1998	1999	2000	2001	2002	2003	2004	2005	2006	2007	2008	2009	2010	2011	2012	2013	Average	Median	
15-Apr	Central (cnrm)	8	11	6	5	9	0	28	3	3	9	0	6	4	1	21	0	-7	-5
	Hot/Dry (hadgem2)	16	21	11	6	20	1	36	6	4	7	0	8	6	2	42	1	-11	-7
	Hot/Very Wet (miroc)	-29	-38	-21	-15	-23	-4	-42	-11	-10	-31	-1	-19	-15	-6	-27	0	-18	-17
	Warm/Wet (giss)	-2	-2	-1	0	-4	0	-13	-1	-1	-1	0	-1	0	0	-10	0	-2	0
	Warm/Dry (fio)	-4	-5	-1	-1	-4	0	-22	-1	-1	-2	0	-2	-2	0	-13	0	-3	-2
1-May	Central (cnrm)	12	16	10	19	21	2	30	2	11	17	0	8	10	1	31	3	-11	-11
	Hot/Dry (hadgem2)	-24	-29	-26	-29	-36	-7	-39	-18	-20	-19	-1	-15	-24	-3	-46	-6	-21	-22
	Hot/Very Wet (miroc)	-32	-43	-30	-33	-34	-9	-47	-3	-21	-38	-2	-26	-21	-6	-55	-9	-24	-28
	Warm/Wet (giss)	-4	-5	-5	-6	-13	-1	-16	-1	-3	-3	0	-2	-3	0	-15	0	-4	-4
	Warm/Dry (fio)	-6	-6	-3	-6	-11	-1	-23	0	-3	-5	0	-2	-6	0	-22	-1	-5	-5
15-May	Central (cnrm)	-23	-21	-24	-29	-26	-4	-36	-14	-23	-29	-2	-22	-14	-4	-33	-10	-18	-23
	Hot/Dry (hadgem2)	-43	-37	-52	-47	-47	-13	-54	-36	-37	-38	-11	-41	-31	-10	-53	-27	-35	-39
	Hot/Very Wet (miroc)	-40	-48	-40	-39	-39	-14	-53	-27	-32	-45	-7	-38	-23	-10	-56	-17	-31	-39
	Warm/Wet (giss)	11	8	15	13	17	1	19	8	8	9	1	7	5	1	17	2	-8	-9
	Warm/Dry (fio)	12	9	13	15	15	2	22	7	8	11	1	7	5	1	21	3	-8	-10

Table 5-6: ROMO Snowcovered Area (5 mm SWE threshold) Top: Area (km²) in historical average (2000-2013) and five future scenarios. Bottom: percent change in future simulations compared to historical. Average and Median values also shown. The representative dry year is 2002, wet is 2011, and near normal is 2007. The representative wet year is the same for both areas, but the wet and dry years are different.

5.12.2 Area and Number of years with ≥ 0.5 m Snow Depth

Because of interest in wolverine denning sites, we analyze snow depth ≥ 0.5 m, which we will refer to here as “significant snow.” Figure 5-19 shows the area with snow depth ≥ 0.5 m within the study area. Because of the more stringent threshold for snow, the effects are somewhat larger than for the light snowcover. The numerical values of snowcovered area at the ≥ 0.5 m threshold are shown in Table 5-7 for all years, as well as percent changes for these quantities. In this table, we note that dry years such as 2002 see increases in snowcovered area for the Hot/Very Wet and Warm/Wet scenarios. As in GLAC, dry years are somewhat buffered against change, and in fact can see increases in high-altitude “significant” snow for scenarios with increased precipitation. This is a result of the elevational dependence of snowpack change that will be discussed in the next sub-section.



ROMO		Snow Covered Area sq-km (0.5 m depth threshold)																	
Scenario		1998	1999	2000	2001	2002	2003	2004	2005	2006	2007	2008	2009	2010	2011	2012	2013	Average	Median
15-Apr	historical	1000	803	1176	1021	776	1571	924	1008	1178	1336	1536	1111	768	1529	710	935	1086	1014
	Central (cnrm)	914	727	1170	929	765	1475	757	1039	1023	999	1533	1035	747	1478	583	967	1009	983
	Hot/Dry (hadgem2)	796	660	963	922	699	1372	692	891	1042	1076	1482	994	737	1417	485	887	945	906
	Hot/Very Wet (mitroc)	781	588	948	897	724	1271	629	990	1071	811	1500	845	761	1361	426	1043	915	871
	Warm/Wet (giss)	1006	789	1184	1098	781	1553	862	1019	1217	1313	1559	1157	806	1531	677	1051	1100	1074
	Warm/Dry (fio)	823	690	1062	821	728	1499	742	817	960	1123	1442	987	700	1462	565	826	953	825
1-May	historical	871	852	1029	819	719	1536	841	987	983	1147	1365	1148	837	1519	594	1119	1024	985
	Central (cnrm)	835	747	944	713	661	1423	710	888	811	847	1286	980	769	1454	472	1052	912	841
	Hot/Dry (hadgem2)	742	636	742	672	561	1234	636	725	797	840	1136	817	703	1354	356	845	801	742
	Hot/Very Wet (mitroc)	736	596	772	694	595	1182	583	819	845	706	1251	825	759	1326	315	1105	819	766
	Warm/Wet (giss)	890	822	980	799	691	1521	782	915	981	1110	1406	1093	837	1510	541	1141	1000	938
	Warm/Dry (fio)	773	720	927	723	665	1464	716	792	800	965	1191	1004	762	1441	490	962	900	796
15-May	historical	852	864	705	712	681	1549	532	1017	943	995	1357	1005	981	1454	577	1041	954	962
	Central (cnrm)	738	699	569	556	569	1377	406	834	728	709	1151	744	854	1328	429	853	784	733
	Hot/Dry (hadgem2)	584	546	296	398	406	1104	238	611	640	610	925	505	691	1080	262	635	596	597
	Hot/Very Wet (mitroc)	636	558	451	534	497	1136	298	753	724	610	1110	627	818	1175	271	907	694	631
	Warm/Wet (giss)	809	797	629	670	632	1502	487	911	895	936	1320	902	957	1421	513	988	898	898
	Warm/Dry (fio)	753	721	608	617	610	1455	402	826	778	832	1190	866	859	1343	484	897	828	802
ROMO		Snow Covered Area % change (0.5 m depth threshold)																	
Scenario		1998	1999	2000	2001	2002	2003	2004	2005	2006	2007	2008	2009	2010	2011	2012	2013	Average	Median
15-Apr	Central (cnrm)	-9	-9	-1	-9	-1	-6	-18	3	-13	-25	0	-7	-3	-3	-18	3	-7	-3
	Hot/Dry (hadgem2)	-20	-18	-18	-10	-10	-13	-25	-12	-12	-19	-4	-11	-4	-7	-32	-5	-13	-11
	Hot/Very Wet (mitroc)	-22	-27	-19	-12	-7	-19	-32	-2	-9	-39	-2	-24	-1	-11	-40	12	-16	-14
	Warm/Wet (giss)	1	-2	1	8	1	-1	-7	1	3	-2	1	4	5	0	-5	12	1	6
	Warm/Dry (fio)	-18	-14	-10	-20	-6	-5	-20	-19	-19	-16	-6	-11	-9	-4	-20	-12	-12	-19
1-May	Central (cnrm)	4	12	8	13	8	9	16	10	17	26	6	15	8	4	21	6	-11	-15
	Hot/Dry (hadgem2)	-15	-25	-28	-18	-22	-19	-24	-27	-19	-27	-17	-29	-16	-11	-40	-24	-22	-25
	Hot/Very Wet (mitroc)	-15	-30	-25	-15	-17	-24	-31	-17	-14	-38	-8	-28	-9	-13	-47	-1	-20	-22
	Warm/Wet (giss)	2	3	7	3	4	2	7	7	0	3	3	5	0	1	9	2	-2	-5
	Warm/Dry (fio)	-11	-15	-10	-12	-7	-6	-15	-20	-19	-16	-13	-13	-9	-5	-18	-14	-12	-19
15-May	Central (cnrm)	13	19	19	22	17	11	24	18	23	29	15	26	13	9	26	18	-18	-24
	Hot/Dry (hadgem2)	-31	-37	-58	-44	-40	-29	-55	-40	-32	-39	-32	-50	-30	-26	-55	-39	-38	-38
	Hot/Very Wet (mitroc)	-25	-35	-36	-25	-27	-27	-44	-26	-23	-39	-18	-38	-17	-19	-53	-13	-27	-34
	Warm/Wet (giss)	5	8	11	6	7	3	9	10	5	6	3	10	2	2	11	5	-6	-7
	Warm/Dry (fio)	-12	-17	-14	-13	-10	-6	-25	-19	-17	-16	-12	-14	-14	-8	-16	-14	-13	-17

Table 5-7: ROMO Snowcovered Area (0.5 m snow depth threshold) Top: Area (km²) in historical average (2000-2013) and five future scenarios. Bottom: percent change in future simulations compared to historical. Average and Median values also shown. Figures 5-11 and 5-12 illustrate these quantities in bar graphs. The representative dry year is 2002, wet is 2011, and near normal is 2007.

Figure 5-20 shows a map of the number of years (out of 16 possible) where each model pixel had at least 0.5 m of snow depth on May 15th. This summary statistic is analogous to that used by the Copeland study, except that there are more years of data, and these maps use a much higher threshold of snow. The projections show declines in the number of years with significant snow. Visually, the changes depicted are more subtle than those for GLAC. The areas with frequent (14-16 years) availability of significant snow become concentrated in smaller, relatively higher elevation areas in the study area.

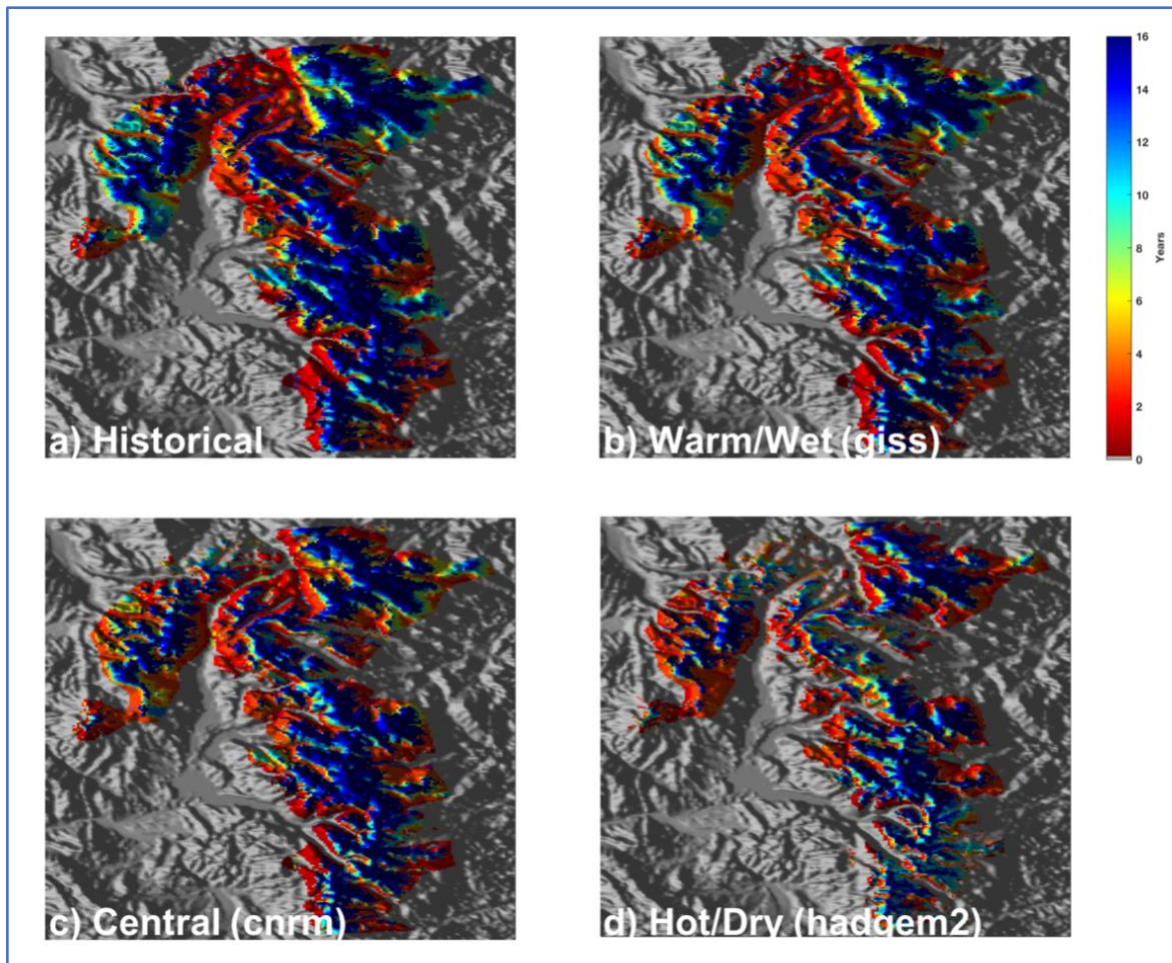


Figure 5-20. Number of years (out of 1998-2013) with Snow Depth ≥ 0.5 m on May 15th for ROMO. Historical simulation at each model gridcell compared to the Warm/Wet (giss), Central(cnrm), and Hot/Dry(hadgem2) future scenarios. Scenarios are described in Table 5-3. Note that scenarios were chosen independently for the two study areas.

The effects of climate change on snow melt have been presented as analogous to a “time shifting” of the melt season earlier in the year. For example, McKelvey (2011) used the May 31st vs. May 15th snowcovered area as a proxy for a 2-week shift in the melt season. Figure 5-21 contrasts the evolution of the snowpack with respect to the number of years with significant snow from April 15th to May 15th in the historical simulations (Top Row) with the Warm/Wet scenario (giss, Middle Row) and Hot/Wet (hadgem, Bottom Row) scenarios. We see that the Warm/Wet scenario, shows the least change in the number of years compared to the historic

snowcover in terms of the availability of significant snow. The Hot/Dry “greatest change” scenario, illustrates that the combination of drying and warming leads to very large declines in the persistence of snow that are evident by May 15th, however with smaller changes on April 15th and May 1st.

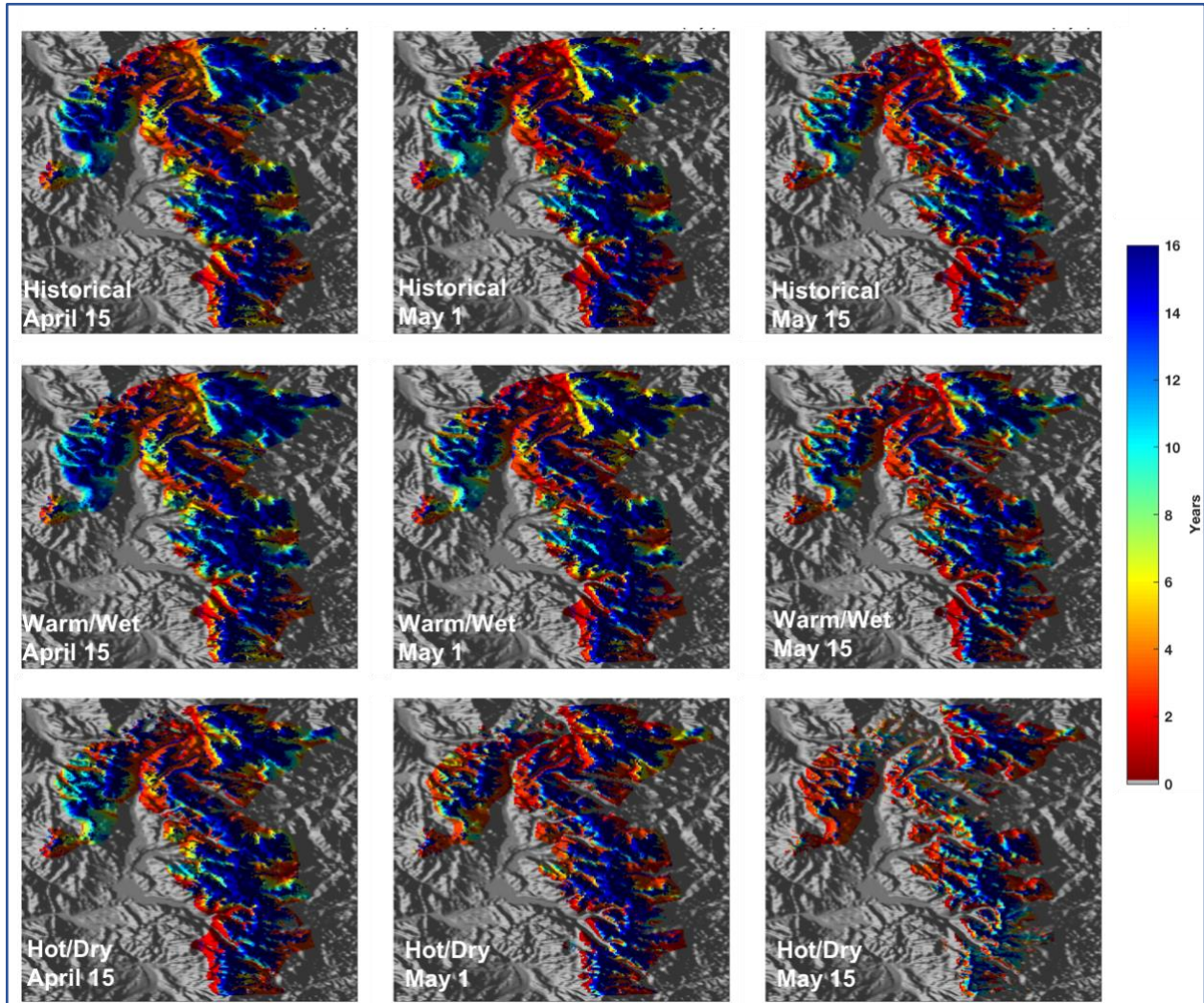


Figure 5-21. Number of years (out of 1998-2013) with Snow Depth ≥ 0.5 m for historic and two future climate scenarios for ROMO. The “number of years” indicates the yearly availability of deep snow at each model gridcell across all years in the DHSVM simulations, including wet, dry, and near normal years. Top Row: Historical Simulations on April 15th, May 1st, and May 15th. Middle Row: Warm/Wet future scenario (giss model, “Least Change”) at the same dates, Bottom Row: Hot/Dry future scenario (hadgem2 model, “Greatest Change”) at the same dates. The reduction in the number of years on May 1 for each future scenario can be compared to the historical simulation at a later calendar date, showing little shift for the Warm/Wet scenario and a > 2 week shift for the Hot/Dry scenario. Scenarios are listed in Table 5-3.

5.13 Elevation Dependence of Snowpack Change in the DHSVM model

Snowpack accumulation and melt depends critically on temperature and hence on elevation. In the Warm/Dry and Hot/Dry scenarios, both the reduction in precipitation and the warming act to reduce Spring snowpack. For the scenarios with warming and increased precipitation there are two countervailing forces that play out along an elevational gradient. A warmer, wetter future is one in which the freezing level and snow line tends to be higher, but with the potential for greater snowpack accumulation during the cold season at high elevations. The warming also tends to lead to an earlier snowmelt, so that the increased high-elevation snowpack is more evident early in the Springtime than later

Figure 5-22 shows the percent change in April 15 and May 15 snowcovered area (SCA; ≥ 0.5 meters depth) for GLAC, computed for 200 m elevation bands. The elevation of observed den sites is noted by triangles, with den sites ranging from approximately 1500m to 2300 m (personal communication, John Guinotte). For April 15 in mid-century, there is little change ($<20\%$) in SCA for 4 of the 5 scenarios above 2000m. There is loss of $\sim 60\%$ or greater of SCA below 1400m for 3 of the 5 scenarios. For May 15, there is $\sim 10\text{-}35\%$ loss in SCA above 2000m, and 4 of the 5 scenarios, and below 1400m there is loss of $\sim 60\%$ or greater in 4 of the 5 scenarios. Between these two elevations – and in the regions where most observations of dens have been observed – the snowpack change is very sensitive to elevation and to the particular future climate scenario. Most of the dens are at 1800 to 2000, below that band large losses predicted, above that elevation band minimal losses predicted except in maximum warming scenario. For May 1, see the supplementary material.

Figure 5-23 shows this elevation dependence measured in terms of snow water equivalent (SWE). Viewing snowpack in terms of SWE illustrates more clearly that the snowpack in the Hot/Very Wet future scenario has increased between 2300 – 2900 m elevation despite completely loss of snowpack at 1000m elevation. Comparing Figure 5-22 (SCA) with Figure 5-23 (SWE) illustrates that SWE can have modest declines without affecting the area with significant snow depth. The implication is that wet, cold climate of the GLAC study area can act as a “buffer” to change in the area of ≥ 0.5 meter deep snow on May 1st, at least at relatively high elevations within the study area. For May 1, see the supplementary material.

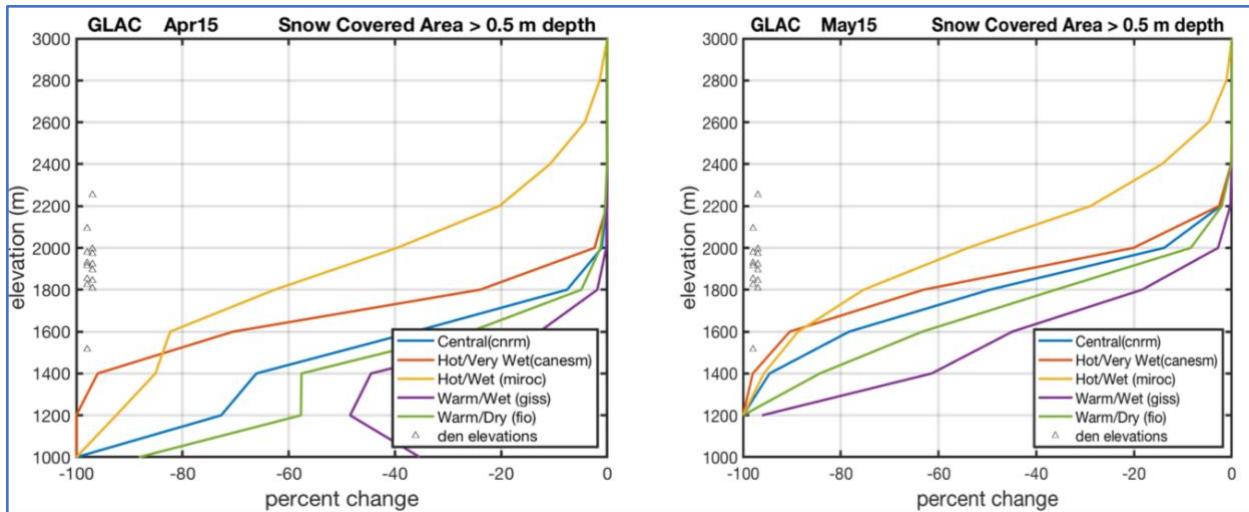


Figure 5-22. Elevation dependence of snow covered area (SCA) for GLAC: Percent change in average Snow Covered Area (km² with depth ≥ 0.5 m) on April 15 (left) and May 15 (right) at elevation bands for GLAC for five future scenarios in mid-century. The five scenarios are Central (cnrm, blue), Hot/Very Wet (canesm, red), Hot/Wet (miroc, yellow), Warm/Wet (giss, purple), Warm/Dry (fio, green). Black triangles on the y-axis show the elevations of documented wolverine den sites, elevation range 1500m ~2250. All but three of these dens are between 1800 and 2000m; two are above 2000m and one is below ~1500m. See also Table 5-2 for Modeled Snow Depth on May 15 at reported den sites in the Glacier Study Area.

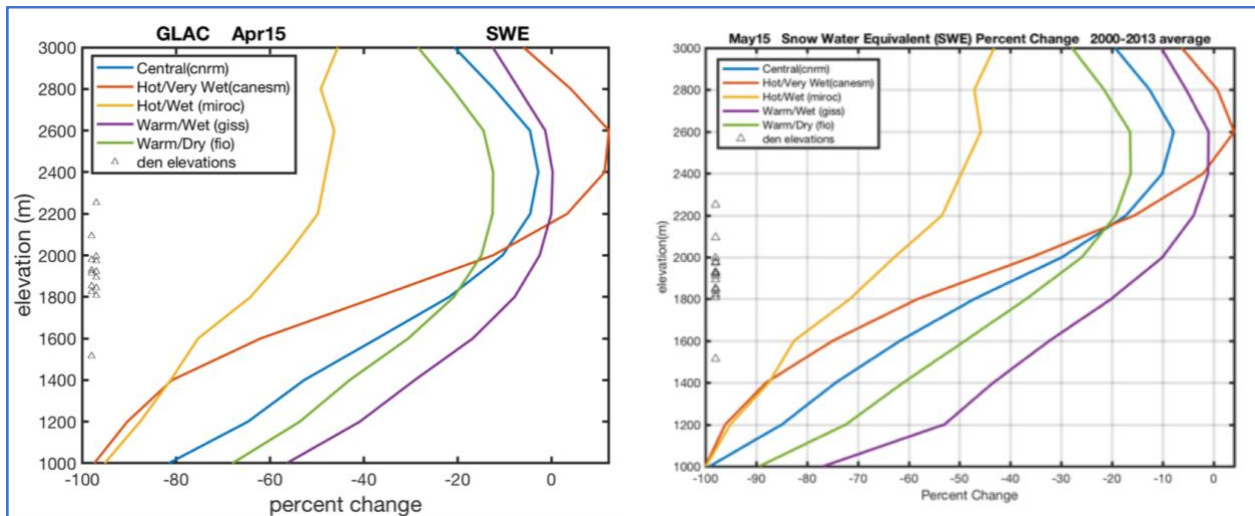


Figure 5-23. Average Snow Water Equivalent (SWE, percent change) on April 15(left) and May 15 (right) at elevation bands for GLAC for five future scenarios in mid-century. SWE is shown in this figure in addition to SCA in the previous figure to emphasize that a Hot/Very Wet projection can have increased snowpack at high elevations despite the significantly warmer temperatures. The five scenarios are Central (cnrm, blue), Hot/Very Wet (canesm, red), Hot/Wet (miroc, yellow), Warm/Wet (giss, purple), Warm/Dry (fio, green). As in the previous figure, known wolverine den site elevations are shown by black triangles. All but three of these dens are between 1800 and 2000m; two are above 2000m and one is below ~1500m (From John Guinotte, FWS). SWE is shown in addition to the snow covered area to emphasize that a Hot/Very Wet projection can have increased snowpack at high elevations despite the significantly warmer temperatures. See Supplementary material for SWE change on May 1

Figure 5-24 shows percent change in April 15 and May 15 snowcovered area (SCA; ≥ 0.5 meters depth), computed for 200 m elevation bands for ROMO. For elevations above 3400m only modest (under 20%) losses of SCA are seen for April 15, and a slight increase from 3000-3600m. For May 15th, losses below 3000 range from 20-100%, whereas at 3400 and above losses are 30% and less. As a proxy, for den site elevation, linear regression of den site elevations and latitude in the contiguous U.S. indicated that den sites in the ROMO would be located in an elevation range of 2700-3600 m (pers comm, John Guinotte, FWS). For May 1, see the supplementary material.

Figure 5-25 shows this elevation dependence measured in terms of snow water equivalent (SWE). Viewing snowpack in terms of SWE illustrates more clearly that the snowpack in two future scenarios (Hot/Wet, Warm/Wet) has increased slightly between 3000-3800 m elevation despite over 70% loss of snowpack at 2600m elevation for the Hot/Wet scenario. For the other three scenarios for April 15th, there are only modest (under ~20%) losses in SWE for ~3200 and above. Below 3400m the losses in SWE become larger, the lower the elevation. Comparison of Figures 5-24 (SCA) and 5-25 (SWE) shows that the relationship between SWE loss and SCA loss is not always straightforward (as for GLAC), with a more complicated elevation dependence for SCA than for SWE. For May 1, see the supplementary material.

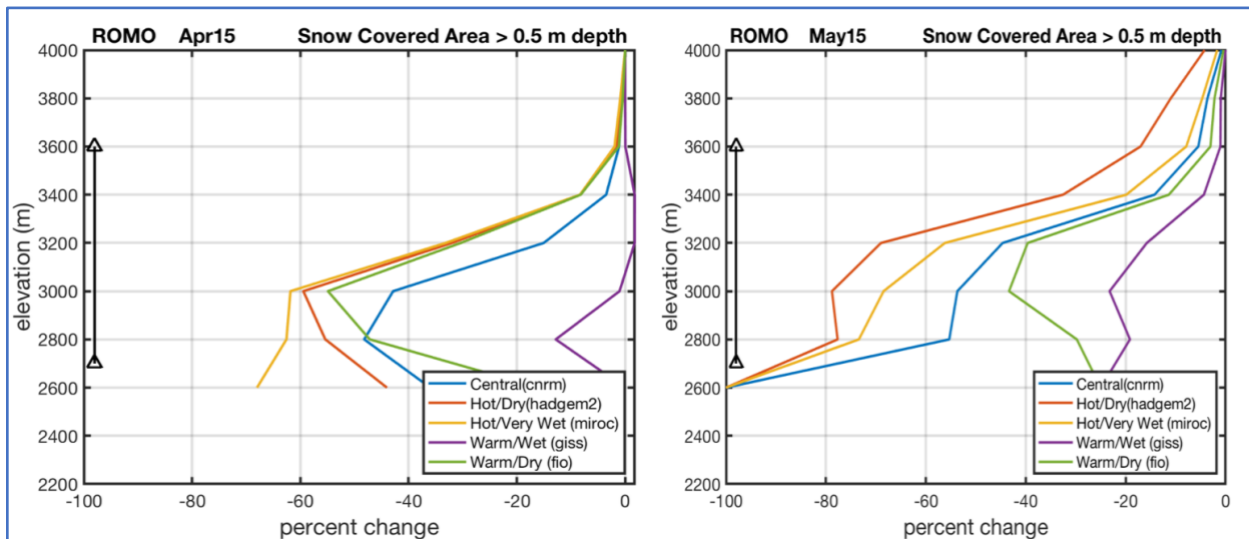


Figure 5-24. Percent change in average Snow Covered Area (depth ≥ 0.5 m) on April 15(left) and May 15 at elevation bands for ROMO for five future scenarios: The five scenarios are Central (cnrm, blue), Hot/Dry (hadgem2, red), Hot/Very Wet (miroc, yellow), Warm/Wet (giss, purple), Warm/Dry (fio, green) for mid-century. Note that the highest elevation band at ROMO tops out at 4000m, whereas the highest elevation band at GLAC tops out at 3000m. No documented den sites exist in ROMO. As a proxy, linear regression of den site elevations and latitude in the contiguous U.S. indicated den sites in the ROMO study area would be located in an elevation range of 2700-3600 m (pers comm, John Guinotte, FWS). See Supplementary material for SCA change on May 1.

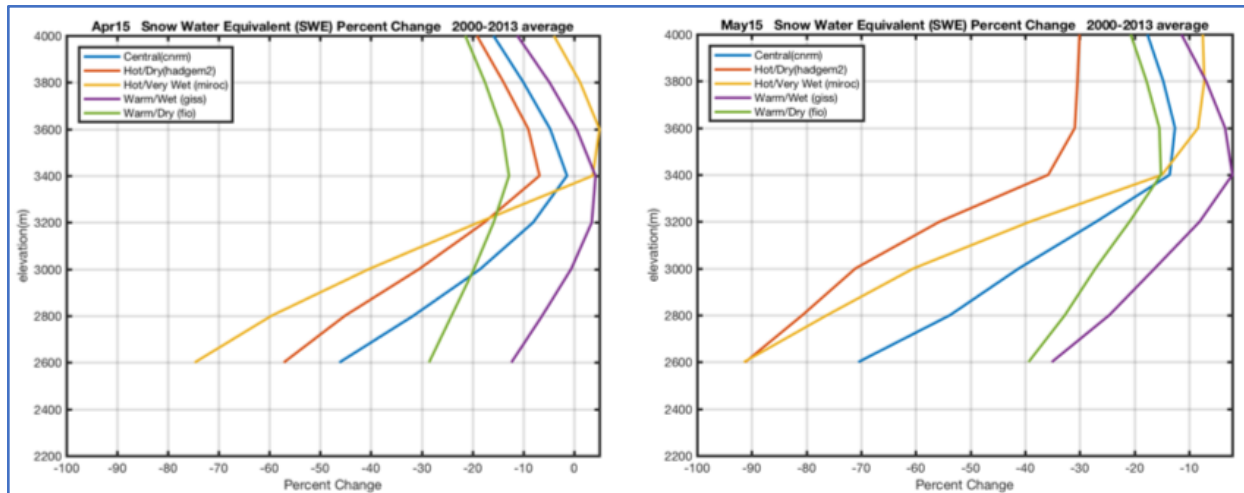


Figure 5-25. Average Snow Water Equivalent (SWE, percent change) on April 15(left) and May 15 at elevation bands for ROMO for five future scenarios. The scenarios are: Central (cnrm, blue), Hot/Very Wet (hadgem, red), Hot/Wet (miroc, yellow), Warm/Wet (giss, purple), Warm/Dry (fio, green) for mid-century. Note that the highest elevation band at ROMO tops out at 4000m, whereas the highest elevation band at GLAC tops out at 3000m. The vertical black lines near the y-axis show the *possible den site elevations (2700-3600 m) from John Guinotte, FWS, (pers comm)*. See Supplementary material for SCA change on May 1.

This phenomenon of elevation-dependent snowpack change in the Western US is well supported in the literature. Regonda et al. (2005) found little historical change in snowpack in the Western United States above approximately 2500m elevation despite observed warming trends, and Lettenmaier (2007) considered VIC hydrology model projections and reported as strong elevation dependence for snowpack loss in the Colorado River basin below 2500 m elevation (their data was visualized in Ray et al. 2008, Fig. 24). Two recent studies are of special interest because they focus on areas near those considered here. Sospendra-Alfonso et al (2015), on an area near the GLAC study area, find that historically, temperature has been a larger driver of April 1st snowpack only below about 1560 m elevation, with precipitation the main driver of variability above that elevation. Scalzitti et al. (2016) investigated a single climate change scenario using a high-resolution weather model and found that the critical elevation below which temperature dominates snowpack rises by about 250m in the Colorado Rockies, and rises by about 191 m in the Northern Rockies near the GLAC study area. While it is difficult to these results directly to the present study due to differences in methodology, the qualitative picture remains – projected warming has a larger effect at lower elevations whereas projected precipitation changes may dominate the Springtime snowpack in the high country.

6 Comparing results with McKelvey

An overview of the methodological similarities and differences between this study and McKelvey et al (2011) was presented in section 2.2. The differences in aims of these studies leads to challenges in making a direct comparison. The primary difference is in the choice of study areas – west-wide vs. much smaller selected areas near treeline, which has implications for the biological hypotheses that may be addressed. Their work focused on May 1st snow depth as a proxy for May 15th snow disappearance, while we directly estimated the May 15th snow disappearance. McKelvey investigated persistence of even a snowcover to May 15th as a correlate of wolverine habitat, as noted in Aubry et al (2008). This study focuses on high-elevation terrain and on the persistence of deeper snowpack. We also analyze our model results for the presence or absence of deeper snow (nominally greater than or equal to 0.5 meters depth) on April 15th and May 1st.⁸

Nonetheless some general statements can be made relating the two studies. Figure 5-26 shows snowcover under McKelvey’s historic and “miroc 2080’s” (or hotter, greatest change) scenario. The GLAC and ROMO areas have been outlined. A close examination of this figure shows that snowcover persists in our study areas, even for their hotter scenario of change (miroc “2080’s”). The greatest loss of snowcover in McKelvey occurs at lower elevations than were included in GLAC or ROMO. Because of the increased resolution of our study we are able to consider whether any pockets of snow with depth ≥ 0.5 meters will persist.

Our choice of future climate scenarios differs somewhat from McKelvey. We have intentionally included scenarios that represent the range of possibilities of temperature and precipitation indicated by the CMIP5 climate models. McKelvey used climate model output from Littell, who chose scenarios based solely on projected warming. For GLAC, this choice fortuitously included a range of precipitation changes as well. For ROMO, however, McKelvey’s scenarios include only a narrow range of precipitation change, where we include scenarios with significantly increased wintertime precipitation as well as scenarios with drying. This is a significant factor, given the buffering effect that increased precipitation has on snowpack loss at high elevations.

While McKelvey focused snowpack projections entirely on the long-term average, we investigate how climate variability – the sequences of wet and dry years -- intersects with scenarios of change. For ROMO in particular we find that dry years behave differently than wet years, with dry years benefitting from the increased precipitation in several of our future scenarios. This emphasizes the importance of planning for a range of possible climate scenarios, particularly regarding the direction of change in wintertime precipitation.

⁸ The study originally focused on May 15th to compare to the McKelvey, et al (2011) study, and June 1st to bracket the snowmelt season. However, as the study progressed, biologists became more interested in April snow.

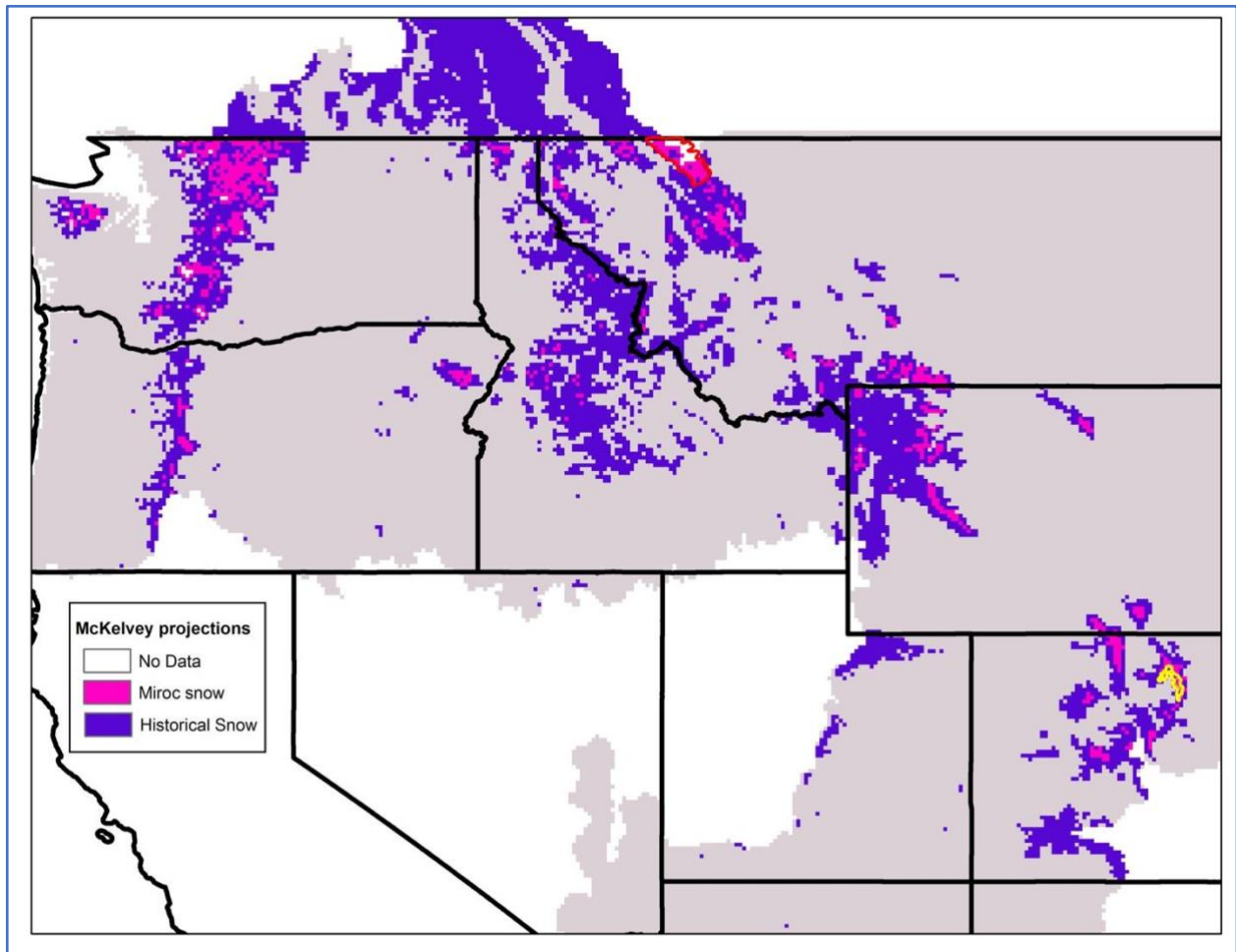


Figure 5-26. Figure 5-26: Simulated May 15 average snow cover inferred from 13cm snow depth on May 1 from McKelvey et al. (2011). Snowcover persists in our study areas even for their hotter scenario of change. Snow cover is shown for their historical simulation (purple) and their hotter, or greatest change scenario (“miroc 2080s”, pink). GLAC (red outlines) and ROMO (yellow outlines) show the study areas for this report. The greatest loss of snowcover in McKelvey occurs at lower elevations than were included in GLAC or ROMO. The higher resolution of our study allowed us to consider whether any pockets of snow with depth ≥ 0.5 meters will persist. Note that McKelvey used May 1st to infer May 15 and the domain simulated in McKelvey et al. (2011) did not include all of the GLAC study area, and did not include projection data for Canada. (Data were generously provided by Jeff Copeland. Graphic prepared by John Guinotte.

The question arises as to how the fine-scale projections of snow persistence in other areas might reasonably be inferred from the two study areas considered here. Figure 5-26 indicates many areas in the western United States that show persistence of snowcover in McKelvey’s scenarios, even in the more extreme scenarios. We have investigated two study areas: a northern, relatively wet and low-elevation area GLAC, and a southern, relatively dry, and very high elevation area (ROMO). In both areas we find general declines in snowcovered area under most future scenarios. The GLAC study area is broadly similar in its climate to much of the high northern Rockies, while ROMO shares features with the high mountain ranges of the Central Rockies. For areas in the McKelvey maps that show retention of snow on the higher mountain ranges it is physically reasonable to presume that a finer scale simulation would show the retention of areas

of snow ≥ 0.5 m on May 15th. Extending this beyond the general area of the Rocky Mountains is problematic. Even within the Rockies, in regions where McKelvey's results show widespread loss of snowpack it is probably not reasonable to conclude one way or the other whether a finer scale analysis would identify snow refugia.

7 References

Aubry, K. B., K. S. McKelvey, and J. P. Copeland. 2007. Distribution and broadscale habitat relations of the wolverine in the contiguous United States. *Journal of Wildlife Management* 71:2147–2158.

Barsugli, J.J. Jr., Ray, A.J., Livneh, B., Dewes, C.F., Rangwala, I., Heldmyer, A., Guinotte, J., Torbit, S. 2020. Projections of mountain snowpack loss for wolverine denning elevations in the Rocky Mountains, *Earth's Future*, in press (Sept 2020).

Bradley, R. S., F. T. Keimig, H. F. Diaz, and D. R. Hardy (2009), Recent changes in freezing level heights in the Tropics with implications for the deglaciation of high mountain regions, *Geophys. Res. Lett.*, 36, L17701, doi:10.1029/2009GL037712.

Copeland, JP, McKelvey, KS, Aubry, KB, Landa, A, Persson, J., Inman, RM, Krebs, J, Lofroth, E, Golden, H, Squires, JR, Magoun, A, Schwartz, MK, Wilmot, J, Copeland, CL, Yates, RE, Kojola, I, and May, R.. 2010. The bioclimatic envelope of the wolverine (*Gulo gulo*): do climatic constraints limit its geographic distribution? *Canadian Journal of Zoology* 88:233–246.

Christensen, N. S. and Lettenmaier, D. P. 2007. A multimodel ensemble approach to assessment of climate change impacts on the hydrology and water resources of the Colorado River Basin, *Hydrol. Earth Syst. Sci.*, 11, 1417-1434

Curtis JA, Flint LE, Flint AL, Lundquist JD, Hudgens B, et al. (2014) Incorporating Cold-Air Pooling into Downscaled Climate Models Increases Potential Refugia for Snow-Dependent Species within the Sierra Nevada Ecoregion, CA. *PLoS ONE* 9(9): e106984.

doi:10.1371/journal.pone.0106984

- Snow depth, cold air pooling

Elsner, MM, et al. 2010. Implications of 21st century climate change for the hydrology of Washington State. *Climatic Change* 102:225–260 DOI 10.1007/s10584-010-9855-0

- This paper describes some of the methods that were later used by Littell et al.

Fischelli, N., G. Schuurman, A. Symstad, A. Ray, B. Miller, M. Cross, E. Rowland. 2016. Resource management and operations in southwest South Dakota: Climate change scenario planning workshop summary January 20-21, 2016, Rapid City, SD. Natural Resource Report NPS/NRSS/NRR—2016/1289. National Park Service, Fort Collins, Colorado.

- The two Fischelli citations and references therein describe the strategy for selecting a range of divergent future scenarios.

Fisichelli, N., G. Schuurman, A. Symstad, A. Ray, J. Friedman, B. Miller, E. Rowland. 2016. Resource management and operations in central North Dakota: Climate change scenario planning workshop summary November 12-13, 2015, Bismarck, ND. Natural Resource Report NPS/NRSS/NRR—2016/1262. National Park Service, Fort Collins, Colorado.

Garfin, G., G. Franco, H. Blanco, A. Comrie, P. Gonzalez, T. Piechota, R. Smyth, and R. Waskom, 2014: Ch. 20: Southwest. *Climate Change Impacts in the United States: The Third National Climate Assessment*, J. M. Melillo, Terese (T.C.) Richmond, and G. W. Yohe, Eds., U.S. Global Change Research Program, 462-486. doi:10.7930/J08G8HMN.

- Description of southwest regional climate, including Colorado, from the National Climate Assessment

Hall, D. K. and G. A. Riggs. 2016. *MODIS/Terra Snowcover Daily L3 Global 500m Grid, Version 6*. Tiles h09v04 and h10v04. Boulder, Colorado USA. NASA National Snow and Ice Data Center Distributed Active Archive Center. doi:

<http://dx.doi.org/10.5067/MODIS/MOD10A1.006>. Accessed on 09/06/2016.

- Reference for MODIS collection 6 data

Hawkins, E., and Sutton, R. 2012. Time of emergence of climate signals, *Geophys. Res. Lett.*, 39, L01702, doi:10.1029/2011GL050087.

Hawkins, E., Sutton, R. 2011. The potential to narrow uncertainty in projections of regional precipitation change. *Clim Dyn* 37, 407–418. <https://doi.org/10.1007/s00382-010-0810-6>

IPCC, 2013: *Climate Change 2013: The Physical Science Basis*. Contribution of Working Group I to the Fifth Assessment Report of the Intergovernmental Panel on Climate Change [Stocker, T.F., D. Qin, G.-K. Plattner, M. Tignor, S.K. Allen, J. Boschung, A. Nauels, Y. Xia, V. Bex and P.M. Midgley (eds.)]. Cambridge University Press, Cambridge, United Kingdom and New York, NY, USA, 1535 pp, doi:10.1017/CBO9781107415324.

IPCC, 2007: *Climate Change 2007: The Physical Science Basis*. Contribution of Working Group I to the Fourth Assessment Report of the Intergovernmental Panel on Climate Change [Solomon, S., D. Qin, M. Manning, Z. Chen, M. Marquis, K.B. Averyt, M. Tignor and H.L. Miller (eds.)]. Cambridge University Press, Cambridge, United Kingdom and New York, NY, USA.

Littell, J.S., M.M. Elsner, G. S. Mauger, E. Lutz, A.F. Hamlet, and E. Salathé. 2011. *Regional Climate and Hydrologic Change in the Northern US Rockies and Pacific Northwest: Internally Consistent Projections of Future Climate for Resource Management*. Project report: April 17, 2011. Latest version online at: http://cse.washington.edu/picea/USFS/pub/Littell_etal_2010/

- Report by Univ of Washington Climate Impacts Group describing in detail the climate, hydrologic and snow modeling that were used in the McKelvey et al. 2011 study

Livneh, B., Bohn, T. J., Pierce, D. W., Munoz-Arriola, F., Nijssen, B., Vose, R., & Brekke, L. (2015). A spatially comprehensive, hydrometeorological data set for Mexico, the US, and Southern Canada 1950–2013. *Scientific data*, 2. Article number: 150042 (2015) doi:10.1038/sdata.2015.42

- This and the two references below are the key references for the DHSVM modeling.

Livneh, B., Deems, J. S., Schneider, D., Barsugli, J. J., & Molotch, N. P. 2014 . Filling in the gaps: Inferring spatially distributed precipitation from gauge observations over complex terrain. *Water Resources Research*, 50(11), 8589-8610.

Livneh B., E.A. Rosenberg, C. Lin, B. Nijssen, V. Mishra, K.M. Andreadis, E.P. Maurer, and D.P. Lettenmaier. 2013: A Long-Term Hydrologically Based Dataset of Land Surface Fluxes and States for the Conterminous United States: Update and Extensions, *Journal of Climate*, 26, 9384–9392.

Lukas, J., J.J. Barsugli, N. Doesken, I. Rangwala, and K.E. Wolter. 2014. Climate change in Colorado—A synthesis to support water resources management and adaptation. Report by the Western Water Assessment for the Colorado Water Conservation Board. 108 pp.

<http://cwcb.state.co.us/environment/climate-change/Pages/main.aspx>.

- Description of Colorado and interior West regional climate; primer on climate models, emissions scenarios, and downscaling (Ch. 3)

Lundquist, J. D., and A.L. Flint. 2006. Onset of Snowmelt and Streamflow in 2004 in the Western United States: How Shading May Affect Spring Streamflow Timing in a Warmer World. *J. Hydromet.* ,7,1199-1215.

Magoun Audrey J. and Jeffrey P. Copeland. 1998. Characteristics of Wolverine Reproductive Den Sites. *Journal of Wildlife Management*, Vol. 62, No. 4 (Oct., 1998), pp. 1313-1320. DOI: 10.2307/3801996

- Study of denning in Idaho that finds that April 15th is the date when most dens are abandoned and 1-m of snow is the minimum denning depth.

McKelvey, K. S., J. P. Copeland, M. K. Schwartz, J. S. Littell, K. B. Aubry, J. R. Squires, S. A. Parks, M. M. Elsner, and G. S. Mauger. 2011. Climate change predicted to shift wolverine distributions, connectivity, and dispersal corridors. *Ecological Applications* 21:2882–2897.

- Used Littell et al (2011) climate and hydrology data as well as analyzing MODIS snowcover to investigate wolverine habitat. Our study attempts to extend the science in this study.

McWethy D. B., S. T. Gray, P. E. Higuera, J. S. Littell, G. T. Pederson, A. J. Ray, and C. Whitlock. 2010. Climate and terrestrial ecosystem change in the U.S. Rocky Mountains and Upper Columbia Basin: Historical and future perspectives for natural resource management. Natural Resource Report NPS/GRYN/NRR—2010/260. National Park Service, Fort Collins, Colorado.

- Description of southwest regional climate, including Colorado, from the National Climate Assessment, see case study on N. Rockies and drought variability and ecosystem dynamics in Glacier and section on 20th century observations

Maier, H. R., Guillaume, J. H., van Delden, H., Riddell, G. A., Haasnoot, M., & Kwakkel, J. H. 2016. An uncertain future, deep uncertainty, scenarios, robustness and adaptation: How do they fit together? *Environmental Modelling & Software*, 81, 154-164.

Morelli TL, Daly C, Dobrowski SZ, Dulen, DM, Ebersole JL, Jackson ST, et al. 2016. Managing Climate Change Refugia for Climate Adaptation. *PLoS ONE* 11(8): e0159909.doi:10.1371/journal.pone.0159909

Murphy, D., C. Wyborn, L. Yung, D. Williams, C. Cleveland, L. Eby, S. Dobrowski, and E. Towler. 2016. Engaging Communities and Climate Change Futures with Multi-Scale, Iterative Scenario Building (MISB) in the Western United States. *Human Organization*. Vol. 75, No. 1, 2016.

National Park Service, 2013. Using Scenarios to Explore Climate Change: A Handbook for Practitioners. National Park Service Climate Change Response Program. Fort Collins, Colorado. <https://www.nps.gov/subjects/climatechange/upload/CCScenariosHandbookJuly2013.pdf>

- scenario planning

Peacock, S. 2011. Projected 21st century climate change for wolverine habitats within the contiguous United States. *Environmental Research Letters* 6:014007.

Ray, A.J., Joseph J. Barsugli, Jr., Klaus E. Wolter, Jon K. Eischeid. 2010. Rapid-Response Climate Assessment to Support the FWS Status Review of the American Pika. NOAA Report to the U.S. Fish and Wildlife Service. 53pp. Available at: <http://www.esrl.noaa.gov/psd/news/2010/020210.html>

- Includes discussion of how differences among mid-21st century climate responses are limited compared to later in the century; and elevation dependence for snowpack loss in the Colorado River basin below 2500 m elevation.

Ray, A.J., J.J. Barsugli, K.B Averyt, K. Wolter, M. Hoerling, 2008. Colorado Climate Change: A Synthesis To Support Water Resource Management and Adaptation, a report for the Colorado Water Conservation Board by the NOAA-CU Western Water Assessment, [http://wwa.colorado.edu/publications/reports/WWA_ClimateChangeColoradoReport_2008 .pdf](http://wwa.colorado.edu/publications/reports/WWA_ClimateChangeColoradoReport_2008.pdf)

Reclamation (U.S. Bureau of Reclamation) 2013. Downscaled CMIP3 and CMIP5 Climate Projections – Release of Downscaled CMIP5 Climate Projections, Comparison with Preceding Information, and Summary of User Needs. U.S. Department of the Interior, Bureau of Reclamation, 104 pp., available at: http://gdo-dcp.ucllnl.org/downscaled_cmip_projections/techmemo/downscaled_climate.pdf.

- documentation for downscaled climate projections used in this report

Regonda, S. K. , B. Rajagopalan, M. Clark, and J. Pitlick. 2005. Seasonal Cycle Shifts in Hydroclimatology over the Western United States. *J. Climate*, **18**, 372–384.

Rowland, E.R., Cross, M.S., Hartmann, H. 2014. Considering Multiple Futures: Scenario Planning to Address Uncertainty in Natural Resource Conservation. Washington, DC: US Fish

and Wildlife Service. <https://www.fws.gov/home/climatechange/pdf/Scenario-Planning-Report.pdf>

Scalzitti J, Strong C, Kochanski A. 2016. Climate change impact on the roles of temperature and precipitation in Western U.S. snowpack variability. *Geophys Res Lett* 43, 5361-5369.

Shafer, M., D. Ojima, J. M. Antle, D. Kluck, R. A. McPherson, S. Petersen, B. Scanlon, and K. Sherman, 2014: Ch. 19: Great Plains. *Climate Change Impacts in the United States: The Third National Climate Assessment*, J. M. Melillo, Terese (T.C.) Richmond, and G. W. Yohe, Eds., U.S. Global Change Research Program, 441-461. doi:10.7930/J0D798BC.

- Description of Great Plains regional climate, including Montana, from the National Climate Assessment

Sofaer, H.R., S.K. Skagen, J.J. Barsugli, B.S. Rashford, G.C. Reese, J.A. Hoeting, A.W. Wood, and B.R. Noon. 2016. Projected wetland densities under climate change: habitat loss but little geographic shift in conservation strategy. *Ecological Applications* 26: 1677-1692.

- includes discussion of advantages and disadvantages of the delta method

Sospedra-Alfonso, R., J. R. Melton, and W. J. Merryfield. 2015. Effects of temperature and precipitation on snowpack variability in the central Rocky Mountains as a function of elevation, *Geophys. Res. Lett.*, **42**, 4429–4438.

Star, J., Rowland, E. L., Black, M. E., Enquist, C. A., Garfin, G., Hoffman, C. H., ... & Waple, A. M. 2016. Supporting adaptation decisions through scenario planning: enabling the effective use of multiple methods. *Climate Risk Management*, 13, 88-94.

Symstad, A.J., N.A. Fisichelli, B.W. Miller, E. Rowland, and G.W. Schuurman. 2017. *Climate Risk Management*, <http://dx.doi.org/10.1016/j.crm.2017.07.002>.

Taylor, K.E., Stouffer, R.J. and Meehl, G.A. 2012. An overview of CMIP5 and the experiment design. *Bulletin of the American Meteorological Society*, 93(4): 485.

USGS. 2009. National Elevation Dataset (NED), Second Edition.

Wigmosta, M.S., Vail, L.W., Lettenmaier, D.P., 1994. A distributed hydrologyvegetation model for complex terrain. *Water Resour. Res.* 30, 1665–1679.

- DHSVM model primary reference

Zappa, Massimiliano. 2008. Objective quantitative spatial verification of distributed snowcover simulations—an experiment for the whole of Switzerland. *Hydrological Sciences Journal*, 53: 179-191, DOI: 10.1623/hysj.53.1.179

8 Glossary

- **Aspect:** Compass direction that slope faces
- **Baseline period 1916-2000:** Deltas (changes) computed (monthly average delta) for “2040’s and “2080’s” compared to the 1916-2000 baseline.
- **CanESM or cansm:** A CMIP5 climate model the Canadian Centre for Climate Modeling and Analysis (canesm2.1.rcp85), forced with the RCP 8.5 higher emissions pathway, used in this report as a future scenario (Hot/Dry scenario for GLAC only) that has relatively higher increase in temperature (+~4.5 C) and about +20% increase in precipitation (See Figure 5-7)
- **Climate sensitivity:** Regionally speaking, it is the response of a climate model for a given amount of greenhouse gas increase. More narrowly defined it is the global average temperature increase that results from a doubling of carbon dioxide over pre-industrial values.
- **CMIP3, CMIP5:** Coupled Model Intercomparison Project Phases 3 and 5. “Foundational” collections of climate model projections, used in the Intergovernmental panel on Climate Change (IPCC) 2007 and IPCC 2013 reports, respectively.
- **CNRM:** A CMIP5 climate model from the French National Centre of Meteorological Research (cnrm-cm5.1.rcp85), used in this report as a future scenario (Central scenario for both GLAC and ROMO) that is relatively close to the ensemble mean in temperature increase (+~2.5 °C) and +~5-8% increase in precipitation (See Figure 5-7).
- **DEM:** Digital elevation model
- **DSHVM:** Distributed Hydrology Soil Vegetation Model
- **ESM:** earth system models, see GCM.
- **FIO:** A CMIP5 earth system model from the First Institute of Oceanography, State Oceanic Administration of China (fio-esm.1.rcp85), used in this report as a future scenario (Warm/Dry scenario for both areas) that is relatively lower in temperature increase (+~0.8-1.6 °C) and ~5% decrease in precipitation (See Figure 5-7).
- **FLH:** Atmospheric freezing level height is the altitude in the free atmosphere at which the temperature is 0 °C
- **GCM:** Global Climate Model, 6 were used for this report from the IPCC 2013 class of models; some of these are actually earth system models (ESM), an advanced type of GCM which have the added capability to explicitly represent biogeochemical processes that interact with the physical climate. GCM is used as a general term referring to both kinds of models, ESM is used specifically for earth system models.
- **GISS:** A CMIP5 climate model from the NASA Goddard Institute for Space Studies (giss-e2-r.1.rcp45), used in this report as a future scenario (Warm/Wet scenario for both areas). Referred to as the “Least Change” scenario because it that is relatively lower temperature increase (+~1-1.3 °C) and +~7-10% increase in precipitation (Figure 5-7).
- **GLAC:** Area in Glacier National Park used as a spatial unit of analysis in this report
- **HADGEM:** A CMIP5 earth system model from the United Kingdom Meteorological Office Hadley Center (hadgem2-es.1.rcp85) used in this report as a future scenario (Hot/Very Wet scenario for ROMO only) that has relatively higher temperature increase (+~ 3.5 °C) and ~5% decrease in precipitation.

- **Internal climate variability:** The variations in the climate, even for 30-year and longer averages, that can occur due to the interactions of the atmosphere, ocean, inland surface and cryosphere. This occurs even in the absence of anthropogenic climate change.
- **MODIS:** Moderate Resolution Imaging Spectroradiometer, a satellite remote sensing instrument carried on the Terra satellite
- **MIROC:** A CMIP5 earth system model from the Japanese Agency for Marine-Earth Science and Technology, Atmosphere and Ocean Research Institute (The University of Tokyo), and National Institute for Environmental Studies (miroc-esm-chem.1.rcp85), used in this report as a future scenario (Hot/Wet scenario for both areas). Referred to as the “Greatest Change” scenario because it has the highest temperature increase of the scenarios (+~4 °C) and +~10-18% increase in precipitation (see Figure 5-7). This ESM has an atmospheric chemistry (CHEM) component coupled to the MIROC-ESM (<http://maca.northwestknowledge.net/GCMs.php>).
- **NDSI:** Normalized Difference Snow Index, a measure of snowcover, has a linear relationship to fractional snowcover (FSC) (see text in 4.2.2 and 5.4.2. for discussion)
- **North American Freezing Level Tracker:** NCEP/NCAR Global Reanalysis 2.5° x 2.5° grid data (<http://www.wrcc.dri.edu/cwd/products/>)
- **Octants:** Topographic aspect, or compass direction, was classified into eight directional bins, each representing 45° of compass arc, e.g; NW, N, NE, E, SE, S, SW, and W
- **Resolution:** The VIC modeling that was the basis for McKelvey was performed on a regular grid in latitude and longitude, with a grid size of 1/16 degree on a side. The distance between degrees of longitude varies due to the curvature of the Earth, and the east-west dimension of a gridbox is smaller than the north-south distance by a factor of the cosine of latitude. At 40°N latitude, the southern extent of Rocky Mountain National Park, the gridbox is ~5km by 7 km (~37km²). Grid boxes at Glacier National Park (~48°N) are slightly smaller. When referring to the McKelvey study we will use the “1/16 degree” notation. The DHSVM modeling used in this study was performed on a uniform grid in the Universal Transverse Mercator (UTM) map projection, which allows a near-uniform grid size of 250m by 250m (0.0625 km²) in both of the study areas.
- **ROMO:** Area in and around Rocky Mountain NP used as a spatial unit of analysis
- **SCA:** Snowcovered Area (km²)
- **SDD:** Snow Disappearance Date, the first Day of Year after March 1 where pixel is snow-free, defined as the date which NDSI/100 was less or equal to 0.1.
- **Significant snow:** Snow depth ≥ 0.5 m, referred to in this report as “significant snow,” because of interest in snow depth at wolverine denning sites, see Sec 5.12.2.
- **SNODAS:** Snow Data Assimilation System, a product of the NOAA National Weather Service's National Operational Hydrologic Remote Sensing Center (NOHRSC)
- **SWE:** Snow water equivalent (mm). For May, snow depth is assumed to be ~ 2.5 *SWE
- **TopoWx:** 800m-resolution gridded temperature dataset, <https://www.sciencebase.gov/>
- **Snowcovered area, total:** Total area covered by snow within the study boundaries in square kilometers (km²)
- **Snowcovered area, fractional:** Percentage of the total land area that is covered by snow; this can be within the study boundaries, aspect area, or elevation bands (see text in 4.2.2 and 5.4.2. for discussion)
- **VIC:** Variable Infiltration Capacity hydrologic model
- **UTM:** Universal Transverse Mercator spatial coordinates

9 Supplementary Material

Supplementary Material is presented using the report section number where it is mentioned,.

Section 4.2.1 Data sub-setting and re-projection

Table S4-1: MODIS reprojection tool parameters for the two study areas.

GLAC	ROMO
SPATIAL_SUBSET_TYPE = INPUT_LAT_LONG SPATIAL_SUBSET_UL_CORNER = (49.4 - 115.1666666666) SPATIAL_SUBSET_LR_CORNER = (47.0 - 112.3333333333) RESAMPLING_TYPE = NEAREST_NEIGHBOR OUTPUT_PROJECTION_TYPE = UTM DATUM = NAD83 UTM_ZONE = 12 OUTPUT_PIXEL_SIZE = 250	SPATIAL_SUBSET_TYPE = INPUT_LAT_LONG SPATIAL_SUBSET_UL_CORNER = (41.0 - 106.064513) SPATIAL_SUBSET_LR_CORNER = (39.907169 - 105.116666666) RESAMPLING_TYPE = NEAREST_NEIGHBOR OUTPUT_PROJECTION_TYPE = UTM DATUM = NAD83 UTM_ZONE = 13 OUTPUT_PIXEL_SIZE = 250

Section 4.3.2 Aspect Dependence of Snowpack (GLAC)

The following figures for GLAC show total SCA as a function of aspect, in contrast with the figures in Section 4.3.2 in the main text, which show fractional snow covered area.

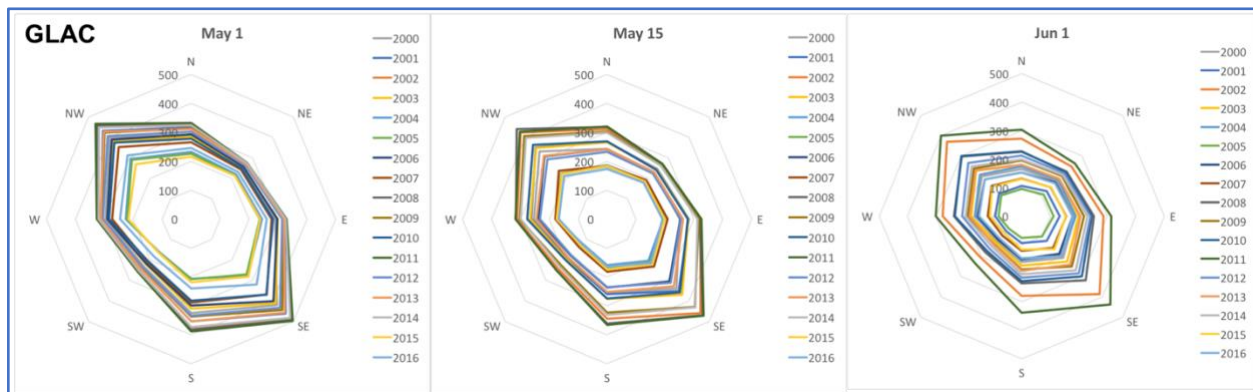


Figure S4-1: Total snow covered area (km^2) as a function of aspect for May 1, May 15, and June 1 for the GLAC study area from MODIS observations. Data for each year is shown by a separate line. Aspect of the slope is determined from a digital elevation model and is binned into eight octants according to the compass direction. The shape of the curves is strongly determined by the total land area in each aspect bin. Concentric octagons (gray) denote the magnitude scale ranging from 0 to 500 km^2 .

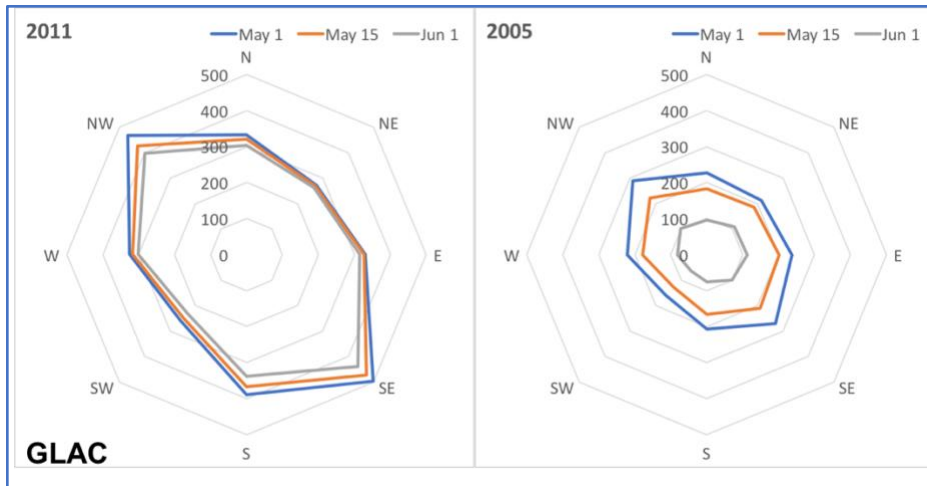


Figure S4-2: Total snow covered area (km²) as a function of aspect for representative Wet (2011) and Dry (2005) years for the GLAC study area from MODIS observations. For each year, the snowcovered area is shown for May 1 (blue), May 15 (red), and June 1 (thick gray) Concentric octagons (thin gray) denote the magnitude scale ranging from 0 to 500 km².

Section 4.4.2 Aspect Dependence of Snowpack (ROMO)

The following figures for ROMO show total SCA as a function of aspect, in contrast with the figures in Section 4.4.2 in the main text, which show fractional snow covered area.

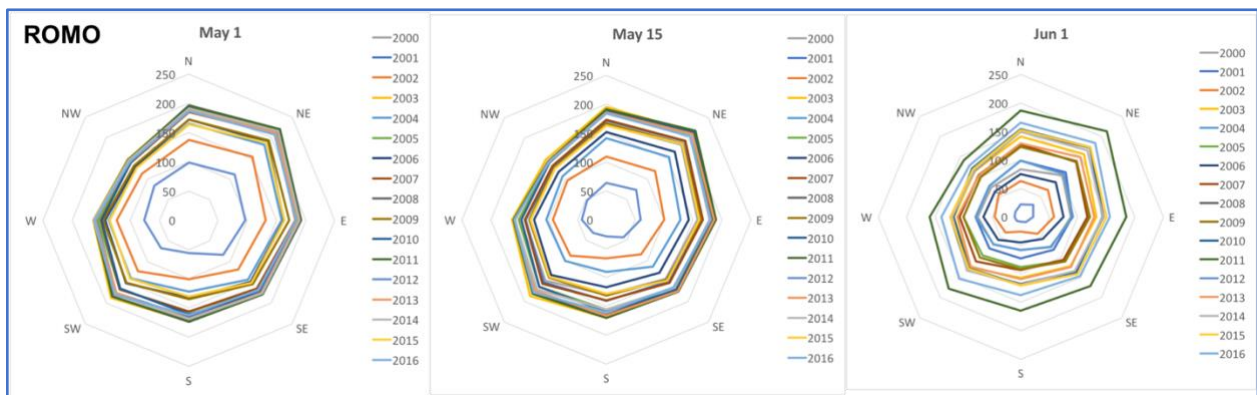


Figure S4-3: Total snow covered area (km²) as a function of aspect for May 1, May 15, and June 1 for the ROMO study area from MODIS observations. Data for each year is shown by a separate line. Aspect of the slope is determined from a digital elevation model and is binned into eight octants according to the compass direction. The shape of the curves is strongly determined by the total land area in each aspect bin. Concentric octagons (gray) denote the magnitude scale ranging from 0 to 500 km².

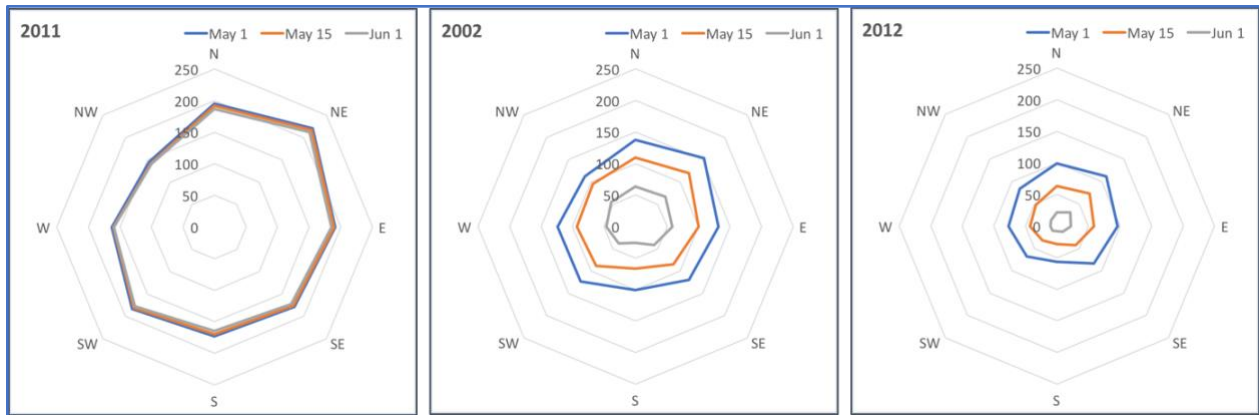


Figure S4-4: Total snow covered area (km²) as a function of aspect for “wet” (2011) and “dry” (2002) representative years for the ROMO study area from MODIS observations. For each year the snow covered area is shown for May 1 (blue), May 15 (red), and June 1 (thick gray) Concentric octagons (thin gray) denote the magnitude scale ranging from 0 to 500 km². Note that while 2012 had the least snow cover in late Spring, 2002 was adopted as a representative dry year due to modeling considerations in Section 5. We show both dry years here which exhibit similar features.

Section 5.3 Meteorological Inputs

The Livneh data are gridded at a spatial resolution of 1/ 16 degree in latitude and longitude and are derived from daily temperature and precipitation observations from approximately 20,000 NOAA Cooperative Observer (COOP) stations, with a minimum requirement of 20 years of data for CONUS grids. The gridding procedure uses the SYMAP algorithm. An orographic scaling procedure is also applied using PRISM climatology for precipitation and a constant 6.5 K/km lapse rate for minimum and maximum temperature. More information on the dataset is found in Livneh et al. (2015) and Livneh et al. (2013).

Section 5.4.2 Comparison to MODIS Snowcover

Table S5-1: Parameter settings that were adjusted and objective values obtained for DHSVM model runs in ROMO. Ten parameter sets tested for parameter adjustment in ROMO, including snow roughness (SR) and liquid water content (LWC), as well as an alternative precipitation scaling method.

Run Name	LWC	SR	Alt. Precip. Scaling?
C03R01 (Default; (GLAC)	0.03	0.01	No
C01R01	0.01	0.01	No
C05R01	0.05	0.01	No
C03R0001	0.03	0.0001	No

C03R1	0.03	0.1	No
C05R001 (ROMO)	0.05	0.001	No
C03R01P	0.03	0.01	Yes
C03R0001P	0.03	0.0001	Yes
C05R01P	0.05	0.01	Yes
C05R001P	0.05	0.001	Yes

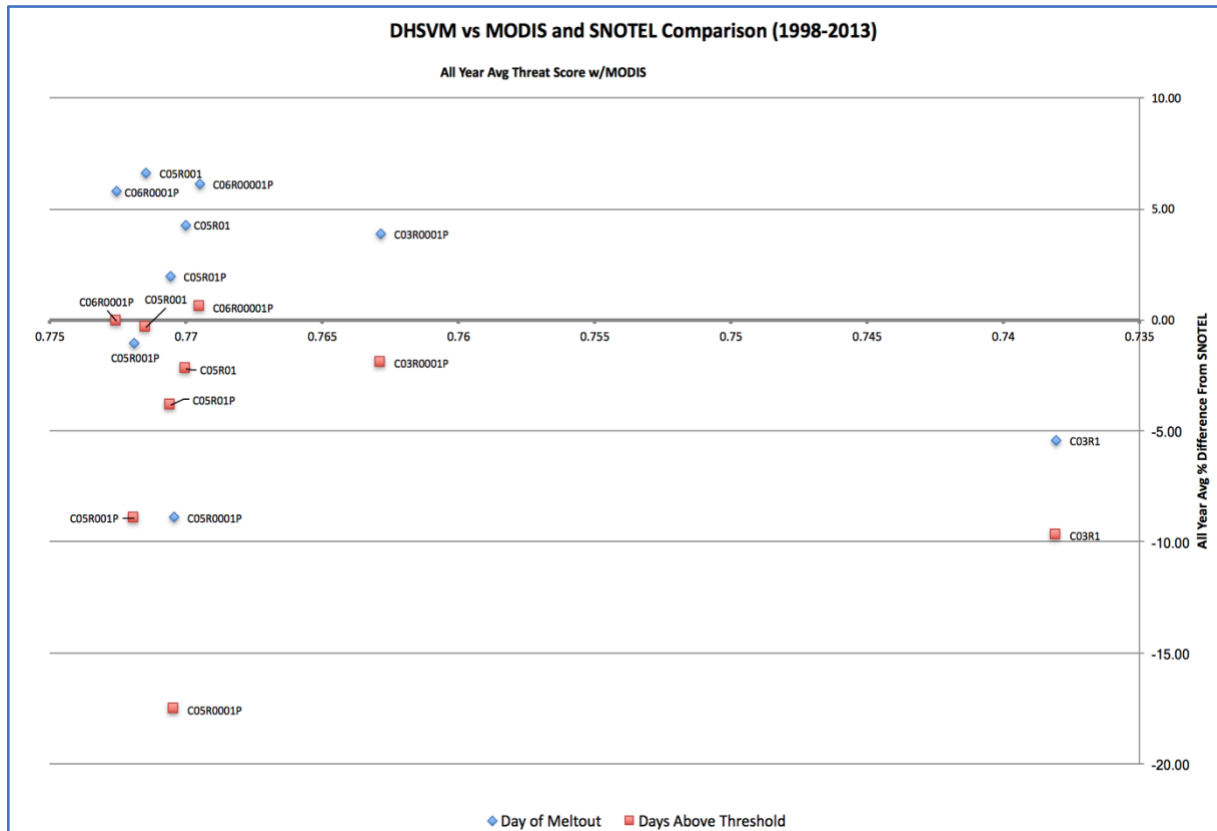


Figure S5-1. Performance metrics for parameter adjustment runs. The horizontal axis is the average CSI threat score for the spatial comparison against MODIS snow cover. Vertical axis shows percentage error in comparison to SNOTEL point observations for day of meltout and days above threshold (snow season length). Points are labeled with run number (See Table S5-1). C05R001 parameter settings were implemented for the final model runs.

5.5 Determination of Snow Depth from DHSVM model output

This supplement describes the method used to convert snow water equivalent (SWE) to snow depth (SD) in late Spring for use in the US Fish and Wildlife Service sponsored study of the future of snowpack regarding potential denning sites for the Wolverine. Three lines of evidence support using an approximate conversion factor of $SD = 2.5 * SWE$ for May snowpack.

For the purposes of this report we desired an estimate of snow depth during the late Spring months, particularly in May. Snow depth was desired as it was easier to communicate with wolverine biologists as regards the snowpack in commonly observed denning locations. However, the Distributed Hydrology Soil Vegetation Model (DHSVM) that was used to generate projections of snowpack outputs SWE, but not snow depth. Furthermore, the McKelvey study analyzed May 1st snow depth (with a threshold of 13 cm) as determined from the Variable Infiltration Capacity (VIC) hydrology model from the Littell (2011) dataset. They used this as a proxy for May 15th snow disappearance. In their paper they also noted that the maps of SWE and maps of Snow Depth from the Littell dataset were correlated at > 99.5%. This high correlation motivates the use of a simple conversion factor between SWE and snow depth. We bring three lines of evidence to our estimate of this conversion factor based on the ratio of SD to SWE: in-situ observations at SNOTEL (Snow Telemetry) sites; Snow Data Assimilation System (SNODAS) estimates based on a fusion of data and model results, and finally, modeled SWE and SD from Littell et al (2011).

Snow Depth and SWE were reported for the three SNOTEL sites near the GLAC study area. We find the following estimates (Table S5-2) of the SD:SWE ratio by looking at the average over the years 2002-2016.

Table S5-2

SNOTEL SITE (GLAC AREA)	2002-2016 Average SD:SWE ratio	Density
Flattop Mountain	2.3:1	0.43
Pike Creek	2.4:1	0.42
Many Glacier	Insufficient years with snow	

To corroborate these approximate values we present maps of snow density for May 1, 2017 obtained from the Natural Resources Conservation Service website (Figure S5-1)⁹. The bulk snow density $\rho = \text{SWE}/\text{SD}$ is simply the inverse of the ratio SD:SWE. These maps indicate widespread areas with density between 0.3 and 0.5, corresponding to a range of 2:1 and 3.3:1 ratios. However, SNOTEL sites are not representative of the entire domain. To do that we proceed to the other sources of snow data that are spatially distributed.

⁹ <https://www.wcc.nrcs.usda.gov/gis/snow.html>

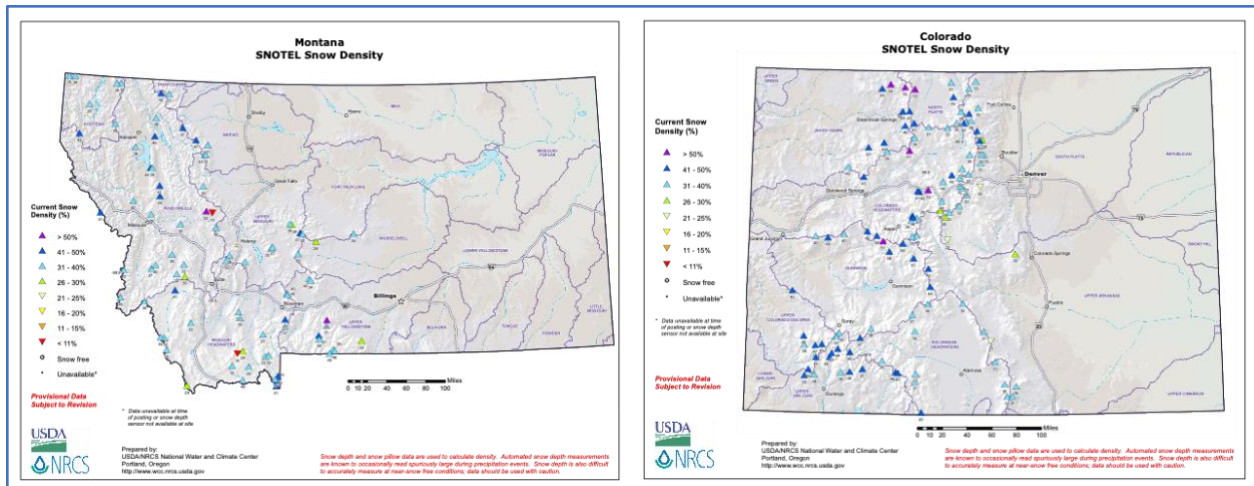


Figure S5-2. Snow Density (%) at SNOTEL sites for May 1, 2017. Montana (left) and Colorado (right). Snow density is the inverse of the SD:SWE ratio. Downloaded from the Natural Resources Conservation Service website.

The second line of evidence comes from the Snow Data Assimilation System (SNODAS) which is a blend of modeled and observed snow variables. The data is available for 2004 – 2016 and was downloaded from the National Snow and Ice Data Center. Because of problems encountered with the NSIDC data server (their server had just been permanently taken offline), extensive processing was necessary for this step and was only done for the GLAC area. The SD:SWE ratio was computed as the least squares regression slope between SD and SWE from all available years at each 1 km pixel. Figure S5-3 below shows that the vast majority of the area in and near the GLAC study area has ratios between 2.6 and 3.0 with the deeper snow areas (background image) having the lower ratios. It is rather remarkable how uniform this product is. However, the paucity of snow depth measurements means that the values in this product rely heavily on the modeled snow depth and are not influenced by the few observations available.

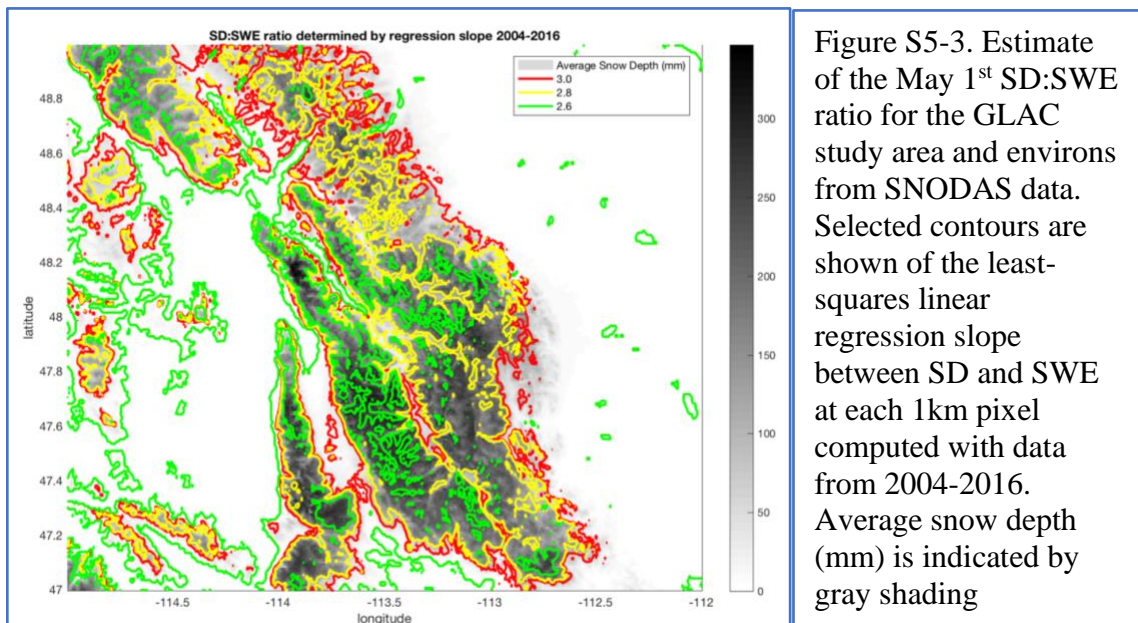


Figure S5-3. Estimate of the May 1st SD:SWE ratio for the GLAC study area and environs from SNODAS data. Selected contours are shown of the least-squares linear regression slope between SD and SWE at each 1km pixel computed with data from 2004-2016. Average snow depth (mm) is indicated by gray shading

The third line of evidence used the modeled SWE and SD from the Littell (2011) dataset. The SWE and SD were derived entirely from the VIC hydrologic model. The VIC hydrologic model has a component that computes the snow depth. These were available for the entire Western United States domain with the exception California. Figure S5-4 below shows the scatter plot of the long-term average May 1 SD vs. May 1 SWE. Each data point is a gridpoint in the VIC simulation. Considering that we are looking at grids throughout the West, we see a remarkably tight cluster of points that lie between the 2.0:1 and 2.5:1 and ratios. The ratio is closer to 2.5:1 for values near 50cm of snow depth that concerns us in this report.

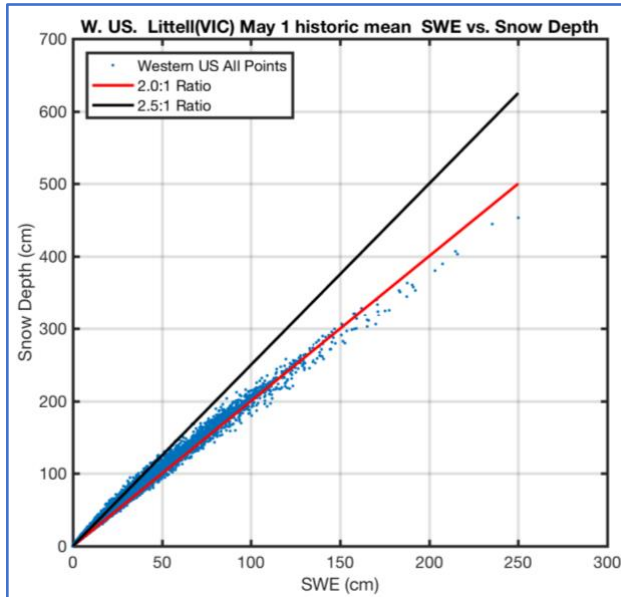


Figure S5-4. Scatterplot of long-term average snow depth vs SWE at all gridpoints from the historical simulation in the Littell (2011) dataset. Lines with slopes of 2.0:1 and 2.5:1 are indicated.

Looking specifically at model gridpoints near GLAC and ROMO we see the following scatter of SD vs SWE:

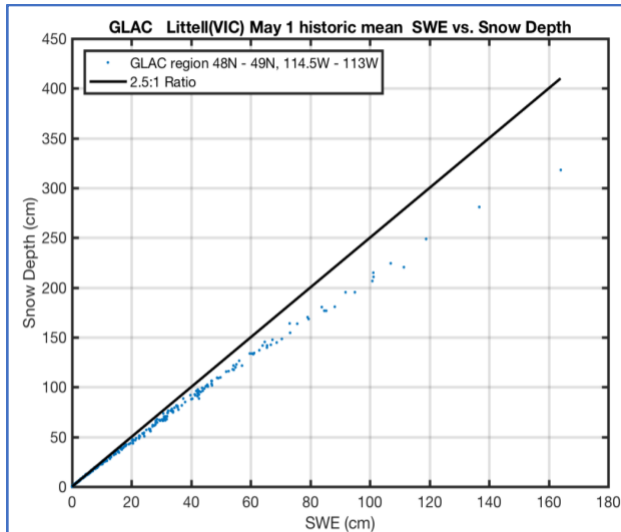


Figure S5-5. Scatterplot of long-term average snow depth vs SWE at all gridpoints from the historical simulation in the Littell (2011) dataset. Same as Figure S5-4, except only for grids in a region near the GLAC study area. Only the 2.5:1 ratio line is indicated.

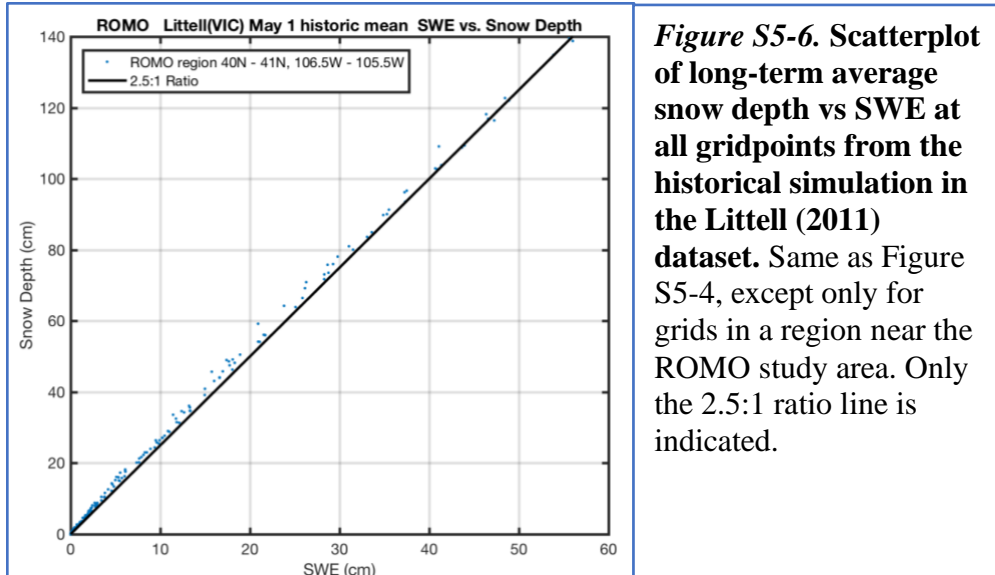


Figure S5-6. Scatterplot of long-term average snow depth vs SWE at all gridpoints from the historical simulation in the Littell (2011) dataset. Same as Figure S5-4, except only for grids in a region near the ROMO study area. Only the 2.5:1 ratio line is indicated.

The GLAC scatter is slightly below the 2.5:1 line whereas the ROMO scatter is slightly above. It might be speculated that the rather tight clustering of ratios for the Springtime snowpack in the SNODAS and the VIC products is a result of the snow depth model

Based on these lines of evidence we adopted a uniform value of 2.5:1 for the SD:SWE ratio, corresponding to a snow density of 0.4. As we have noted in the report, we desired only an approximate value that was appropriate to the season. Note that values of SD:SWE computed earlier in the year for the VIC product are considerably higher. Subsequent analysis for April 15th snowpack indicated a typical bulk density of 0.33. The conclusions of the report are not sensitive to the choice of conversion factor within the ranges indicated by the above analysis.

Section 5.9 Climate Projections Evaluation and Scenarios Selection

Table S5-3. The CMIP5 GCMs from which the five scenarios were chosen for each study area. Only run 1 from RCP4.5 and RCP 8.0 were used where available (rcp4.5 after the model name denotes where a single RCP was used).

Model	Institution
access1-0	CSIRO (Commonwealth Scientific and Industrial Research Organisation, Australia), and BOM (Bureau of Meteorology, Australia)
access1-3	
bcc-csm1-1	Beijing Climate Center, China Meteorological Administration
bcc-csm1-1-m	
canesm2	Canadian Centre for Climate Modelling and Analysis
ccsm4	National Center for Atmospheric Research
cesm1-bgc	National Science Foundation, Department of Energy, National Center for Atmospheric Research
cesm1-cam5	
cmcc-cm	Centro Euro-Mediterraneo per I Cambiamenti Climatici
cnrm-cm5	Centre National de Recherches Meteorologiques / Centre Europeen de Recherche et Formation Avancees en Calcul Scientifique
csiro-mk3-6-0	Commonwealth Scientific and Industrial Research Organisation in collaboration with the Queensland Climate Change Centre of Excellence
ec-earth.2.rcp45	EC-Earth Consortium
fgoals-g2	LASG, Institute of Atmospheric Physics, Chinese Academy of Sciences
fgoals-s2.2.rcp45	
fio-esm	The First Institute of Oceanography, SOA, China
gfdl-cm3	NOAA Geophysical Fluid Dynamics Laboratory
gfdl-esm2g	
gfdl-esm2m	
giss-e2-r	NASA Goddard Institute for Space Studies
hadgem2-ao	National Institute of Meteorological Research/Korea Meteorological Administration
hadgem2-cc	Met Office Hadley Centre (additional HadGEM2-ES realizations contributed by Instituto Nacional de Pesquisas Espaciais)
hadgem2-es	
inmcm4	Institute for Numerical Mathematics
ipsl-cm5a-lr	Institut Pierre-Simon Laplace
ipsl-cm5a-mr	
ipsl-cm5b-lr	
miroc-esm	Japan Agency for Marine-Earth Science and Technology, Atmosphere and Ocean Research Institute (The University of Tokyo), and National Institute for Environmental Studies
miroc-esm-chem	
miroc5	Atmosphere and Ocean Research Institute (The University of Tokyo), National Institute for Environmental Studies, and Japan Agency for Marine-Earth Science and Technology
mpi-esm-lr	Max Planck Institute for Meteorology (MPI-M)
mpi-esm-mr	
mri-cgcm3	Meteorological Research Institute
noresm1-m	Norwegian Climate Centre
noresm1-me	

Section 5.11 GLAC Study Area Results

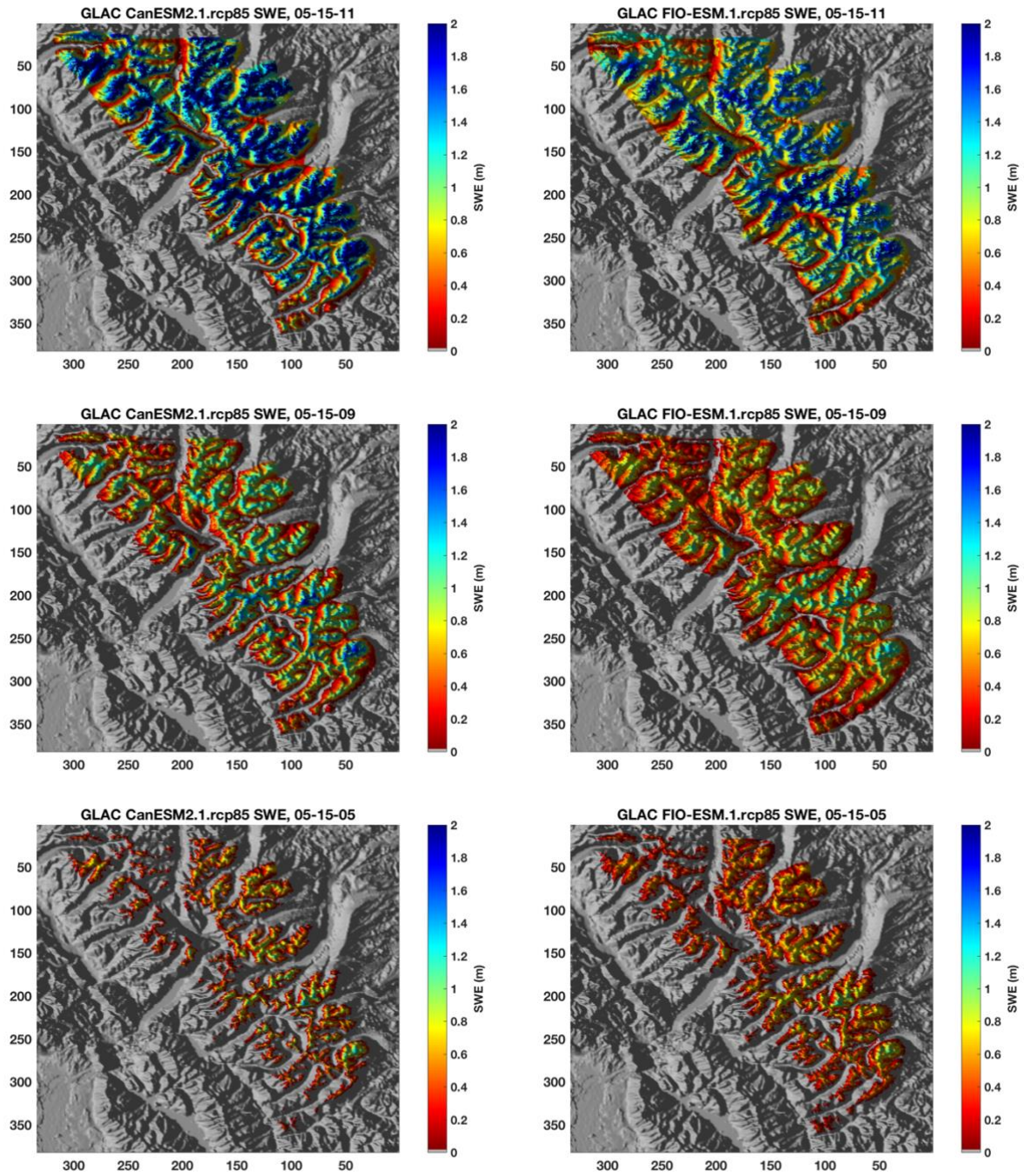


Figure S5-7. Additional scenarios for May 15th GLAC snow water equivalent based on representative wet (2011), near normal (2009) and dry (2005) years.

Section 5.12 ROMO Study Area Results

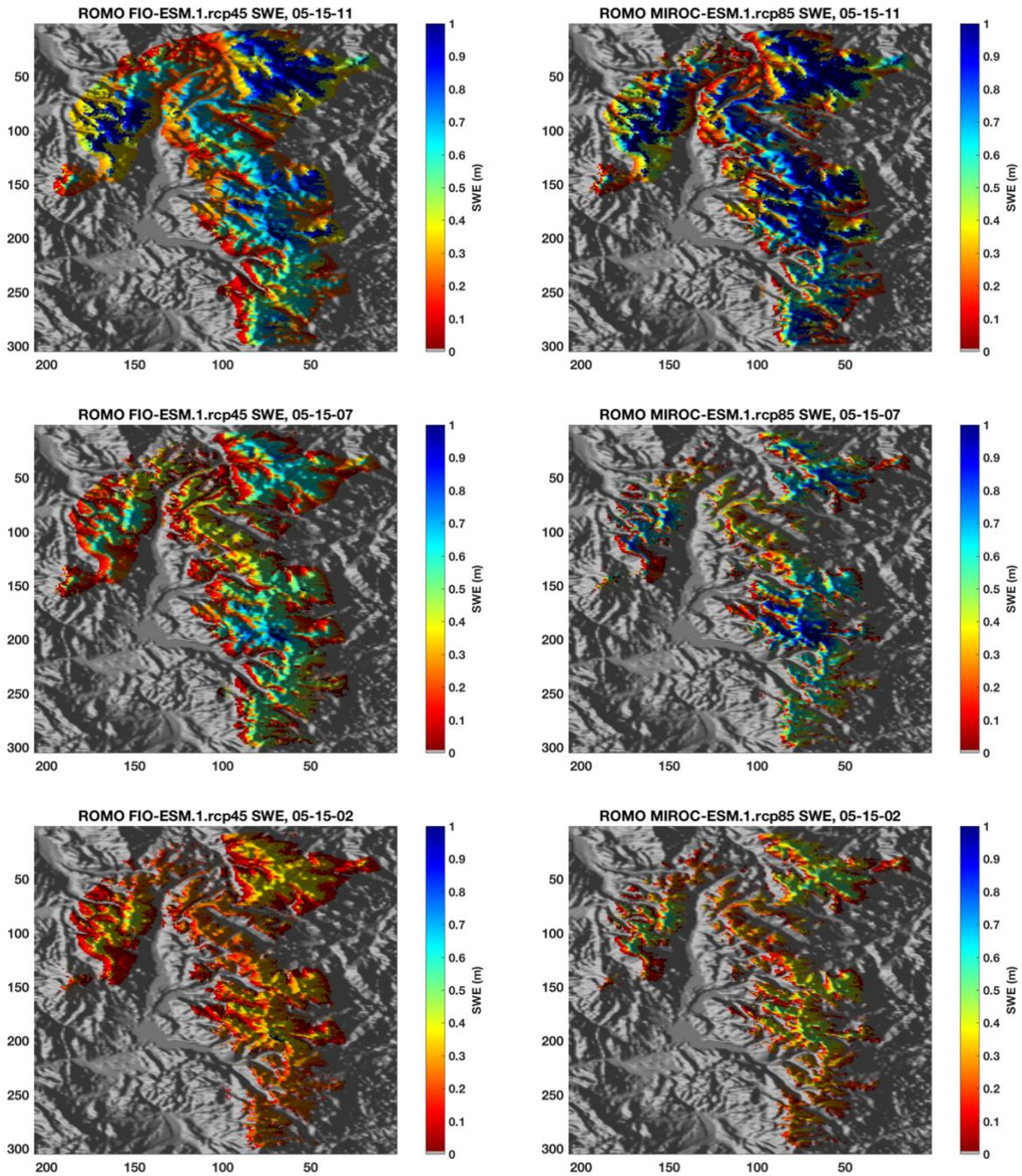


Figure S5-8. Additional scenarios for May 15th ROMO snow water equivalent based on representative wet (2011, top), near normal (2007, middle) and dry (2002, bottom) years.

Fig S5-22 and S5-23 show May 1st for comparison with April 15 and May 15 in Fig 5-22 and 23. Fig S5-22 shows the percent change in May 1st snowcovered area (SCA; ≥ 0.5 meters depth) for GLAC, computed for 200 m elevation bands. The elevation of observed den sites is noted by triangles, with den sites ranging from approximately 1500m to 2300 m. There is little change ($<10\%$) in SCA for 4 of the 5 scenarios above 2000m. There is greater than 60 % loss of SCA

below 1400m for 4 of the 5 scenarios. Between these two elevations – and in the regions where most observations of dens have been noted – the snowpack change is very sensitive to elevation and to the particular future climate scenario. Most of the dens are at 1800 to 2000, below that band large losses predicted, above that elevation band minimal losses predicted accept in maximum warming scenario. Figure 5-23 shows the elevation dependence of the May 1st snowpack measured in terms of snow water equivalent (SWE). Viewing snowpack in terms of SWE illustrates more clearly that the Hot/Very Wet future scenario has increased its snowpack between 2300 – 2900 m elevation despite completely losing its snowpack at 1000m elevation. Comparing Figure 5-22 (SCA) with Figure 5-23 (SWE) illustrates that SWE can have modest declines without affecting the area with significant snow depth. The implications is that wet, cold climate of the GLAC study area can act as a “buffer” to change in the area of ≥ 0.5 meter deep snow on May 1st, at least at relatively high elevations within the study area.

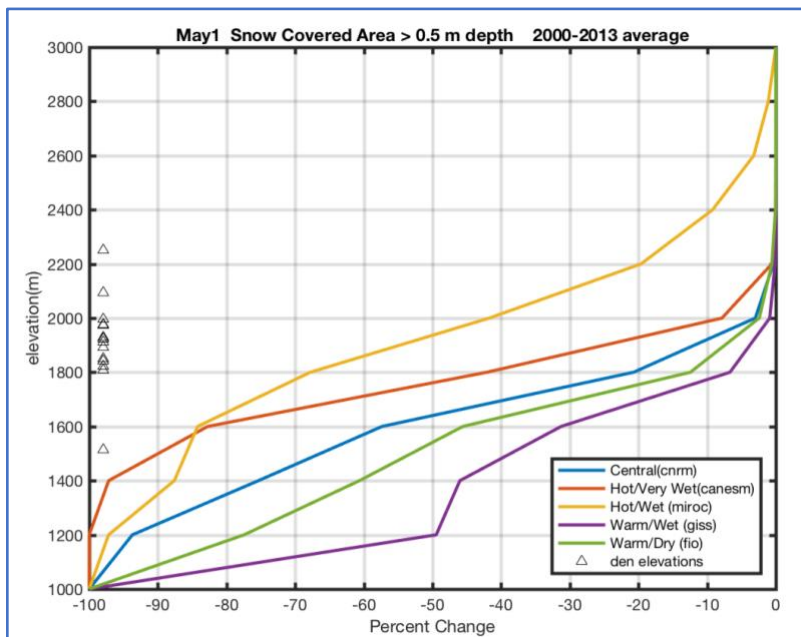


Figure S5-22: Elevation dependence of snow covered area (SCA) for GLAC: **Percent change in average Snow Covered Area (km² with depth ≥ 0.5 m) on May 1 at elevation bands for GLAC for five future scenarios.** As in Fig 5-22, line plot of percent change in SCA (x-axis, -100% to 0%) and elevation (y-axis 1000-3000m). The five scenarios are Central (cnrm, blue), Hot/Very Wet (canesm, red), Hot/Wet (miroc, yellow), Warm/Wet (giss, purple), Warm/Dry (fio, green). Black triangles on the y-axis show the elevations of documented wolverine den sites, elevation range 1500m ~2250. All but three of these dens are between 1800 and 2000m; two are above 2000m and one is below ~1500m. See also Table 5-2 for Modeled Snow Depth on May 15 at reported den sites in the Glacier Study Area.

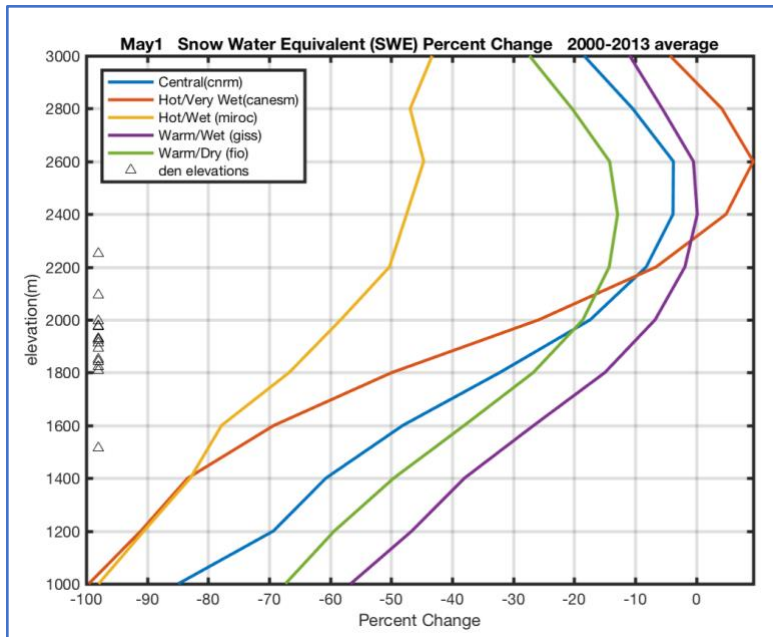


Figure S5-23. Percent change in average Snow Covered Area (depth ≥ 0.5 m) on May 1 at elevation bands for ROMO for five future scenarios: The five scenarios are Central (cnrm, blue), Hot/Dry (hadgem2, red), Hot/Very Wet (miroc, yellow), Warm/Wet (giss, purple), Warm/Dry (fio, green). Note that the highest elevation band at ROMO tops out at 4000m, whereas the highest elevation band at GLAC tops out at 3000m. No documented den sites exist in ROMO. As a proxy, linear regression of den site elevations and latitude in the contiguous U.S. indicated den sites in the ROMO study area would be located in an elevation range of 2700-3600 m (pers comm, John Guinotte, FWS).

Figure S5-24 shows the May 1st SCA (≥ 0.5 m depth) for ROMO. For elevations above 3400m only modest (under 20%) losses of SCA are seen. Figure 5-25 shows only modest (under $\sim 20\%$) losses in SWE for that elevation band as well with two scenarios (Warm/Wet (giss) and Hot Very Wet (miroc) having slight increases. Below 3400m the losses in SWE become much larger, the lower the elevation. Comparison of Figures 5-24, 5:25, and S5-24 and S5-25 shows that the relationship between SWE loss and SCA loss is not always straightforward, with a more complicated elevation dependence for SCA than for SWE.

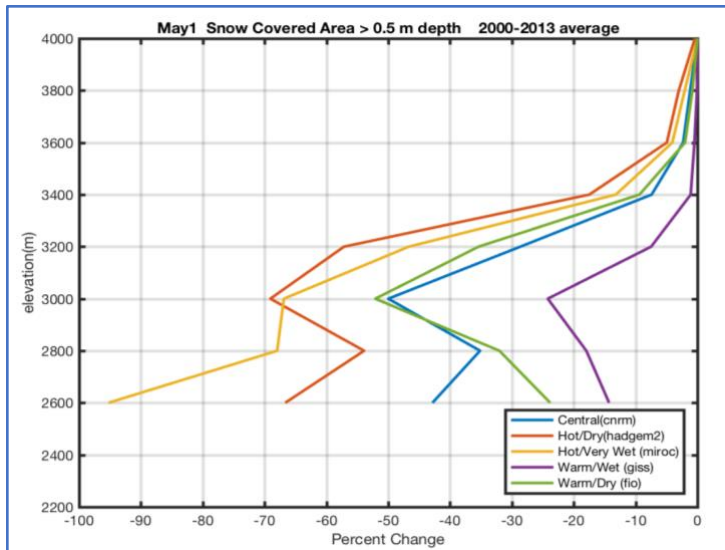


Figure S5-24: Percent change in average Snow Covered Area (depth ≥ 0.5 m) on May 1 at elevation bands for ROMO for five future scenarios: The five scenarios are Central (cnrm, blue), Hot/Dry (hadgem2, red), Hot/Very Wet (miroc, yellow), Warm/Wet (giss, purple), Warm/Dry (fio, green). Note that the highest elevation band at ROMO tops out at 4000m, whereas the highest elevation band at GLAC tops out at 3000m. No documented den sites exist in ROMO. As a proxy, linear regression of den site elevations and latitude in the contiguous U.S. indicated den sites in the ROMO study area would be located in an elevation range of 2700-3600 m (pers comm, John Guinotte, FWS).

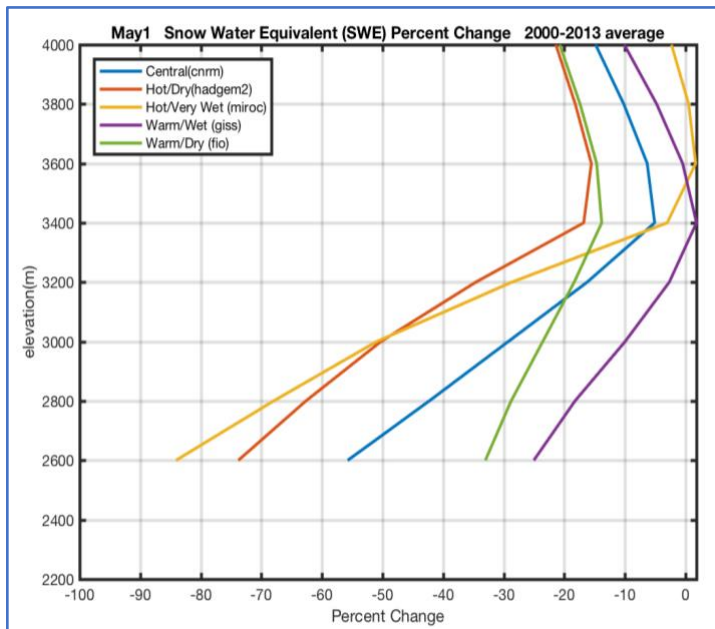


Figure S5-25: Average Snow Water Equivalent (SWE, percent change) on May 1 at elevation bands for ROMO for five future scenarios. The scenarios are: Central (cnrm, blue), Hot/Very Wet (hadgem, red), Hot/Wet (miroc, yellow), Warm/Wet (giss, purple), Warm/Dry (fio, green). Note that the highest elevation band at ROMO tops out at 4000m, whereas the highest elevation band at GLAC tops out at 3000m. See the main text for April 15 and May 15.